Master's thesis

NTNU
Norwegian University of Science and Technology
Faculty of Engineering
Department of Civil and Environmental Engineering

Elene Gotsiridze

Assessment Of Greenhouse Gas Emissions From Hydropower Projects Using G-RES Tool

Master's thesis in Hydropower Development
Supervisor: Tor Haakon Bakken
Co-supervisor: Mahmoud Kenawi
June 2023

NTNU
Norwegian University of Science and Technology

SINTEF iha

Elene Gotsiridze

Assessment Of Greenhouse Gas Emissions From Hydropower Projects Using G-RES Tool

Master's thesis in Hydropower Development
Supervisor: Tor Haakon Bakken
Co-supervisor: Mahmoud Kenawi
June 2023

Norwegian University of Science and Technology
Faculty of Engineering
Department of Civil and Environmental Engineering

NTNU
Norwegian University of
Science and Technology

Abstract

2050 net zero transition requires analyzing and calculating GHG emissions from different renewable energy sources. Hydropower in this big transition plays a vital role, as it serves as a green battery capable of generating electricity when other renewables like wind and solar may be hindered by weather conditions. Energy storage, provided by hydropower, becomes essential in such scenarios.

Although hydropower is a renewable energy source, which has a minimum emission, it still produces GHG emissions from reservoirs and during construction, hence, it is important to calculate GHG emissions related to hydropower projects.

In this study, the focus is on evaluating emissions from existing or expanded reservoirs, excluding emissions from the construction phase.

To study and analyze GHG emissions from reservoirs G-RES tool was used, which is led by International Hydropower Association and the UNESCO Chair in Global Environmental Change, The G-res Tool was developed using a conceptual framework created with scientists from the University of Quebec at Montreal (UQAM), the Norwegian Foundation for Scientific and Industrial Research (SINTEF) and the Natural Resources Institute of Finland (LUKE), with assistance from the World Bank. The study utilized the G-RES tool to investigate 15 Norwegian reservoirs, comparing the results with emissions from eight Norwegian wind farms and the global solar project emissions intensity.

The simulations conducted highlighted the importance of factors such as land cover and soil type within reservoirs, as they significantly impact the quantity of emissions released into the atmosphere. Thoroughly studying these factors before embarking on reservoir construction is crucial.

The study showed that the lowest emissions intensity from reservoirs can be $0gCO_2e/kWh$, while the highest is $5.7gCO_2e/kWh$, in a comparison from Norwegian onshore wind the lowest emissions rate is $11gCO_2e/kWh$, and from the offshore wind concepts the lowest 18 gCO_2e/kWh, and the highest $31.4gCO_2e/kWh$, while the lowest global solar emissions rate is $38gCO_2e/kWh$, while the highest is $48gCO_2e/kWh$.

Further examination and improvement of the G-RES tool are necessary, to ensure that all requirements are met. The proper utilization of this tool can save considerable time, expenses, and resources, enabling hydropower project owners to attain certification and generate green electricity.

The study is done with SINTEF and IHA (International Hydropower Association) collaboration.

Acknowledgements

I am deeply grateful to my supervisor, Professor Tor Haakon Bakken, for his unwavering guidance, valuable advice, and constant motivation throughout my study. Without his support, this endeavour would not have been possible. I would also like to express my gratitude to my co-supervisor, Mahmoud Saber Kenawi, whose constructive suggestions, extensive support, encouragement, and dedicated time have played a pivotal role in my growth and development during this learning journey.

I extend my sincere thanks to Håkon Sundt and Atle Harby from SINTEF, as well as the G-RES team from the International Hydropower Association (IHA). Their knowledge, expertise, and generous contributions have significantly enriched my research, while their encouraging suggestions have inspired me to strive for continuous improvement and excellence. I am grateful for their valuable feedback and prompt responses.

Finally, I cannot overlook the importance of acknowledging my family, supportive friends and loved ones. Their unwavering belief in my abilities has been instrumental in keeping my spirits high and my motivation strong throughout the course of this study.

Contents

List of Figures

List of Tables

List of Abbreviations and terms

- CO_2 : Carbon dioxide
- CH_4 : Methane
- g : grams
- GHG : Greenhouse Gas
- GWP : Global Warming Potential
- G-RES : Greenhouse gas REServoirs
- HRW : Highest Regulated Water Level
- LRW : Lowest Regulated Water Level
- IPCC : Intergovernmental Panel on Climate Change
- km^2 : Squared kilometers
- m^2 : Squared meters
- KWh : Kilowatt hours
- m.a.s.l : Meters Above Sea Level
- m/s : Meters per second
- N_2O : Nitrous Oxide
- tCO_2eqv : Tons of Carbon dioxide equivalent
- UAS : Unrelated Anthropogenic Sources
- yr : Year
- ^oC : Degree Celsius
- EE – Earth Engine
- LCA – Life Cycle Assessment
- Pre-impoundment – the GHG balance associated with the area subsequently occupied by the reservoir, which is calculated based on the land-cover and a set of emission factors which represent the flux of emissions for land cover at the location of the reservoir
- Post-impoundment – the GHG balance associated with the reservoir after inundation, which is calculated using a semi-empirical model based on a comprehensive dataset collated from the published peer-reviewed literature on measured GHG fluxes for diffusive, bubbling, and degassing emission pathways
- Construction – the GHG emission associated with materials, plant and transport required to construct the dam and other infrastructure to form the reservoir, calculated based on the use of materials and emission factors (Optional). The results for each module are presented in terms of annual emissions, total missions, and areal emissions
- Gross emissions - Gross emission is the amount of pollution released into the atmosphere by the natural environment after the reservoir has been built. This definition does not take into account earlier emissions in the system.
- Net emissions - The net emission however is the total emission that has resulted after the reservoir has been constructed minus emission the area under the reservoir used to emit or would emit minus the emission from Unrelated Unthropogenic Sources
- Ebullition / Bubbling - Gases with low water solubility such as CH_4 (mole fraction solubility 2.81 x 10-5 at 20^oC) are often released to the

atmosphere in the form of bubbles also known as ebullition. These bubbles usually rise from the sediments

- Degassing - The concentration of gases in the water decreases after passing through the generating stations and spillways known as degassing
- CO_2 equivalent - A carbon dioxide equivalent or CO_2 equivalent, abbreviated as CO_2-eq is a metric measure used to compare the emissions from various greenhouse gases on the basis of their global-warming potential (GWP), by converting amounts of other gases to the equivalent amount of carbon dioxide with the same global warming potential
- Soil Carbon content under the impoundment - A region is flooded in preparation for the building of an artificial reservoir. Prior to floods, the region most likely had a variety of land uses and soil carbon. The soil carbon content under the impounded region is the soil carbon content inundated by the artificial reservoir. It is measured in kilograms of carbon per square meter (Kg C/m^2).
- GHG emission intensity - It is the quantity of carbon dioxide equivalent emissions per unit of electricity generation. It is represented by gCO_2eqv/kWh.
- Units of emission - The areal emission is measured in grams of carbon dioxide equivalent per square meter per year ($gCO_2eqv/m^2/yr.$)
- Reservoir-wide emissions - The reservoir-wide emissions are computed in tons of carbon-dioxide equivalent per year ($tCO_2eqv/yr.$)
- Total lifetime emission - The total lifetime emission of the reservoir is computed in tons of carbon-dioxide equivalent (tCO_2eqv).
- Power density - Power density is a measure of the average power output per unit area used for generation. The world uses just over 100,000 billion kWh of final energy each year to run transport, industry, and convenience living. That includes the oil burnt in your car engine, the coal fed into manufacturing facilities, the natural gas heating your home, and the electricity used to power your appliances. Divide that total annual energy use over 365 days, and the 24 hours in each day, and this equates to an average of nearly 12 billion kW (12 TW) to power the planet at any given time

1 Introduction

In today's world where everyone tries to achieve sustainability and be net zero by 2050, hydropower plays a vital role in this chain, which offers a steady and renewable energy source of electricity. Considering this it is crucial to examine and study the environmental impacts of hydropower projects, especially of GHG emissions. To meet this there are different possibilities. On-site studies offer the opportunity to directly measure GHG emissions at the reservoir location, enabling a comprehensive understanding of the environmental footprint. Additionally, the G-RES tool provides a valuable resource for conducting desk studies, empowering users to accurately calculate GHG emissions stemming from hydropower projects.

Hydropower provides a variety of advantages as a sustainable energy source. However, reservoirs have potential GHG emissions which need to be assessed. These emissions are mostly caused by the decomposition of organic materials in reservoirs, which ends in the release of methane emissions. Furthermore, operational activities like turbine discharges and spillway operations can add to indirect emissions. Understanding the magnitude and origins of these emissions is thus critical for successful environmental management and the development of sustainable energy policies.

The G-RES tool offers a practical and efficient approach to evaluating GHG emissions from hydropower projects. It provides users with the ability to calculate emissions throughout the entire lifecycle, from reservoir impoundment to operation, and considers the land covering of catchment and reservoir, climate, wind, and other important factors which can influence emissions from reservoirs. By integrating advanced modelling techniques and leveraging robust data inputs, the tool delivers reliable estimates of GHG emissions, enabling project developers, operators, and policymakers to make informed decisions and implement effective mitigation strategies.

Despite its importance, there are not enough studies done on greenhouse gas (GHG) emissions associated with these projects, particularly with regard to the effects of land covering changes within reservoir areas and the long-term response of impoundment areas. Objective 1 of this thesis is to find an answer to a question: "What are the GHG emissions from reservoirs?" To achieve this, the study will focus on analyzing 15 reservoirs in Norway, taking into account a range of factors including different climate patterns, elevations, and variations in land cover within the reservoir areas.

Conducting a thorough analysis of these reservoirs, the research aims to uncover vital insights and calculate accurate GHG emissions from each case. By filling the existing knowledge gap, this study will contribute to a more comprehensive

understanding of the environmental impact of reservoirs in terms of GHG emissions.

The second main objective is to compare the GHG emissions among renewable energy projects. This study aims to present and compare the GHG emissions associated with wind and solar energy projects in contrast to the GHG emissions calculated using the G-RES tool for reservoirs.

To achieve this objective, data was gathered from eight wind projects in Norway, as well as global studies on solar energy. These datasets provided valuable information to assess and compare the emissions intensity across different renewable energy sources.

By presenting the emissions intensity from wind and solar energy projects alongside the GHG emissions from reservoirs, readers will gain insights into the relative environmental impact of different renewable energy technologies.

1.1 Objectives

Key questions to be addressed in the thesis are;

- To identify and select 5-10 reservoirs for the assessment of greenhouse gas emissions in Norway, based on hydropower projects where land use changes (due to hydropower regulations) have been detailed assessed
- To get familiar with the G-RES tool hosted by the International Hydropower Association (IHA) and configure the model for the selected reservoirs
- To calculate the net greenhouse gas emissions from the selected case studies and discuss the results.
- To compare the calculated results from hydropower projects in Norway, with published values on the greenhouse gas emissions from wind power projects (and possibly other renewable sources), from similar/comparable climatic conditions.

2 Basic Theory and Literature Review

2.1 Climate change mitigation and transition to renewable from fossil fuels

Climate change refers to a change in the state of the climate *that can be identified (e.g., by using statistical tests) by changes in the mean and/or the variability of its properties and that persists for an extended period, typically decades or longer. Climate change may be due to natural internal processes or external* forcings *such as modulations of the solar cycles, volcanic eruptions and persistent* anthropogenic *changes in the composition of the* atmosphere *or in* land use*.* (IPCC Glossary , n.d.)

In order to mitigate climate change, greenhouse gas emissions have to be reduced into the atmosphere. To make this greenhouse gas emissions from the main sources have to be decreased, like power plants, industry, automobiles and agriculture. Forests, oceans and soil can collect and store all these gases, that's why it is important to take care and maintain the natural mitigation possibilities. (EEA - European Environment Agency, Climate change mitigation : reducing emissions)

However, not only natural sources are enough to decrease emissions. Switching from fossil fuels to renewables such as solar, wind, and hydropower will lessen the emissions that are causing climate change. While an increasing number of nations are pledging to achieve net zero emissions by 2050, emissions must be cut in half by 2030 in order to keep the temperature below 1.5°C. To achieve this, massive reductions in the usage of coal, oil, and gas are required: more than two-thirds of today's proven supplies of fossil fuels must be maintained in the ground by 2050 in order to avoid catastrophic levels of climate change. (United Nations - Renewable energy - Powering a safer future). That's why it is important to switch to renewable energy sources. With renewable energy, it is possible to have a transition from coal, natural gas and oil. With wind, solar and hydropower we can produce green electricity and help the earth, and society to continue life without major changes.

2.1.1 Hydro Power

The use of falling or fast-running water to generate energy or power machinery is known as hydropower. This is accomplished by transforming a water source's gravitational potential or kinetic energy into power. It can be achieved by guiding water through a series of turbines, which transform the potential and kinetic energy of the water into the turbine's rotating motion after this the turbine is connected to a generator, and the motion of the turbine is utilized to create power. It can be used as the base load when wind and solar can't produce the energy due to weather conditions. That's why hydropower is considered the natural green battery storage, thanks to the reservoir. The amount of energy

available is determined by reservoir size, reservoir head difference, and turbine efficiency.

Hydropower has the following main components:

- Reservoir or water source
- Dam and intake structure
- Waterways (penstock, channels, canals, tunnel shafts)
- Turbine
- Generator
- Powerhouse
- Transmission lines and substations
- Control systems and monitoring

Power can be calculated from the following equation:

$$P = \eta * \rho * g * h * Q$$

Equation 1 Power production equation

η – Efficiency factor

ρ – Water density 1000 kg/m^3

g- Gravitational acceleration 9.81 m/s^2

h – Height of fall (Head)

Q – Discharge

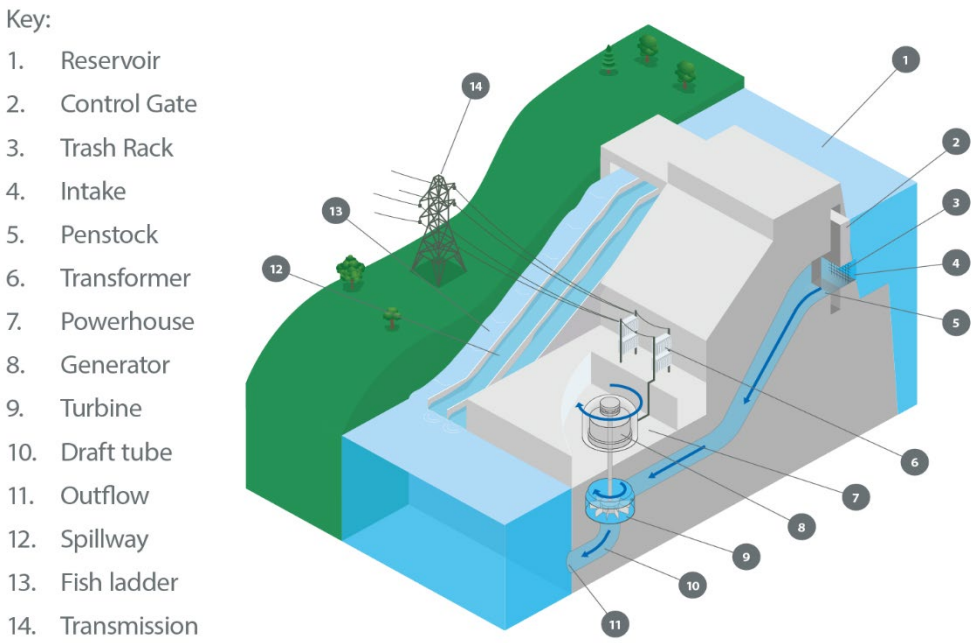

Figure 1 Hydropower plant with the main components (IHA - International Hydropower Assosication , n.d.)

Hydropower projects are classified into four types. These technologies frequently overlap. Storage projects, for example, may include some pumping to supply the water that naturally flows into the reservoir, and run-of-river projects may have some storage capabilities.

- Run-of-river-hydropower (ROR) - an infrastructure that uses flowing water from a river to spin a turbine via a canal or penstock. A run-of-river project will often have little or no storage capacity. Run-of-river offers a constant supply of energy (base load), with some operational flexibility for daily shifts in demand via controlled water flow.
- Storage hydropower - A large system that stores water in a reservoir using a dam. Water from the reservoir is released through a turbine, which runs a generator, producing electricity. Storage hydropower offers a base load as well as the capacity to be shut down and restarted quickly in response to system needs (peak load). It has the potential to provide enough storage capacity to function independently of hydrological input for many weeks or perhaps months.
- Pumped storage hydropower (PHES) - offers peak-load supply by capturing water that is cycled between a lower and upper reservoir by pumps that utilise excess energy from the system when demand is low. When there is a high demand for energy, water is discharged back into the lower reservoir using turbines to generate electricity.
- Offshore hydropower - a newer but expanding class of technology that employ tidal currents or the strength of waves to generate electricity from seawater.

Hydropower remains the largest renewable electricity technology by capacity and generation, current capacity growth trends are not sufficient to place it on the trajectory under the Net Zero Scenario. Reaching about 5 700 TWh of annual electricity generation by 2030 will require approximately 3%, which may be additionally challenging taking into account accelerating disturbances to water availability caused by climate change. (Hydroelectricity , IEA)

2.1.2 Wind Power

Wind energy is used to generate power by transforming the kinetic energy of moving air into electricity. The wind transforms the rotor blades of contemporary wind turbines, converting kinetic energy into rotational energy. This rotational energy is transmitted to the generator through a shaft, resulting in the generation of electrical energy. Wind power is a sustainable, renewable energy source that has a far lower environmental effect than burning fossil fuels. Because wind power is variable, it requires energy storage or other dispatchable generation energy sources to ensure a consistent supply of electricity. Wind power is one of the least expensive sources of electricity per unit of energy produced. In many places, new onshore wind farms are less expensive than new coal or gas facilities.

Depending on the location we can have two types of wind energy – onshore and offshore. Per unit of energy generated, land-based (onshore) wind farms have a bigger aesthetic impact on the landscape than most other power plants. Offshore wind farms have less aesthetic effect and better capacity factors, although they are often more costly. Offshore wind power presently accounts for around 10% of new installations. (Global Wind Energy Council, Global Wind Report, n.d.)
The quantity of wind energy that can be captured is determined by the size of the turbine and the length of its blades. The output is proportional to the rotor size and the cube of the wind speed. In theory, doubling the wind speed increases the wind power potential by a factor of eight. (Wind Energy, n.d.)

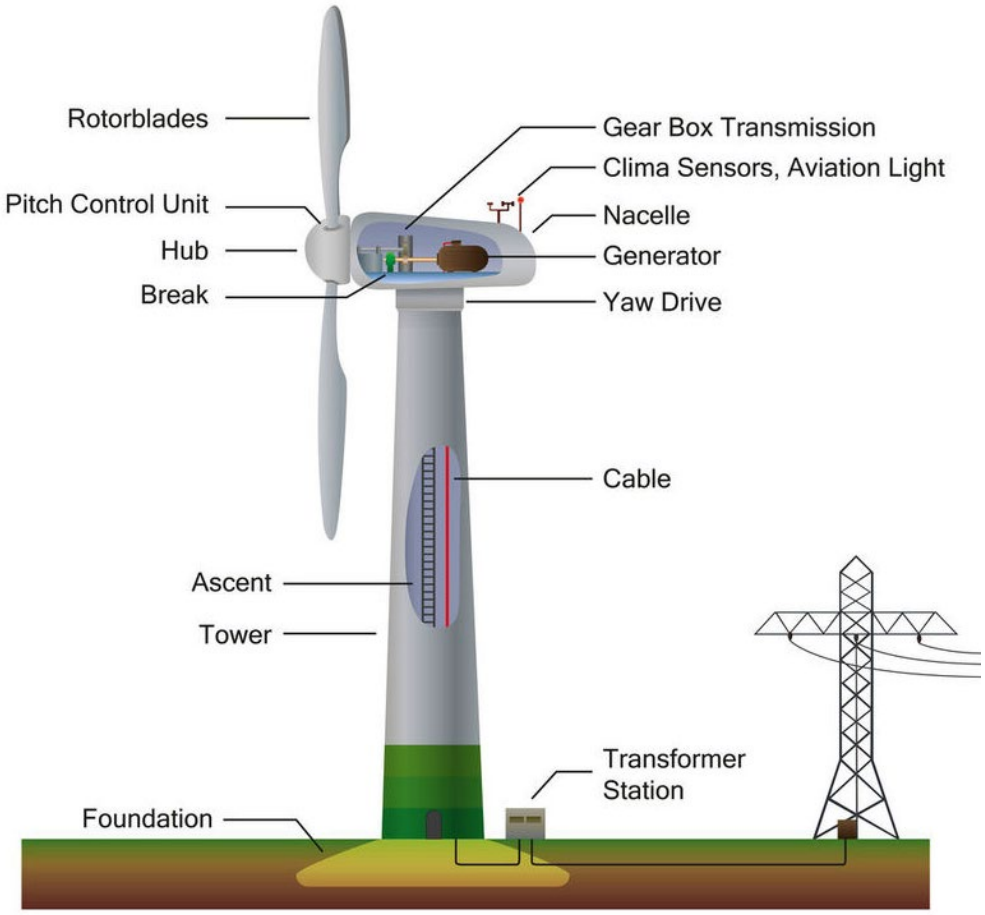

Figure 2 Typical components of wind power generation (What is the wind energy , n.d.)

The amount of electricity generated by wind increased by almost 273 TWh in 2021, 55% higher growth than that achieved in 2020. Wind remains the leading non-hydro renewable technology, aligning with the Net Zero Scenario's wind power generation level of about 7 900 TWh in 2030 calls for an average expansion of approximately 18% per year during 2022-2030. (IEA, Wind Electricity, n.d.)

2.1.3 Solar Power

Solar energy is any sort of energy that is produced by the sun.

Even in cloudy weather, energy may be extracted directly from the sun. Solar energy is utilized all around the world and is becoming increasingly popular for generating power, heating, and desalinating water. Solar energy is produced in two ways:

Solar photovoltaic (PV) technology converts sunlight directly into electricity using electrical devices known as solar cells. It is one of the most rapidly expanding renewable energy technologies, and it is becoming increasingly essential in the global energy change. (IRENA, Solar Energy , n.d.)

Solar PV power output climbed by a record 179 TWh in 2021, representing a 22% increase over 2020. Solar PV accounted for 3.6% of worldwide electricity output in 2016, and it is still the third largest renewable energy technology after hydropower and wind. To attain an annual solar PV generating level of around 7 400 TWh in 2030, aligned with the Net Zero Scenario, yearly average generation increase of nearly 25% is required during 2022-2030. (IEA, Solar PV , n.d.)

Solar PV systems are very flexible and range in size from tiny solar home kits and rooftop installations of 3-20 kW capacity to systems with hundreds of megawatts of capacity. It has democratized the production of power.

Solar panel production costs have dropped drastically in the last decade, making them not only inexpensive, but often frequently the cheapest type of power. Between 2010 and 2020, solar module prices plummeted by up to 93%. During the same time frame, the worldwide weighted-average levelized cost of electricity (LCOE) for utility-scale solar PV plants dropped by 85%. (IRENA, Solar Energy , n.d.)

2.2 Concerns of Renewable energies

Renewable energy (RE) *is any form of energy from solar, geophysical or biological sources that is replenished by natural processes at a rate that equals or exceeds its rate of use. Renewable energy is obtained from the continuing or repetitive flows of energy occurring in the natural environment and includes low-carbon technologies such as solar energy, hydropower, wind, tide and waves and ocean thermal energy, as well as renewable fuels such as biomass. For a more detailed description see specific renewable energy types in this glossary, for example, biomass, solar, hydropower, ocean, geothermal and wind.* (IPCC Glossary , n.d.)

2.2.1 Positive impacts of renewable energies

- Evnironmentlal benefits
  When compared to traditional fuel sources such as natural gas, renewable energy generating methods produce little to no greenhouse gas emissions. This results in a lower carbon footprint and a beneficial overall influence on the natural environment. During the combustion process, fossil fuels generate significant amounts of greenhouse gases, which have been shown to worsen climate change, resulting in rising global temperatures and an increase in the frequency of extreme weather events. The use of fossil fuels not only generates greenhouse gases, but also other toxic chemicals that cause respiratory and heart problems. You can help reduce the incidence of these contaminants and contribute to a healthier environment by using renewable energy.

- Cleaner water and air
  When fossil fuels are used to generate energy, they pollute the air and water we use. Coal power plants, for example, emit large amounts of carbon dioxide and nitrous oxide, as well as hazardous pollutants such as mercury, lead, and sulfur dioxide. Ingesting these components can cause serious and even deadly health consequences. Investing in renewable energy is an excellent strategy to mitigate these risks because renewables have a far lower negative impact on our air and water.

- Energy availability
  Renewable energy methods create electricity directly from the environment. Sunlight, wind, tides, and biomass are just a few of the more prevalent energy sources. Renewable resources will not run out, however many types of fossil fuels will become increasingly difficult to access as we utilize them, possibly increasing both the expense and environmental effect of extraction.

2.2.2 Negative impacts of renewable energies

- Periodicity
  Though renewable energy resources are accessible all around the world, many of them are not available 24/7. Some days may be windier than others, the sun may not shine at night, and droughts may occur. Unpredictable weather occurrences can damage these technologies, and the quantity of energy we can acquire from renewable energy sources can vary. Fossil fuels are not intermittent, and power plants may be turned on and off at any moment to supply electricity. That is one of the main

reasons why hydropower is crucial in renewable energy sources since it gives grids stability and flexibility possibilities, also thanks to the reservoir it has storage capabilities.

- Higher initial investment
  While adopting renewable energy might save money, the technologies are often more expensive up front than standard energy providers. To mitigate this, financial incentives such as tax credits and rebates are frequently given to assist offset the early expenses of renewable technologies.
- Not completely carbon-free
  Although solar panels and other kinds of renewable energy cut carbon emissions significantly, they are not always fully clean. Renewable energy, such as wind turbines, can have a carbon footprint since they are often manufactured in facilities that use fossil fuels, not to mention the diesel and gasoline required to fuel the transport trucks.

2.3 General concept of GHG (Green Houses Gases) emissions

Greenhouse gases are those gaseous constituents of the atmosphere, both natural and anthropogenic, that absorb and emit radiation at specific wavelengths within the spectrum of thermal infrared radiation emitted by the Earth's surface, the atmosphere itself, and by clouds. This property causes the greenhouse effect. Water vapor (H_2O), carbon dioxide (CO_2), nitrous oxide (N_2O), methane (CH_4) and ozone (O3) are the primary greenhouse gases in the Earth's atmosphere. Moreover, there are a number of entirely human-made greenhouse gases in the atmosphere, such as the halocarbons and other chlorine- and bromine-containing substances, dealt with under the Montreal Protocol. Beside CO_2, N_2O and CH_4, the Kyoto Protocol deals with the greenhouse gases sulphur hexafluoride (SF6), hydrofluorocarbons (HFCs) and perfluorocarbons (PFCs).
(IPCC Glossary , n.d.)

2.3.1 GHG emissions in the reservoirs

Reservoirs can be major sources of greenhouse gas (GHG) emissions. Factors, like climate, catchment characteristics, reservoir age and area, water residence time, soil carbon content, global mean horizontal radiance, land covering within the reservoir, elevation and other factors all have an impact on the rate of GHG emissions.

GHG emissions from reservoirs can occur through various mechanisms, including surface diffusion, bubbling, and vegetation decay. Natural reservoirs release GHG through these processes. However, manmade reservoirs introduce additional emission pathways downstream. These include degassing or diffusive emissions in the turbulent waters downstream of the reservoirs and diffusion and bubbling in the river downstream of the power-producing plant.

- Surface Diffusion: GHGs like methane (CH_4) and carbon dioxide (CO_2) can spread over reservoir water-air interfaces. This happens when dissolved gases in water come into contact with the atmosphere and are released. Natural reservoirs, as well as manmade reservoirs, contribute to surface diffusion emissions.
- Bubbling: Bubbling is another mechanism through which GHGs are released from reservoirs. Methane, in particular, can be generated through anaerobic microbial processes in the sediment and then released as bubbles that rise to the water's surface. These bubbles burst, releasing methane into the atmosphere. Bubbling is a significant pathway for methane emissions
-

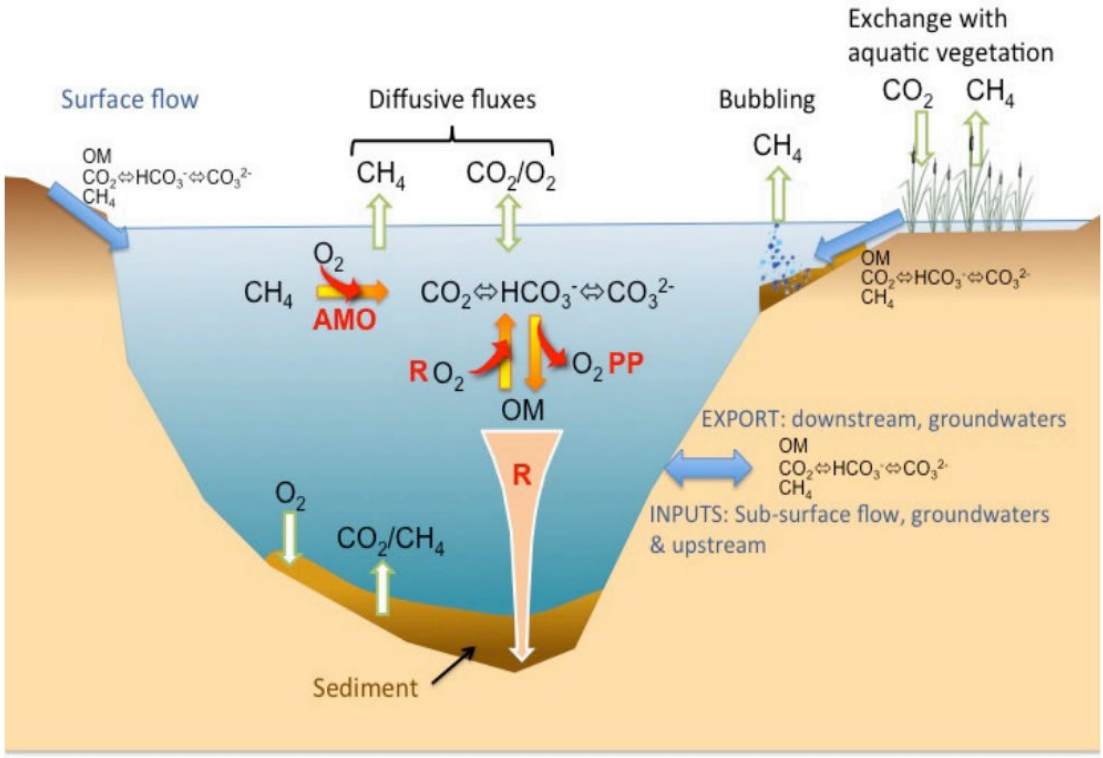

Figure 3 Carbon cycle in waterscape (CEDREN, 2023)

3 Thesis Workflow

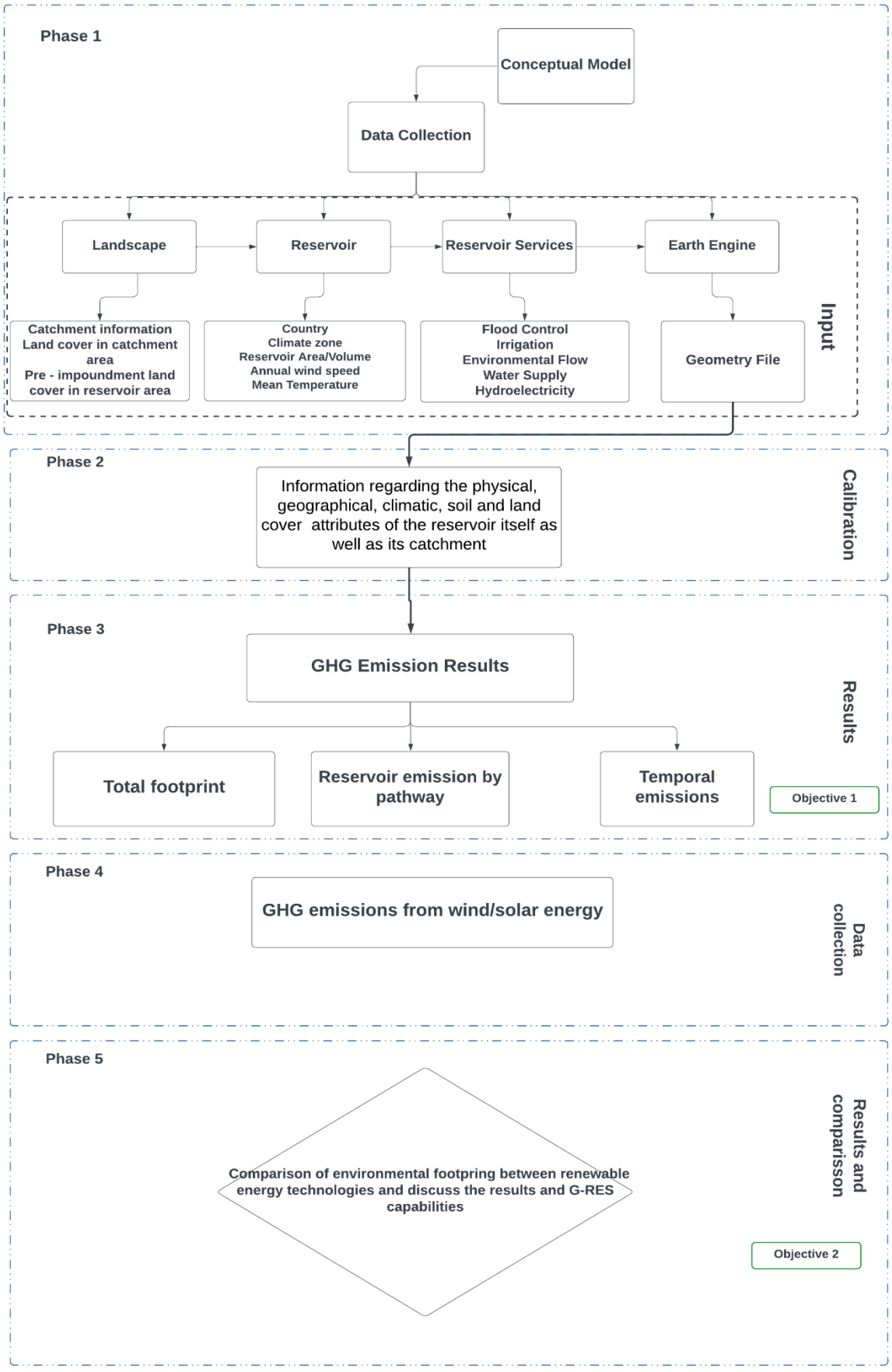

3.1 Phase 1: Data Collection

For Hydropower production:

Nevina, NVE Atlas, Earth Engine (a built-in G-RES tool), Norge i bilder and NINA were used to collect data. Working with various cases, the findings for the reservoir from Earth Engine and NINA were varied, therefore Earth Engine data were only utilized for the catchment land coverage, while NINA data was picked for the reservoir land coverage. The key reason for the disparity in data between these two is that NINA data was collected by a site visit and comprehensive description of the location, whereas shape files for Earth Engine are derived from NVE Atlas, which uses satellite pictures.

Reservoir area, reservoir volume, latitude and longitude of the dams, impoundment year, exact catchment size, and the highest and lowest regulated water level, with shape files were retrieved using NVE Atlas. Shapefiles were extracted from NVE Atlas for use in the G-RES tool, which additionally validated the exact position, river path, catchment area, and reservoir size

The weather prediction is a key input for the G-RES tool. The data for the weather prediction for certain reservoirs came from the Earth Engine (Mean Temperature per Months ^{o}C), while data for other reservoirs came from the Seklima.met.no. The major reason for this is that the measuring station was extremely far away from several reservoir sites, resulting in more questionable figures for the reservoirs, that's why the weather informaton was takes from EE.

In order to check how the pre-construction location of reservoirs looked Norge i bilder were used. With this website, it was possible to understand the before impoundment area of the reservoir, also since the website information comes as satellite images, it gives us the possibility to see the vegetation area covered. This website was used also to double-check the shapefiles, and maps to have the exact information regarding the reservoirs, and catchment.

To determine the maximum depth of the reservoirs, a calculation was performed using the formula ((HRW-LRW)+20), additionally, a 20-meter allowance was made to account for the littoral area. The assumed water intake elevation (m.a.s.l.) was set as the lowest regulated water level. Furthermore, the volume of each reservoir was increased by 50% for the purpose of this study, which will be elaborated upon in the results section. This methodology ensured a comprehensive assessment of the reservoirs' maximum depth and allowed for a meaningful analysis of their characteristics. The calculation of results using G-RES relies heavily on the reservoir volume parameter. To determine the most appropriate reservoir volume, the tool's sensitivity was evaluated to assess how it would affect the model's outcomes. Initially, the volume value was obtained from NVE Atlas, and subsequent analyses were conducted by increasing it by various percentages: 10%, 15%, 20%, 50%, and 100%. The purpose of these increments was to observe the resulting changes in the reservoir's gross volume.

The analysis indicated that the model was responsive to changes in volume. Specifically, it revealed that increasing the volume led to a decrease in emission intensity. This phenomenon can be attributed to the fact that in shallow water, sunlight penetration is more pronounced compared to deeper water, facilitating the decomposition of organic materials. Based on this understanding, and to avoid any mistake from NVE Atlas information, a decision was made to augment the volume by 50% and examine the corresponding results. Further details regarding this analysis will be provided in the results section.

The Google Earth Engine function, which is included in the G-Res tool, was used to generate the soil carbon content under the impounded area, the reservoir mean global horizontal radiance, catchment land covering, and temperature/wind, in the case when the station was far away from the reservoir. Wind speed and temperature over the previous 12 months were computed using data from a nearby measurement station from Seklima (Seklima.met.no, n.d.). All of the reservoirs are used primarily for hydroelectricity. GHG emissions from reservoir building materials are not taken into account. The G-Res tool calculates the output based on the inputs.

For wind and solar power:

To find the data on GHG emissions for wind and solar power, after land degradation was a challenging task, due to small number of studies available in this area. However, several comprehensive reports were utilized to explore and discuss the impact of wind power on GHG emissions from the affected land. Additionally, a life cycle assessment (LCA) specific to wind power were conducted to accurately quantify the emissions associated with this renewable energy source. This will be explained in the results section.

3.2 Phase 2: Setting up G-RES tool with collected data

Phase 2 of the study includes model development and sensitivity analysis of the model. Using the data obtained from NEVINA, NVE Atlas, Earth Engine and NINA was used to run the G-RES and make the simulation. Different values for Volume in Reservoir tab and different values for Organic and Mineral soil in landscape were used to check the sensitivity of the inputs in the model. Based on the shape files from NVE Atlas ((Nve Atlas , n.d.) the Earth Engine run and found all the necessary information for the model. To obtain data on the land cover of the reservoirs, image classification techniques were employed on a comprehensive set of aerial photographs capturing the pre-construction state of the land. This process involved analyzing and categorizing the land cover features depicted in the images. To ensure the accuracy and reliability of the classification results, a subsequent accuracy assessment was carried out. This assessment served to validate and confirm the accuracy of the land cover classifications achieved through image analysis. The combination of image classification and accuracy assessment provides a robust methodology for obtaining reliable data on reservoir land cover dynamics.

3.3 Phase 3: Learning solar and wind power GHG emissions

A phase 3 analysis was undertaken on GHG emissions from solar and wind after the findings of reservoir emissions were simulated and compared to wind and solar emissions.

3.4 Phase 5: Discussion

Comparison of GHG emissions intensities from different renewable energies, finding, issues related to G-RES tool, and recommendations.

3.5 Tools and techonologies used

In this thesis to calculate GHG emissions from reservoirs following tools and technology were used: G-RES, GIS, Excel, Python and JavaScript, and ChatGPT for information search purposes.

4 Methods of calculating the GHG emissions in renewable energy technologies

4.1 Tools for calculating GHG emissions in renewable energy technologies

Determining the greenhouse gas (GHG) emissions associated with wind and solar energy requires examining their Life Cycle Assessment (LCA). The primary source of GHG emissions in wind and solar energy production stems from the material manufacturing stage and the type of energy employed (green or grey energy). Unfortunately, there is currently a no comprehensive studies or tools available to calculate the amount of GHG emitted from the land during the construction of solar and wind farms. Further research and development are needed in this area to better understand and quantify the emissions associated with these renewable energy sources

4.1.1.1 Measurments for calculating GHG emissions in reservoir

Since the G-RES tool is the first non-measurement tool, which allows the calculation of GHG, below will be reviewed the onsite measurements. There are several approaches and strategies for measuring GHG emissions in reservoirs, which are following:

- **Floating chambers** - In this approach, the floating chamber(s) play a crucial role in collecting diffusive and potentially ebullition flux from the air-water interface. Typically, this accumulation process takes only a few minutes, and the gas collected within the enclosed chamber serves as a means to calibrate and measure the accumulated greenhouse gases (GHGs). However, if gas measuring devices can be brought to the field, it becomes feasible to continuously calibrate emissions. By employing the same methodology to calculate both types of emissions, the floating chamber that accumulates both diffusive and ebullition flux is considered a cost-effective and simpler option.
- **Funnel traps** - Gas bubbles or ebullition are systematically gathered and measured using an inverted funnel apparatus over a specific time frame. This collection period typically extends from several hours to multiple days, and in certain instances, the observation period may even extend beyond this timeframe to ensure comprehensive data acquisition.
- **Thin boundary layer method** - In this approach, diffusive flux is calculated by comparing observed dissolved GHG levels to a pre-calculated air-water gas exchange rate.

- **Eddy covariance technology -** In this approach, a tower is built on a little island inside the reservoir or within the reservoir itself, and GHG emissions are computed across time and space using mean air density and instantaneous variances in vertical wind speed and gas concentrations. It is used to compute the total diffusive and ebullient flow.
- **Bubble collector -** During these measurements, the gas collector is submerged in the water and positioned to capture the gases that naturally rise to the water's surface. The collector effectively captures and accumulates the gases, enabling subsequent analysis and measurement.

Several factors impact CO_2 and CH_4 emissions. It is quite tough to quantify each one and create a general pattern for all of them. To begin with, the emission of various GHGs begins with the construction of dams and the flooding of areas with varied land uses. Depending on the aerobic or anaerobic character of the process, CH_4, CO_2, and even N_2O are emitted from the breakdown of organic deposits. Microbial fermentation aids in the decomposition of organic carbon into CH_4.

5 G-RES tool

5.1 Introduction

The G-res tool seeks to promote better decision-making throughout the reservoir development process. It is a technology that tries to improve the capacity to explain possible consequences and identify projects that may require mitigation. To broaden its applicability, the G-res tool employs input data that do not necessitate onsite measurements for either pre- or post-impoundment conditions, instead, it employs parameters and data that project developers and environmental professionals should be aware of, such as when planning new reservoirs or assessing existing reservoirs. The G-res tool calculates the 'net GHG footprint' of reservoir construction. This method is based on the Intergovernmental Panel on Climate Change (IPCC, 2011) suggestion that net emissions be included when assessing the effect of reservoir systems. Consequently, an accurate picture of a reservoir's net impact should take into account the GHG balance of the pre-impounded region and subtract or add it to the GHG balance of the reservoir itself post-impoundment. Furthermore, the G-res tool examines the likelihood that certain reservoir emissions are the product of human activities unrelated to the reservoir's construction, which must be compensated for. The tool also incorporates indirect GHG emissions from reservoir infrastructure projects, such as manufacturing, transportation, and installation. This offers a more thorough estimate of the total emissions connected with a reservoir.

The calculation of net GHG footprint in the G-res tool is defined by the following equation:

$$\boldsymbol{Net\ GHG\ footprint} = [\boldsymbol{Post-impoundment\ GHG\ balance\ of\ the\ reservoir}] - [\boldsymbol{Pre-impoundment\ GHG\ balance\ of\ the\ reservoir\ area\ before\ its\ introduction}] + [\boldsymbol{GHG\ due\ to\ construction\ (Optional)}]$$

Equation 2 Net GHG Footprint

The reader can check by themself all the reservoirs which were used for simulation on the following G-RES tool website. The G-RES is asking the inputs to calculate net GHG emissions, if the project is new the inputs have to be written from scratch, in the case of this thesis, all 15 reservoirs inputs are given in the zip file, in this file reader can find 17 files since there are 2 scenarios for 2 reservoirs.

The reader can check the results from these inputs and see how the tool works.

5.2 Earth Engine

The G-res tool requires a lot of information on the reservoir's physical, geographical, climatic, soil, and land cover properties, as well as its catchment, to generate reliable estimates of net GHG emissions from reservoirs. This information, however, must be obtained from reliable and consistent sources. This procedure can be time-consuming and prone to errors or inconsistencies. To aid in this process, the G-res tool has additional capability that allows the user to extract the information in a globally consistent manner before manually entering the missing information into the G-res tool. This feature was created using Google's Earth Engine platform and is hence known as the Earth Engine (EE) functionality in the G-res tool. The information thus obtained can then be saved locally for future use. (The GHG Reservoir Tool (G-RES) Technical Document)

The reservoir specific information that can be derived directly from the EE functionality
are:

For the catchment:
• Catchment Area (in square kilometres)
• Catchment Annual Runoff (in millimeters per year)
• Population in the Catchment (person)
• Land Cover by Soil Type (in percentage)

For the reservoir:
• Dam Coordinates (in degrees, WGS84)
• Reservoir Area (in square kilometres)
• River length before impoundment (in meters)
• Maximum Depth (in meters)
• Mean Depth (in meters)
• Climate Zone
• Monthly Mean Temperature (in degree Celsius)
• Reservoir Mean Global Horizontal Radiance Annual (GHR) (in kilowatt hour per square meter per day)
• Reservoir Mean global horizontal Radiance (GHR) for the months of May to September (in kilowatt hour per square meter per day)
• Reservoir Mean Global Horizontal Radiance (GHR) for the months of November to
March (in kilowatt hour per square meter per day)
• Soil Carbon Content in the Impounded Area (kilogram of carbon per square meters)
• Annual Wind Speed (meters per second)
• Land Cover by Soil Type (in percentage)

For the buffer surrounding the reservoir:
• Soil Carbon Content Buffer (kilogram of carbon per square meters)
• Land Cover by Soil Type (in percentage) (The GHG Reservoir Tool (G-RES) Technical Document)

6 Site selection and methods

6.1 Study areas

The research regions are spread throughout three distinct places in Norway (North, Central, and Southern regions). The major rationale for choosing diverse sites is climate and elevation, since temperature and elevation may have a considerable influence on greenhouse gas (GHG) emissions in reservoirs. The schemes that were chosen are Rana, Orlka, and Sira-Kvina Figure 4. Also, the land cover in these three areas differs, resulting in varying GHG emissions. The biggest difficulty with the G-RES tool is that it does not allow you to select more than four climatic zones (Boreal, temperate, tropical, and subtropical), and several of the reservoir locations were in the arctic climate zone, which may have an impact on the tool's final results. The catchment land coverage information from Earth Engine, on the other hand, is accurate, and the outcomes are not impacted by incorrect information.

These reservoirs were essential for the overall functioning of the scheme and hydropower generation. To accurately calculate the greenhouse gas (GHG) emissions from these reservoirs, the research utilized the G-RES tool. This tool was employed to assess and quantify the environmental impact of the reservoirs in terms of GHG emissions.

Before conducting the GHG emissions calculation, it was necessary to examine the historical data of the reservoirs. This examination aimed to determine whether the reservoirs were formed naturally or if they were man-made structures. To achieve this, Norge i Bilder (Norge i Bilder, n.d.) was used, which provided precise satellite imagery and historical pictures of the reservoirs.

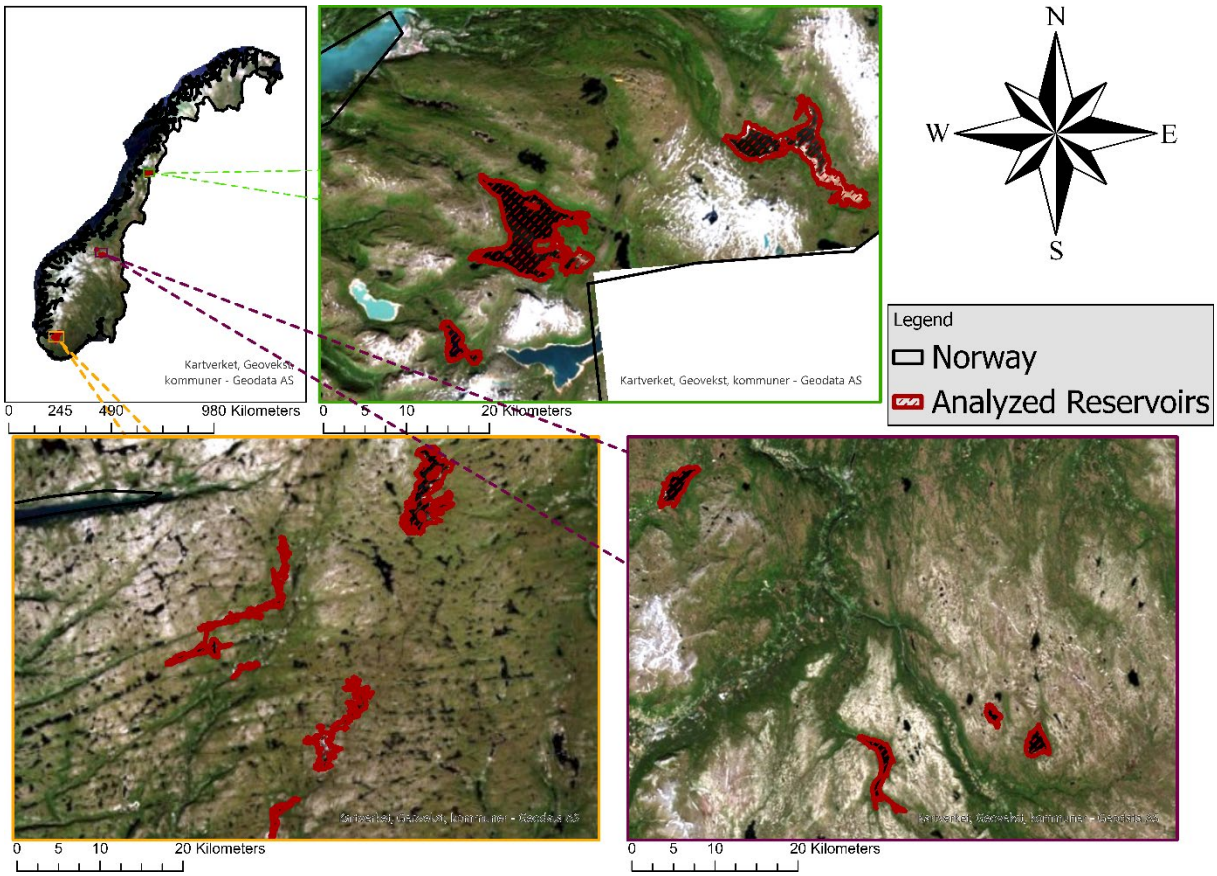

Figure 4 Analyzed Reservoirs

6.1.1 Selection of reservoirs

- Rana Scheme

The Rana hydropower project, located in Troms and Finnmark, Norway, is an ongoing development with a capacity of 500MW. It is situated on the Aker River/basin. The project was implemented as a single-step construction process. Development work commenced in 1967, and the plant began its commercial operations in 1976. Rana is a reservoir-based project, utilizing the gross head of 520m between Lake Akersvatnet and the power plant.

The power station is equipped with four Francis turbines, ensuring efficient power generation. The intake reservoir for the power plant is Lake Store Akersvatnet, while it also draws water from several other lakes, namely Kalvatn, Gressvatnet, Kjennsvatnet, and Durmlsvatn. Additionally, water from Lake Tverrvatnet is pumped up to Lake Akersvatnet to enhance the water supply.

Construction of the Rana power plant took place in multiple phases spanning from 1968 to 1980. This phased approach allowed for the systematic development and expansion of the project over time. (Statkraft/Rana, n.d.)

Figure 5 Rana Scheme

In the Rana scheme, there are the following main reservoirs:

- Kalvatn
- Akersvatn
- Kjensvatn

- Kalvatn

Kalvatn is one of the main reservoirs within the Rana scheme and serves It was commissioned in 1967, and has been instrumental in supplying water for hydroelectric power generation in the region.

The highest regulated water level is 564 (m.o.h), and the lowest regulated water level is 521 m.o.h. With a reservoir volume of 706 (m^3), Kalvatn has a significant capacity for storing water. This large volume allows for the accumulation and controlled release of water, ensuring a steady supply for the power station and other downstream needs.

The area of the reservoir is 28.61km^2. This extensive surface area provides ample space for water storage and serves as a crucial component of the Rana scheme's water management system.

In summary, Kalvatn plays a vital role as one of the main reservoirs in the Rana scheme, supplying water to the Rana power station. With its regulated water levels, substantial reservoir volume, and expansive area, Kalvatn contributes

significantly to hydroelectric power generation and the overall water resource management in the region.

- Akersvatn

Storakersvatnet, also known as Akersvatnet, is a lake located in the municipality of Rana in Nordland County, Norway. The lake lies about 15km south of the town of Mo i Rana and is less than 900 m from the border with Sweden. Originally, the lake covered an area was only 15.9 m^2, in 1968 the dam was constructed at its northern end to change it into a reservoir for the Rana power station. Because of this construction nowadays the area of the reservoir is 42.24 km^2.

The highest regulated water level is set at 523 m.o.h, and the lowest regulated water level is 480 m.o.h. The reservoir volume of Storakersvatnet is 1276 (m^3). This capacity allows for the storage of a significant amount of water, ensuring a stable and reliable water supply for the Rana power station.

Overall, Storakersvatnet serves as an important reservoir in the region, playing a crucial role in hydroelectric power generation and water resource management.

- Kjensvatn

Kjesvatn is another main reservoir in the Rana scheme's reservoirs which stores the water for the Rana powerhouse. Its commissioning took place in 1968, marking its significant contribution to hydroelectric power generation in the region.

The highest regulated water level is 527(m.o.h), and the lowest regulated water level is 520 m.o.h.

With a reservoir volume of 28 (m^3), Kjesvatn has a substantial capacity to store water. This volume allows for the accumulation and controlled release of water, ensuring a steady input to the Rana power station and other downstream needs.

The reservoir covers an area of approximately 4.99m^2. This area provides ample space for water storage and contributes to the efficient management of the Rana scheme's water resources.

In summary, Kjesvatn serves as a crucial reservoir in the Rana scheme, supplying water to the Rana power station. With its regulated water levels, significant reservoir volume, and expansive area, Kjesvatn plays a vital role in hydroelectric power generation and overall water resource management in the region.

Unfortunately for the Rana scheme, it wasn't possible to obtain the historical data, regarding before and after the reservoir construction, since there are no free sources, from where it is possible to check the data.

- Orkla Scheme

The Orkla Hydropower Scheme was meticulously planned and constructed during the 1970s and 1980s to harness hydropower. Spanning across the southern half of Trøndelag County and the northern section of Innlandet County, south of Trondheim, the scheme primarily revolves around the Orkla River. This significant river flows north from a small lake situated at an elevation of 1,058 meters above sea level in Trøndelag, ultimately reaching the sea at Orkanger, located at the southern end of Orkdalsfjorden. Orkanger is approximately 40 kilometres southwest of Trondheim, and Orkdalsfjorden is a branch of the larger Trondheimsfjorden.

With a length of 182 kilometres, the Orkla River encompasses a catchment area of 3,053 km^2 at its mouth. It is fed by around 25 tributaries of varying sizes. While there were no significant natural lakes along the main course of the river, resulting in occasional devastating floods, some of the tributaries possessed small natural lakes, two of which have now been controlled and transformed into reservoirs. Additionally, large artificial reservoirs were created in two additional streams.

The process of designing, obtaining permits, and constructing the artificial reservoirs and dams faced opposition and widespread demonstrations. However, the Orkla hydropower system ultimately came to fruition, comprising five power stations with a combined installed capacity of 320 MW and an annual generating capacity of 1,398 GWh. These power plants were commissioned and put into service between 1982 and 1985. The electricity generated by the scheme is transmitted to the regional 132 kV and 66 kV grids, enabling distribution throughout the area. (NVE - Norway's hydroelectric development, 2021)

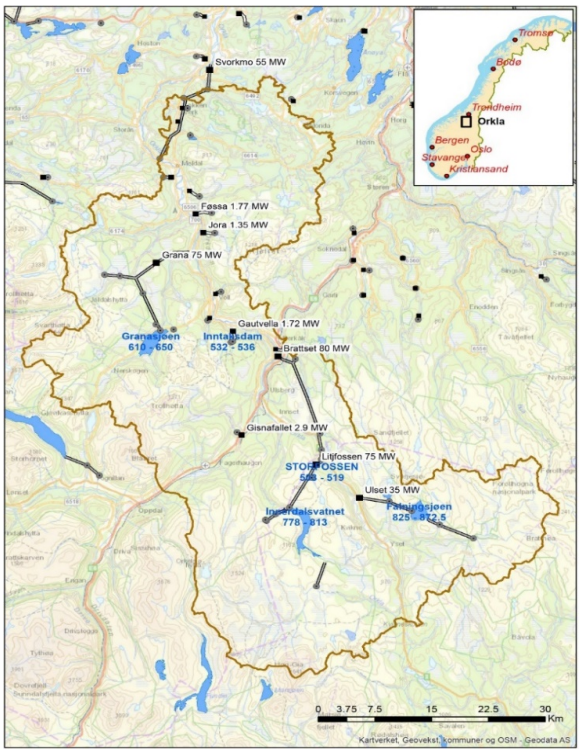

Figure 6 Orkla Scheme (NVE - Norway's hydroelectric development, 2021)

In the Orkla scheme, there are the following main reservoirs:

- Granasjøen
- Litjfossen (Innerdalsvatnet)
- Ulset, which further comprises two main reservoirs: Falningsjøen and Sverjesjøen.

By analyzing data, it was established that Granasjøen and Litjfossen were man-made reservoirs, while Falningsjøen and Sverjesjøen were natural bodies of water transformed into reservoirs.

This comprehensive assessment of the reservoirs' historical background allowed for a more accurate and informed calculation of GHG emissions using the G-RES tool, facilitating a better understanding of the environmental impact of the Orkla hydropower scheme.

- Granasjøen

Granasjøen, located in Nerskogen Rennebu, Trøndelag, is a man-made reservoir that serves as a regulating reservoir for the Grana power plant in Grindal. The reservoir has a head of 462 meters, and the water is transformed into the power plant through a 10-kilometre-long tunnel. The dam is a large rock fill type, with the county road running along its crest.

The highest regulated water level is 650m.o.h, and the lowest regulated water level is 610m.o.h., however, the dam's peak height is 655.5 m.o.h. The reservoir area is 6.61 km² and the volume is 144 m^3.

The reservoir is constructed on loose material and is partially covered with grass. It spans a length of 1,080 meters, stands 55 meters high, and features an eight-meter-wide dam crown. On the eastern side, a closed floodway system has been meticulously engineered, consisting of a concrete overflow dam, collection channel, shaft, and tunnel. To provide an additional layer of security, a side dam has been established in a separate channel. This secondary dam serves as a reserve floodway in the event of exceptionally high reservoir water levels, a feature that is relatively rare in the Norwegian context. (NVE - Granasjøen, n.d.)

The decision to dam Granasjøen in 1978 caused significant protests, both before and after the decision was made, with active demonstrations taking place in the Granada Valley. The proposal to dam Innerdalen and Granadalen faced political opposition from local communities, nature conservation groups, and the Ministry of Agriculture. In addition to natural considerations, the agricultural importance of the valleys played a significant role in the opposition. (Granasjøen, n.d.)

Please refer to the Figure A1 for an overview of the reservoir.

- Litjfossen (Innerdalsvatnet)

Litjfossen - Innerdalsvatnet is a reservoir located in Tynset municipality, Innlandet. Situated on the west side of the valley in Kvikne, it is formed by the Inna River, a tributary of the Orklavassdraget. In 1982, the water level was regulated, raising it by 35 meters. The lake serves as a reservoir for the Litjfossen power plant, which has a head of 285 meters, and the Brattset power plant near Berkåk. Water is transported to the power plants through a seven-kilometre-long tunnel. (Innerdalsvatnen , Wikipedia , n.d.)

The dam at Innerdalsvatnet is of the rock-fill type and features a sealing core made of moraine masses. The reservoir volume is 153 mill m^3, the highest water level is 813 m.o.h and a lowest water level is 778 m.o.h. The area is 6.53 m^2. The reservoir stores water from various sources, including Orkla at Øvre Dølvad, Næringa, Kviknebekken, Storbekken, and Gardåa, which is transferred through a tunnel. The entire lake was created by the process of damming and reaches its highest water level. (NVE -Litjjfossen , n.d.) In order to make this reservoir 6,500 acres of land were dammed. (Innerdalsvatnen , Wikipedia , n.d.)

Please refer to the Figure A2 for an overview of the reservoir.

- Sverjesjøen

Sverjesjøen, situated in Tynset Municipality, Innlandet, is a natural lake that belongs to the river Sverja's catchment area, a tributary of the Orkla River. This pristine lake serves as a regulated reservoir for the Ulset power plant.

The highest reaching 872.5 m.o.h. and the lowest regulated water level is 867.7 m.o.h. The area of lake 1.64m^2.

Please refer to the Figure A3 for an overview of the reservoir.

- Falningsjøen

Falningsjøen, located in Tynset Municipality, Innlandet County, is a natural reservoir and not man-made. This characteristic implies potentially lower environmental issues, such as greenhouse gas emissions, compared to artificial reservoirs. The lake is situated approximately 4.5 kilometres northeast of the village of Yset and serves as the origin of the Ya River. The north end of the lake marks the boundary of Forollhogna National Park.

The reservoir volume is 125 mill m^3 , the highest water level is 813 m.o.h and the lowest water level is 778 m.o.h. The area is 4.23m^2.

At the south end of the lake, a dam is present to regulate the water for hydroelectric power generation. This dam enables the control and management of water flow for harnessing the potential of hydropower. (NVE Atlas, n.d.)

Please refer to Figure A4 for an overviwe of the reservoir

- Sira-Kvina Scheme

The Sira-Kvina watercourse system utilizes water resources from Aust-Agder, Vest-Agder, and Rogaland counties. With a catchment area of approximately 2,700 square kilometers, it plays a significant role in Norway's hydropower generation. The power stations within the watercourse collectively contribute around 5% of the country's total electricity output. Sira-Kvina Kraftselskap, established in 1963, was formed with the purpose of harnessing the power potential of the Sira and Kvina watercourses. Currently, Skagerak Kraft owns a 14.6% stake in Sira-Kvina Kraftselskap, thereby controlling a portion of the power production.

In the system, the Kvina watercourse is redirected into the Sira watercourse to optimize the combined hydraulic head, culminating at the Tonstad Power Plant. Tonstad Power Plant is one of Norway's largest power plants, and from there, the water flows to na-Sira, where it eventually meets the sea. To facilitate this process, a network of seven power stations, along with tunnel systems and regulating reservoirs, has been constructed. Notably, Svartevann and Roskrepp stand out as well-managed multi-year reservoirs in Norway.

Environmental considerations have been voluntarily incorporated into both segments of the watercourse system. On the Kvina side, a minimum flow requirement has been implemented, and specific stone deposits have been placed to facilitate the migration of salmon in certain areas. As part of the dam repair project, an artificial marsh area has been constructed at the base of the Svartevann dam, serving as a crucial environmental mitigation measure in connection with the quarrying activities. These proactive measures demonstrate

the commitment to preserving the ecological balance while harnessing the hydropower potential of the Sira-Kvina watercourse system. (Sira Kvina Scheme, Skagerakkraft , n.d.)

Sira-Kvina hydropower scheme, have 7 reservoirs. GHG results are calculated from all of these 7 reservoirs in this thesis.

The following reservoirs are in Sira-Kvina:

- Flothølen (Dam Kilen)
- Valevatn
- Gravatn
- Kverevatn (Roskeppfjord)
- Øysteinevja
- Kvifjorden (Nesjen)
- Homstølvatnet

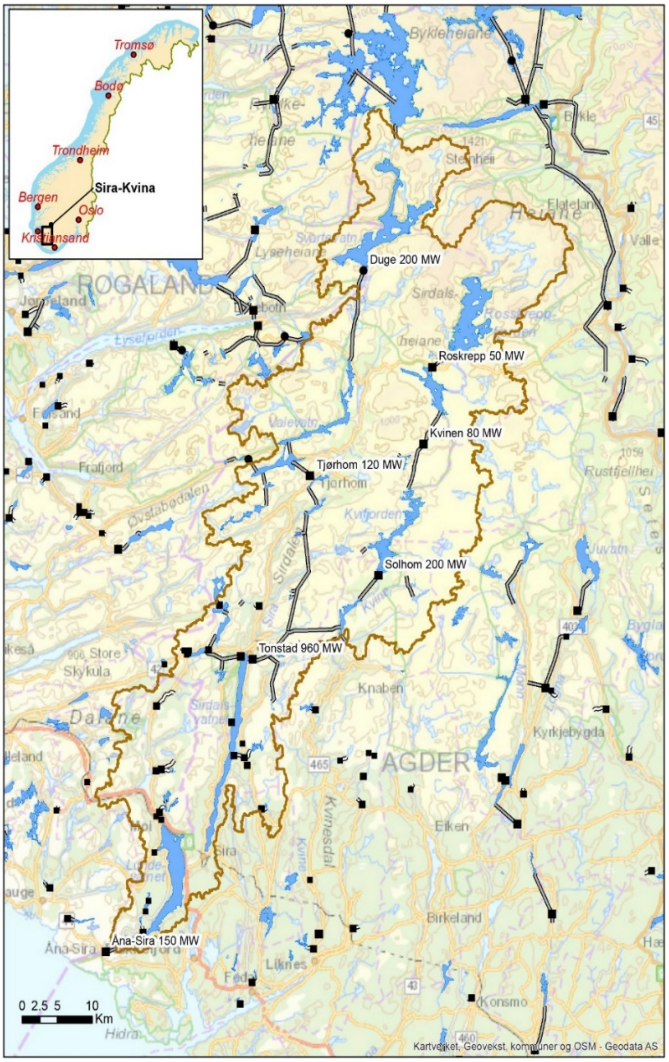

Figure 7 Sira-Kvina Scheme (NVE - Norway's hydroelectric development, 2021)

- Flothølen (Dam Kilen)

Flothølen, also known as Dam Kilen, is an artificial lake that was created in 1970 as part of the Sira-Kvina scheme by constructing a concrete dam across the natural course of the River Sira. It is situated in the Sirdal municipality of Vest-Agder. Along with Valevatn and Gravatn, Flothølen forms a continuous water reservoir.

The water stored in this reservoir serves as a vital resource for the Tjørhom Power Plant, contributing to the generation of hydropower. Dam Kilen, being a concrete dam, ensures the regulation of water levels within the reservoir. The highest water level in the reservoir is 660 m.o.h, while the lowest regulated water level is 628 m.o.h.

With an area spanning 2.04 m^2, the Flothølen reservoir has a significant capacity, holding approximately 317.9 mill m^3 of water. Its strategic location and efficient management make it a crucial component of the Sira-Kvina scheme, supporting sustainable energy production in the region. (Nve Atlas - Flothølen (Dam Kilen) , n.d.)

Please refer to the Figure A5 for an overviwe of the reservoir

- Valevatn

Valevatn, situated in the Sirdal municipality of Agder, is both a lake and a reservoir. It extends from Lortabu in the west to Degdammen in the east, serving as a continuation of Hunnedalen. This lake holds great significance as a central component of the Sira-Kvina development.Valevatn receives water through its natural inlets, primarily from the river Storå, which carries water from Degevatn and Sandvassåna, as well as from the river Bjønnåna. Previously, its natural outlet was located west of the river Deg, which flowed into Lake Fidjelandsvatnet.

The regulation of Valevatn was undertaken as part of the second phase of the Sira-Kvina waterways development, commencing in 1968. The objective was to establish a continuous water reservoir stretching from Sira's natural outlet in Ånesvatnet in the north, through Valevatn, and reaching Gravatn in the south. To accomplish this, two large rock-filled dams, Degdammen and its northern counterpart, along with four smaller secondary dams, were constructed. This resulted in the flooding of extensive outland areas and flood plains, particularly in the northeastern section, as well as the displacement of the homestead Valevatn.

In the northern region, a concrete arch dam named Dam-Kilen was erected to divert the course of the river Sira away from Sirekrok and Ortevatnet. Together with Dam-Farskard and Dam-Flåthølmyra, it formed a sizable reservoir known as Flothølen, which encompassed Ånesvatnet, Svartevatnet, and the surrounding areas that were once occupied by the banks of the river Sira. To connect Flothølen and Valevatn, a smaller channel was excavated.

At Gravatn in the south, the stone fill dam Dam-Gravatn was constructed along with a canal connecting Valevatn and Gravatn. Furthermore, the two lakes were interconnected by means of a transfer tunnel beneath the Gravassryggen. (Sira-Kvina, n.d.)

The highest regulated water level in the Valevatn is 660 m.o.h and the lowest regulated level is 580 m.o.h. With an expansive area of 7.08m^2 and a volume of approximately 267.8mill m^3, Valevatn plays a crucial role in the Sira-Kvina development, ensuring the effective utilization of water resources for energy production. (Nve Atlas , n.d.)

Please refer to the Figure A6 for an overviwe of the reservoir

- Gravatn

Gravatnet is a lake in the municipality of Sirdal in Agder county, Norway. The 5.33m^2 lake is located about 9 kilometres north of the small village of Lunde. The lake lies immediately south of Lake Valevatn, which flows out into Gravatnet. The water in Gravatnet is dammed by a dam on the south side. The highest regulated water level is 660 m.o.h and the lowest regulated water level is 625 m.o.h. The volume is 340 Mill. m³ and it was built in 1970. (NVE Atlas - Gravatn, n.d.)

Please refer to the Figure A7 for an overviwe of the reservoir

- Kverevatn (Roskeppfjord)

The reservoir is dammed back by three dams erected between 1966 and 1968. What makes this dam unique is that Sira-Kvina was not the first to dam the Roskreppfjorden. Traelandsfoss, a Kvinesdal firm, erected a modest dam in the 1920s that blocked up the whole fjord by roughly 2.5 meters. The highest regulated water level is 929 m.o.h and the lowest regulated water level is 890 m.o.h. The area of the reservoir is 29.75 km^2 and the volume 695 mill. m^3.

Please refer to the Figure A8 for an overviwe of the reservoir

- Øyarvatn

Øyarvatnet is a lake in Sirdal and Valle municipalities in Agder . It is part of the Kvinen water pipeline and is regulated as a reservoir for the Kvinen power plant. The highest regulated water level is 837 m.o.h. and the lowest regulated water level is 820 m.o.h. The area of reservoir is 8.08 km² and the volume 104 Mill. m³. (Sira Kvina Oyarvatn, n.d.) Please refer to the Figure A9 for an overviwe of the reservoir

- Kvifjorden (Nesjen)

The reservoir known as Nesjen/Kvifjorden, or simply Nesjen, is formed by damming a series of smaller lakes, including Nesjen, Badstogflona, Kvifjorden, and Kvivatnet. Among these lakes, Kvifjorden is the largest. The damming process involved the construction of three substantial rock-filled dams,

strategically positioned near the mouth of Nesjen, the southernmost lake in the chain. It was built in 1963.

The area of the reservoir is 15.36 km². The highest regulated water level is

715 m.o.h and the lowest regulated water level is 677 m.o.h. The volume of the reservoir is 275 Mill. m³

The reservoir's geographical features also contribute to its significance. Along its eastern shore, it shares proximity with the Setesdal Vesthei - Ryfylkeheiane Landscape Conservation Area, emphasizing the importance of preserving the natural environment and promoting ecological balance in the region. (Nve Atlas Nesjen, n.d.)

Please refer to the Figure A10 for an overviwe of the reservoir

- Homstølvatnet

Homstølvatnet is a lake in the far western part of the municipality of Froland in Agder County. It is located about 12 kilometres east of the village of Byglandsfjord (in Bygland municipality) and about 16 kilometres northwest of the village of Mykland in Froland. The lake was expanded in 1963 when a dam was built for the purposes of hydroelectric power generation. The dam made the lake larger so that it now includes the formerly separate lake Homstølvatnet as one large lake. The lake is now

2.89 km² large and it holds about 55 Mill. m³ as a reservoir for the power station. The highest regulated water level is 497.6 m.o.h and the lowest regulated water level is 471 m.o.h. (NVE atlas Homstvolvatnet, n.d.)

Please refer to the Figure A11 for an overviwe of the reservoir

7 Results

7.1 Results from G-RES

The results of this thesis on CO_2 emissions from hydropower operations will be presented in the following manner. As all the outcomes in this study are derived from the G-RES tool, the graphs illustrating the results will be included in the appendices section. Each graph will be linked to its respective reservoir. Initially, a comprehensive report description, along with all the figures, will be provided exclusively for Kalvatn. Subsequently, for each additional reservoir, the corresponding figure can be found in the appendices and should be cross-referenced.

As already mentioned before, the G-RES tool was used to calculate GHG emissions from reservoirs in Norway. Below will be presented results from this model.

7.1.1 Results from Rana Scheme

The results from Rana Scheme are following:

- Kalvatn

As previously mentioned, an analysis of reservoir volume was conducted, and the resulting simulation outcomes are depicted in the figure. The Figure 8 provides valuable insights, indicating that as the volume increases, emissions result in a noticeable decrease. In order to simulate GHG emissions from the reservoir, the tool utilized a volume that had been augmented by 50% based on the selected depth value. For simulation reservoir volume is 1.059 m which has 1.2 (gCO_2e/kWh) intensity.

Volume		Emissions intensity (gCO2e/kWh)
Initial Volume	0.706	1.3
Volume +10%	0.7766	1.3
Volume +15%	0.812	1.2
Volume +20%	0.8472	1.2
Volume +50%	1.059	1.2
Volume +100%	1.412	1.1

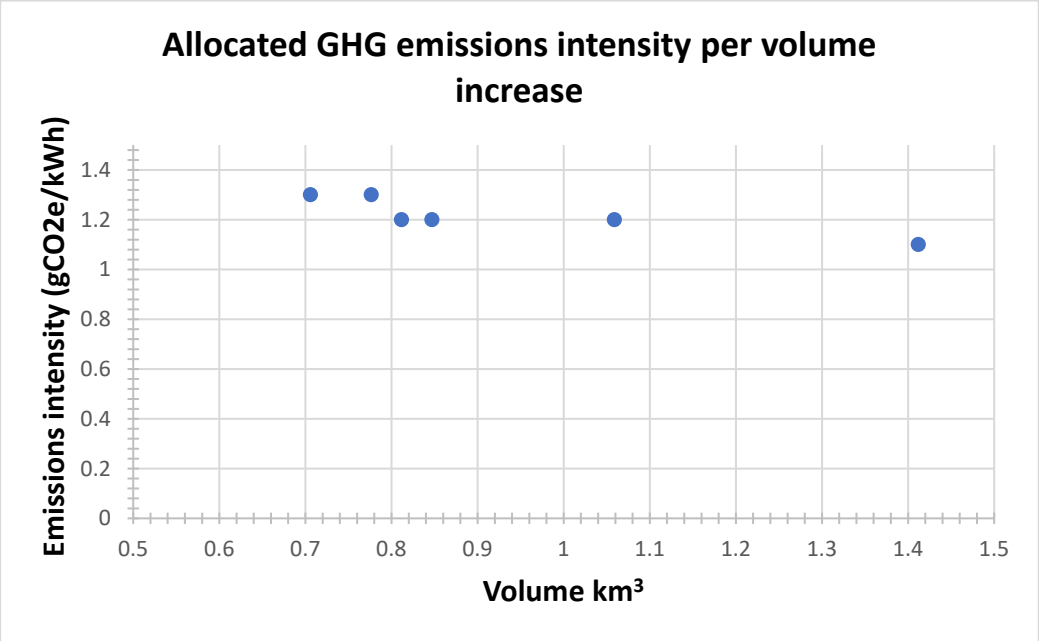

Figure 8 Kalvatn Reservoir volume vs emissions intensity

From the tool, results are following:

Total foot print:

Table 1 presents comprehensive data regarding the total footprint and net greenhouse gas (GHG) emissions from the reservoir. Before the dam construction, the location served as a carbon sink, effectively storing a carbon.

The data reveals that the carbon storage in this pre-dam state amounted to 127,632 tCO_2e.

Table 1 Total footprint - Kalvatn

Name of Reservoir	Total Footprint					
		Post-Impoundment	Pre-Impoundment	Unrelated Anthropogenic Sources	Construcition (Reservoir)	Net GHG Footprint
Kalvatn	Emission Rate (gCO2e/m2/yr)	44	-45	0	0	89.00
	Emission Rate (tCO2e/m2/yr)	1266	-1276	0	0	2542.00
	Total Lifetime Emissions (tC02e)	126623	-127632	0	0	254255.00

However, with the construction of the dam and the subsequent increase in the water level, there was a notable shift from a carbon sink state to a carbon emitter state. The emissions resulting from this change totaled 126,623 tCO_2e.

To calculate the net GHG emissions from the reservoir, Equation 2 was applied. This calculation yielded a total lifetime GHG footprint of 254,255 tCO_2e. Consequently, the annual emission rate was determined to be 2,542 $tCO_2e/m^2/yr$.

It is worth noting that the data indicates an UAS (Unrelated Anthropogenic Sources) value of 0 for this reservoir. This suggests that there are no significant GHG emissions from unrelated human activities in relation to the reservoir.

The findings presented in Table 1 provide important insights into the carbon dynamics of the reservoir. The shift from a carbon sink to a carbon emitter state due to dam construction resulted in substantial emissions. The calculated net GHG footprint further highlights the long-term cumulative emissions associated with the reservoir's operation.

Table 2 represents CO_2 and CH_4 distribution yearly and m^2/yr bases. From a total of 2542 (tCO_2e), CO_2 is 2198 (tCO_2e) and CH_4 is 345 (tCO_2e). In meter per square(m^2) we have following distribution CO_2 = 77 ($gCO_2e/m^2/yr$) and CH_4 =13 ($gCO_2e/m^2/yr$). The increase in CH_4 emissions can be generated by the decomposition of organic material within the flooded area. This can be caused by the forests in the reservoir, accounting for 31.4% (8.9 km^2) of the reservoir area, which contributes to CH_4 emissions.

These findings highlight the importance of considering specific characteristics of reservoir areas, like land use coverage when assessing the GHG footprint.

Table 2 Reservoir emissions by pathway - Kalvatn

Name of Reservoir	Reservoir Emissions by Pathway				
		Post-Impoundment	Pre-Impoundment	Unrelated Anthropogenic Sources	Net GHG Footprint
Kalvatn	**Emission Rate (tCO2e/yr)**	1266	-1276	0	2542
	of which CO2	880	-1318	0	2198
	of which CH4	386	41	0	345
	Emission Rate (gCO2e/m2/yr)	44	-45	0	89
	of which CO2	31	-46	0	77
	of which CH4	13	0	0	13

Power density for this reservoir is 17.5W/m^2, since the number is not low it means that this project doesn't require the larger areas and larger volumes to generate the energy, which also means that less area is necessary to be flooded. This number is higher than the threshold given by the EU Taxonomy for Sustainable Finance (EU Technical Expert Group, 2020), which helps stakeholders and HPP owners to certify their projects as green hydropower, to be defined, one of the requirements to have a power density higher than 5W/m^2, we can see from this reservoir that, it is higher so it has the possibility to have green energy certificate. Allocated GHG emissions intensity is 1.2 gCO_2e/kWh which is low for Norway. For Norway the national number is following: 3.33 gCO_2e/kWh. (Modahl, 2019)

Figure 9 represents the graphs regarding Kalvatn vs worldwide data. As we can see CH_4 diffusive is 13 ($gCO_2e/m^2/yr$) which is lower than the mean, however, CH_4 bubbling is almost the same as worldwide. As already mentioned, the G-RES tool didn't calculate thermocline depth and that's why degassing is zero. CO_2 is lower than the mean which is 31 ($gCO_2e/m^2/yr$). All these give us information that even though we have emissions from Kalvatn, this reservoir has lower emissions than other reservoirs worldwide.

The Figure 10 represents the annual net GHG emissions from Kalvatn. The first year there were significant emissions of 328 ($gCO_2e/m^2/yr$), and in the second year 264 ($gCO_2e/m^2/yr$), and it has been decreasing since then. The dam was built in 1967, and 56 years have been gone since this, from the G-RES forecasting we can read that in 2023 emission is 56($gCO_2e/m^2/yr$), which again is very low after the first year of the reservoir. After 100 years, the emissions will be 47 ($gCO_2e/m^2/yr$).

The Figure 11 illustrates that the Kalvatn reservoir exhibits relatively high CO_2 diffusive emissions, lower CH_4 diffusive emissions, and very low CH_4 bubbling emissions. It is noteworthy that these emissions have been decreasing annually. In the first year of reservoir operation, there was the following information: CO_2 diffusive = 240.371 $gCO_2e/m^2/yr$. CH_4 diffusive = 42.668 $gCO_2e/m^2/yr$ and CH_4 bubbling 0.577 $gCO_2e/m^2/yr$. According to the figure, all of these emissions are

projected to reach zero after 100 years. This raises questions regarding the disparities between the previous and current charts and the potential occurrence of other emissions.

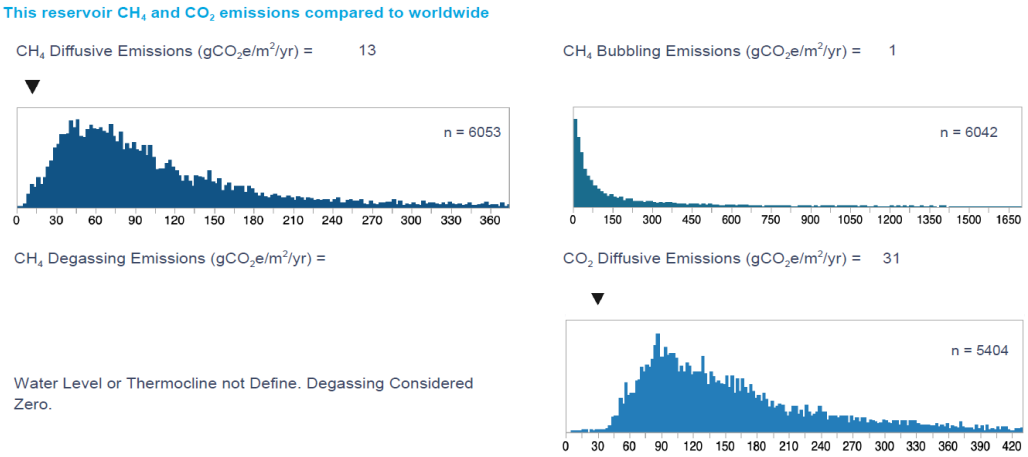

Figure 9 Emissions from Kalvatn compared to worldwide

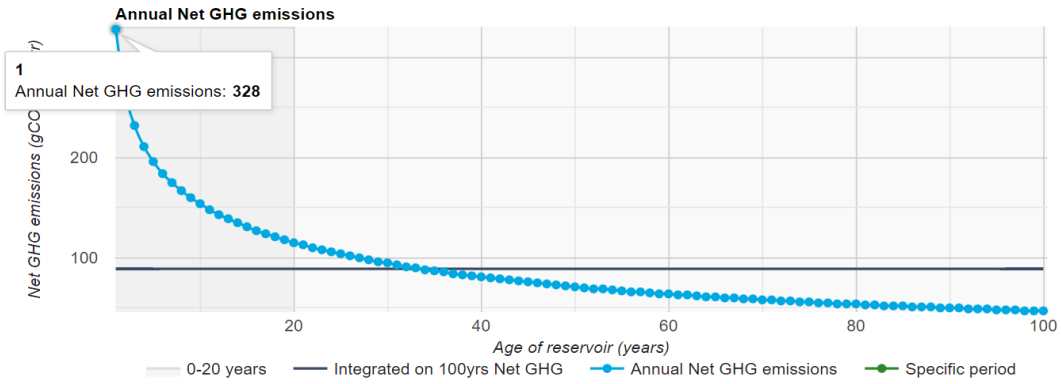

Figure 10 Kalvatn - Annual GHG emissions

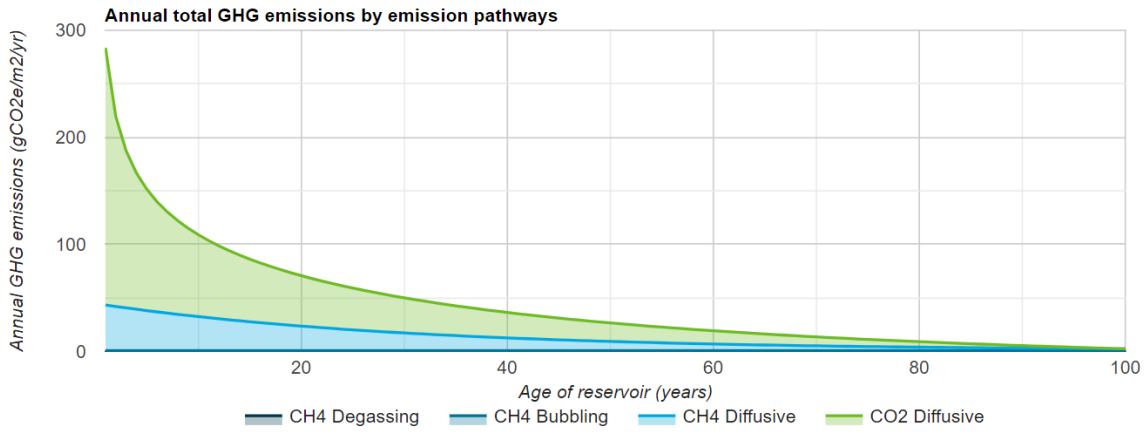

Figure 11 Kalvatn - Annual total GHG emissions by emission pathways

- Akersvatn

Figure 12 represents the reservoir volume analsys results.

Volume		Emissions intensity (gCO2e/kWh)
Initial Volume	1.28	0.8
Volume +10%	1.40	0.8
Volume +15%	1.47	0.7
Volume +20%	1.53	0.7
Volume +50%	1.91	0.7
Volume +100%	2.55	0.5

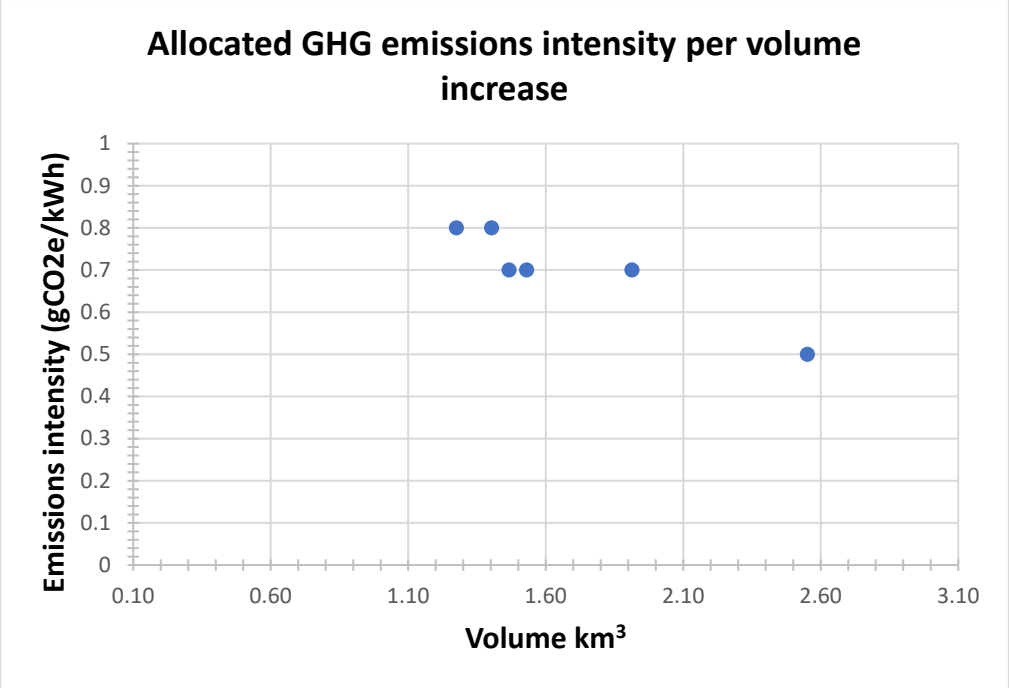

Figure 12 Akersvant Reservoir volume vs emission intensity

From the tool, we have the following results.

Total foot print:

Table 3 Akersvatn total footprint

Total Footprint					
	Post Impoundment	Pre Impoundment	Unrelated Anthropogenic Sources	Constructio n (Reservoir)	Net GHG Footprint
Emission Rate (gCO2e/m2/yr)	23	-11	0	0	34.00
Emission Rate (tCO2e/m2/yr)	961	-483	0	0	1444.00
Total Lifetime Emissions (tC02e)	96127	-48257	0	0	144384.00

Table 3 provides data about the total footprint in the reservoir. We have the same case here as with the previous reservoir. We can see the carbon storage of the location prior to dam construction, indicating a carbon sink state with 48257 tCO_2e stored. However, the construction of the dam resulted in an increased water level, leading to a shift from a carbon sink to a carbon emitter state, with emissions totaling 96127 tCO_2e. Equation 2 Net GHG Footprint highlights the calculation of the Net GHG footprint: Post-impoundment -Pre-impoundment emissions, which resulted in total lifetime emission GHG footprint of 144384 tCO_2e. UAS is 0 from this reservoir.

Table 4 Akersvatn Reservoir emissions by pathway

Name of Reservoir	Reservoir Emissions by Pathway				
		Post-Impoundment	Pre-Impoundment	Unrelated Anthropogenic Sources	Net GHG Footprint
Akersvatn	**Emission Rate (tCO2e/yr)**	961	-483	0	1444
	of which CO2	520	-592	0	1112
	of which CH4	441	110	0	331
	Emission Rate (gCO2e/m2/yr)	23	-11	0	34
	of which CO2	12	-14	0	26
	of which CH4	10	3	0	7

Table 4 represents CO_2 and CH_4 distribution yearly and m^2/y bases. From a total of 1444 (tCO_2e/yr), CO_2 is 1112 (tCO_2e/yr), and CH_4 is 331 (tCO_2e/yr). In meter per square(m^2) we have following distribution CO_2 = 26 ($gCO_2e/m^2/yr$) and CH_4 =7 ($gCO_2/m^2/yr$). In Akersvatn there are no big CH_4 emissions the main reason for this can be the less land coverage in the reservoir area.

Power density for this reservoir is $11.8W/m^2$.Allocated GHG emissions intensity is 0.7 gCO_2e/kWh which is low for Norway. This number is higher than the threshold given by the EU Taxonomy for Sustainable Finance (EU Technical Expert Group, 2020) , which helps stakeholders and HPP owners to certify their projects as green hydropower, to be defined, one of the requirements to have a power density higher than 5, we can see from this reservoir that, it is higher so it has the possibility to have green energy certificate. For Norway the national number is following: 3.33 gCO_2e/kWh. This reservoir has the same characteristics as the previous one.

Figure B1 represents the graphs regarding Akersvatn vs worldwide data. As we can see CH_4 diffusive is 10 ($gCO_2e/m^2/yr$) which is lower than the mean, however, CH_4 bubbling is almost the same as worldwide and it is 0. As already mentioned, the G-RES tool didn't calculate thermocline depth and that's why degassing is zero. CO_2 is a lot of lower than the mean which is 12 ($gCO_2e/m^2/yr$). All these give us information that even though we have emissions from Akersvatn, this reservoir has lower emissions than other reservoirs worldwide. Also, Akersvatn has lower emission then Kalvatn.

Figure B2 represents the annual net GHG emissions from Akersvatn. The first year there were significant emissions of 138 ($gCO_2e/m^2/yr$), and in the second year 113 ($gCO_2e/m^2/yr$), and it has been decreasing since then. The dam was built in 1968, and 55 years have been gone since this, from the G-RES forecasting we can read that in 2023 emission is 23($gCO_2e/m^2/yr$), which again is very low after the first year of the reservoir. After 100 years, the emissions will be 13 ($gCO_2e/m^2/yr$). From this figure we can also read that the Akersvatn reservoir shows relatively high CO_2 diffusive emissions, lower CH_4 diffusive emissions, and very low CH_4 bubbling emissions. It is noteworthy that these emissions have been decreasing annually. In the first year of reservoir operation, there was the following information: CO_2 diffusive = 93.55 $gCO_2e/m^2/yr$. CH_4 diffusive = 33.16 $gCO_2e/m^2/yr$ and CH_4 bubbling 0.055 $gCO_2e/m^2/yr$. According to the figure, all of these emissions are projected to reach zero after 100 years. CH_4 bubbling will maintin its value at the level of 0.055 $gCO_2e/m^2/yr$.

- Kjensvatn

Figure 13 represents the reservoir volume analsys results.

Volume		Emissions intensity (gCO2e/kWh)
Initial Volume	0.028	0.1
Volume +10%	0.0308	0.1
Volume +15%	0.032	0.1
Volume +20%	0.0336	0.1
Volume +50%	0.042	0.1
Volume +100%	0.056	0.1

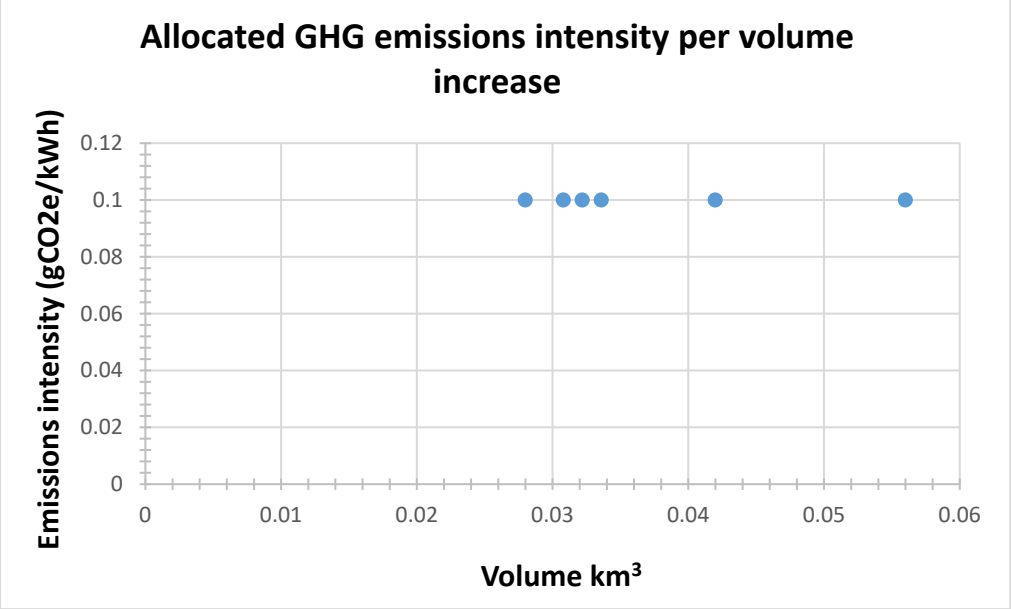

Figure 13 Kjensatn Reservoir volume vs Emission intensity

From the tool, results are following:

Total footprint:

Table 5 Kjensvatn total footprint

Name of Reservoir	Total Footprint					
		Post Impoundment	Pre Impoundment	Unrelated Anthropogenic Sources	Construcition (Reservoir)	Net GHG Footprint
Kjensvatn	Emission Rate (gCO2e/m2/yr)	36	5	0	0	31.00
	Emission Rate (tCO2e/m2/yr)	181	27	6	0	148.00
	Total Lifetime Emissions (tC02e)	18105	2669	616	0	14820.00

Table 5, shows the emissions data associated with the Kjesvatn reservoir. It is important to note that, unlike previously constructed reservoirs, the Kjesvatn reservoir has undergone expansion rather than being built from scratch. Consequently, the emission results differ significantly from those observed in prior reservoir projects.

Before the impoundment phase, the Kjesvatn lake had 27 ($tCO_2e/m^2/yr$). However, following the expansion, the emission value experienced a substantial increase, reaching 181 ($tCO_2e/m^2/yr$), which is nearly seven times higher than the pre-expansion level.

Furthermore, it is pertinent to acknowledge that Kjesvatn is also influenced by unrelated anthropogenic sources. This indicates that human activities in the vicinity contribute to the overall greenhouse gas emissions in the region. UAS is 6 ($tCO_2e/m^2/yr$). These unrelated anthropogenic sources emphasize the significant role of human interaction in shaping the emission dynamics of the Kjesvatn reservoir.

Table 6 presents the annual distribution of CO_2 and CH_4 emissions in the Kjensvatn reservoir. The total emission is 148 (tCO_2e/yr), from where CO_2 is 17 (tCO_2e/yr) and CH_4 is 131 (tCO_2e/yr), on the per square meter m^2 - there is the following distribution of CO_2 = 2 ($gCO_2e/m^2/yr$) and CH_4 = 27 ($gCO_2e/m^2/yr$).

Interestingly, Kjensvatn demonstrates a notable contrast in CO_2 and CH_4 emissions. While the reservoir shows relatively low CO_2 emissions compared to previous cases, the levels of CH_4 emissions are notably higher. This observation indicates a shift in the emissions profile after the expansion of the reservoir.

Prior to the expansion, the lake had the capacity to sequester or absorb CO_2 emissions, resulting in a sinking effect. However, it emitted CH_4 emissions. Following the expansion, both CO_2 and CH_4 emissions increased, with CH_4 showing a more significant rise. This finding highlights the importance of considering the expanded reservoir's impact on greenhouse gas emissions, particularly the dominance of CH_4 despite the relatively low coverage of forest and grass in the reservoir land area (5% for both).

Table 6 Kjensvatn emissions by pathway

Name of Reservoir	Reservoir Emissions by Pathway				
		Post-Impoundment	Pre-Impoundment	Unrelated Anthropogenic Sources	Net GHG Footprint
Kjensvatn	Emission Rate (tCO2e/yr)	181	27	6	148
	of which CO2	10	-7	0	17
	of which CH4	171	34	6	131
	Emission Rate (gCO2e/m2/yr)	36	5	0	31
	of which CO2	2	0	0	2
	of which CH4	34	7	0	27

The power density of the studied reservoir is calculated to be 100.2 W/m^2. This value, being the highest among the cases examined, indicates that this particular project shows exceptional efficiency in energy generation, requiring smaller areas and volumes. This number is the highest from the studied reservoirs in this thesis, which is also higher than the threshold given by the EU Taxonomy for Sustainable Finance (EU Technical Expert Group, 2020), which helps stakeholders and HPP owners to certify their projects as green hydropower, to be defined, one of the requirements to have a power density higher than 5, we can see from this reservoir that, it is higher so it has the possibility to have green energy certificate. Consequently, the need for larger-scale flooding is minimized, presenting an ideal scenario for the project's implementation.

Furthermore, the allocated greenhouse gas (GHG) emissions intensity for this reservoir is determined to be 0.1 gCO_2e/kWh. This value is significantly lower compared to the national emissions intensity for Norway, which stands at 3.33 gCO_2e/kWh. The remarkably low emissions intensity of the studied reservoir further highlights its environmental superiority in comparison to previous reservoir projects in the Rana region.

The findings from this analysis underscore the favourable attributes of the reservoir in terms of power density and GHG emissions intensity. The high-power density signifies its ability to generate a substantial amount of energy while utilizing a smaller area, leading to minimal environmental impact. Moreover, the exceptionally low emissions intensity signifies the reservoir's contribution to reducing carbon emissions, outperforming previous projects in the Rana area.

Figure B3 presents graphical representations comparing the emissions data of the Kjensvatn reservoir with worldwide reservoir data. The analysis focuses on two key metrics: CH_4 diffusive, CH_4 bubbling, and CO_2 emissions.

In terms of CH_4 diffusive is 31 $gCO_2e/m^2/yr$, which is lower than the mean value observed worldwide. This indicates that the diffusive emissions of CH_4 from Kjensvatn are relatively lower compared to other reservoirs on a global scale.

However, CH_4 bubbling in Kjensvatn is nearly equivalent to the worldwide average, CH_4 = 3 $gCO_2e/m^2/yr$.

Additionally, it is important to note that the G-RES tool used for calculations did not consider the thermocline depth, resulting in a degassing value of zero for Kjensvatn. Regarding CO_2 emissions, the Kjensvatn reservoir shows significantly lower emissions compared to the global mean, CO_2 = 2 $gCO_2e/m^2/yr$. This indicates that CO_2 emissions from Kjensvatn are notably reduced in comparison to other reservoirs worldwide.

These findings provide valuable insights into the emissions profile of the Kjensvatn reservoir. Despite emitting some level of greenhouse gases, this reservoir demonstrates lower overall emissions compared to other reservoirs on a global scale. Furthermore, when compared specifically to Kalvatn and Akersvatn reservoirs, Kjensvatn exhibits lower emissions. These observations contribute to the understanding that Kjensvatn represents a reservoir with relatively lower emissions, making it a favorable option in terms of environmental impact compared to other reservoirs worldwide, as well as specific reservoirs in the same region.

Figure B4 illustrates the annual net greenhouse gas (GHG) emissions from the Kjensvatn reservoir. The analysis reveals the emissions trends over time, beginning from the year the reservoir was expanded in 1968 up until the present year of analysis, as well as providing future emission projections.

In the initial year following the expansion, the reservoir exhibited significant emissions, reaching 115 $gCO_2e/m^2/yr$. In the subsequent year, the emissions slightly decreased to 108 $gCO_2e/m^2/yr$. Since then, the emissions have demonstrated a decreasing trend. Using the G-RES forecasting tool, the emissions projection for the current year, 2023, indicates a low emission level of 15 $gCO_2e/m^2/yr$. This represents a substantial reduction in emissions compared to the first year of the reservoir's operation.

Looking ahead, the forecasting predicts a further decline in emissions. In 100 years since the reservoir's expansion, the emissions are estimated to reach 1 $gCO_2e/m^2/yr$. This signifies a remarkable reduction in emissions over a century.

These findings highlight the temporal dynamics of GHG emissions from the Kjensvatn reservoir. Following the initial years with higher emissions, the reservoir has demonstrated a decreasing trend, resulting in significantly lower emissions in the present year. Furthermore, the forecasting provides optimistic insights into the reservoir's future, indicating a continued decline in emissions over time.

The same figure provides a visual representation of the emission patterns observed in the Kjensvatn reservoir, specifically focusing on CH_4 diffusive, CO_2 diffusive, and CH_4 bubbling emissions. The graph highlights the annual changes in these emissions and provides insights into their projected future trajectory.

In the first year of reservoir operation, there was the following information: CH_4 diffusive = 102.321 $gCO_2e/m^2/yr$. CO_2 diffusive = 15.64 $gCO_2e/m^2/yr$ and CH_4 bubbling 2.21 $gCO_2e/m^2/yr$.

It is important to note that the Kjensvatn reservoir shows lower emissions compared to Kalvatn and Akersvatn reservoirs. The significant methane (CH_4) emissions observed in this reservoir raise an important question for investigation. Despite the forest covering only 1% of the reservoir's area and bare areas accounting for merely 4%, the pre-impoundment water area was a substantial 95%. This stark difference between land cover percentages and methane emissions prompts the need for a thorough analysis of real data in order to obtain precise and accurate results, thus minimizing uncertainties in our understanding of the factors contributing to the reservoir's high CH_4 emissions.

Over time, the emissions from the Kjensvatn reservoir have shown a decreasing trend annually. According to the figure, all emissions, including CH_4 diffusive, CO_2 diffusive, and CH_4 bubbling, are projected to reach zero after a span of 100 years. The only exception is CH_4 bubbling emissions, which are expected to remain at a low level of 2.31 $gCO_2e/m^2/yr$.

Among the reservoirs within the Rana scheme, the emissions analysis reveals significant variations in their respective greenhouse gas (GHG) emissions. The Kalvatn reservoir has the highest emissions, measuring at 2543 tCO_2e/yr, followed by the Akersvatn reservoir with emissions of 1146 tCO_2e/yr. In contrast, the Kjensvatn reservoir with the lowest emissions at 138 tCO_2e/yr.

This discrepancy in emissions can be attributed to several factors. The size of the reservoir and the land coverage influence the emissions profile. Kalvatn and Akersvatn are man-made reservoirs. As a result, these reservoirs tend to generate higher emissions compared to Kjensvatn, which is an expanded natural lake. Larger reservoirs typically require larger areas to be flooded, resulting in increased emissions. In the case of Kalvatn and Akersvatn, their larger size and associated land coverage contribute to the higher emissions recorded. On the other hand, the Kjensvatn reservoir, despite being expanded, shows lower emissions due to its natural origin and potentially smaller size. However, this reservoir had the highest CH_4 emissions among the reservoirs. This highlights the importance of considering the reservoir's characteristics and their influence on GHG emissions. These observations emphasize the significance of reservoir type, size, and land coverage when assessing GHG emissions. The data underscores the lower emissions of the Kjensvatn reservoir compared to the man-made reservoirs in the Rana scheme, shedding light on the role of reservoir characteristics in influencing emissions levels.

Understanding these variations is crucial for evaluating the environmental impact of reservoirs and informing decision-making processes related to reservoir construction and management within the Rana scheme. Figure 14 represents the emissions rate distribution in Rana scheme.

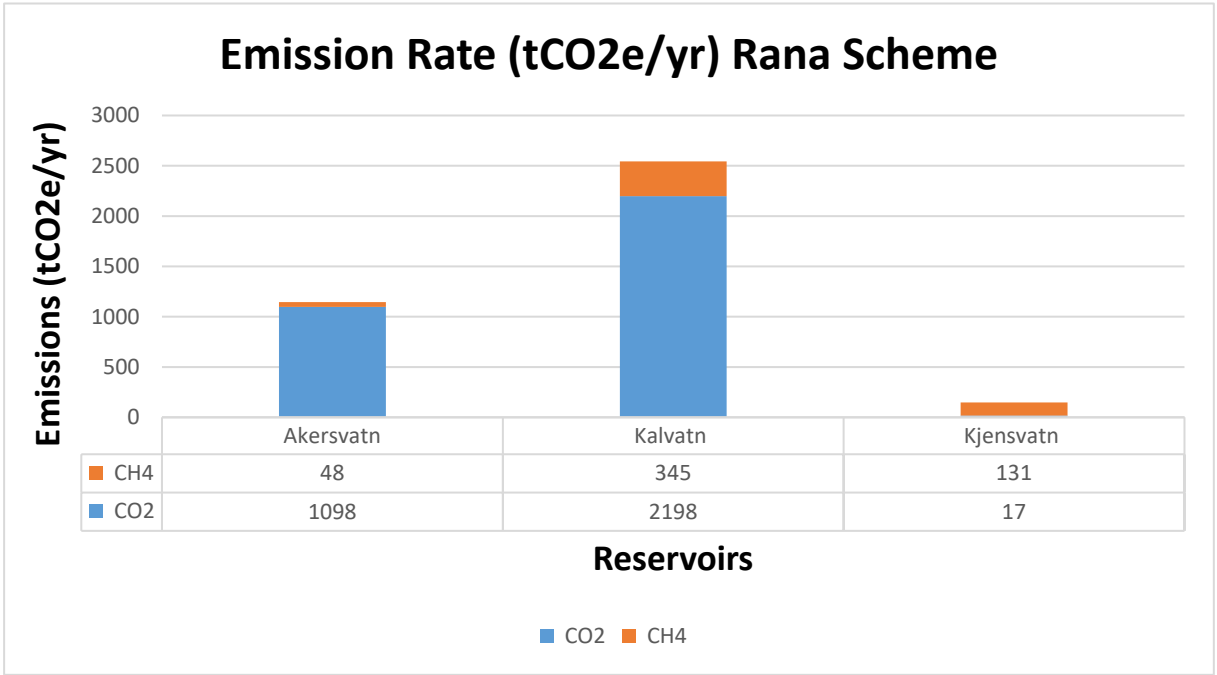

Figure 14 Total Emission rate from Rana Scheme

7.1.2 Results from Orkla Scheme

The results from Orkla Scheme are following:

- Granasjøen

As already mentioned before in the case of this reservoir, comprehensive field studies were conducted to obtain accurate information regarding land coverage. This involved utilizing satellite imagery to determine the land type as mineral and conducting site visits to gather precise data on the soil type. The availability of this detailed information enabled a more accurate simulation and analysis of the reservoir's characteristics.

Two scenarios will be presented in the Granasjøen reservois results: one based on satellite land coverage description and the other incorporating the exact soil type information obtained from site visits with the help of NINA (NINA , n.d.). Both cases will be analyzed and compared to provide a comprehensive understanding of the reservoir's land coverage and its implications.

Scenario 1 – Simulation based on the satellite images with only mineral soil.

Figure 15 represents the reservoir volume analsys results.

Volume		Emissions intensity (gCO2e/kWh)
Initial Volume	0.144	2.7
Volume +10%	0.1584	2.7
Volume +15%	0.1656	2.6
Volume +20%	0.1728	2.6
Volume +50%	0.216	2.5
Volume +100%	0.288	2.5

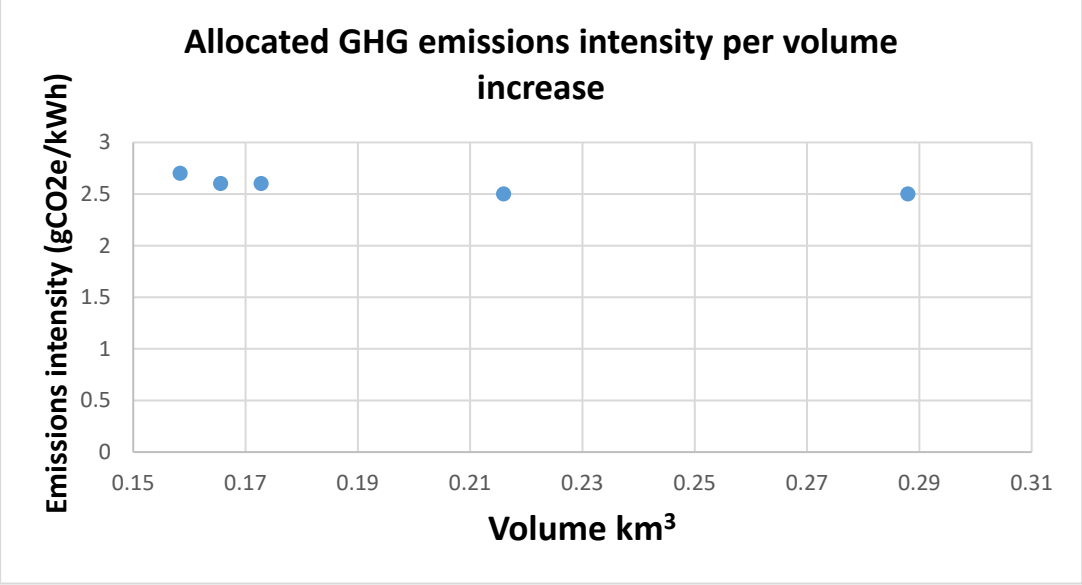

Figure 15 Reservoir volume vs emissions intensity

From the tool, results are following:

Table 7 Total footprint

Name of Reservoir	Total Footprint					
		Post Impoundment	Pre Impoundment	Unrelated Anthropogenic Sources	Construcition (Reservoir)	Net GHG Footprint
Granasjøen	Emission Rate (gCO2e/m2/yr)	57	-73	2	0	128.00
	Emission Rate (tCO2e/m2/yr)	376	-481	14	0	843.00
	Total Lifetime Emissions	37576	-48141	1382	0	84335.00

Table 7 presents important data regarding the total footprint and net greenhouse gas (GHG) emissions from the reservoir. Before the construction of the dam, the location served as a carbon sink, effectively storing a notable amount of carbon. The data reveals that the carbon storage in this pre-dam state amounted to 48,141 tCO_2e. However, with the construction of the dam and the following increase in the water level, there was a notable shift from a carbon sink state to a carbon emitter state. The emissions resulting from this change totalled 37,576 tCO_2e.

To quantify the net GHG emissions from the reservoir, as before cases Equation 2 Net GHG Footprint was applied, which involves subtracting the pre-impoundment emissions from the post-impoundment emissions. This calculation yielded a total lifetime GHG footprint of 84,335 tCO_2e. Consequently, the annual emission rate was determined to be 843 tCO_2e /m^2/yr.

Additionally, the data reveals an Unrelated Anthropogenic Sources (UAS) value of 1,382 tCO_2e for this reservoir. UAS represents the GHG emissions that are unrelated to the reservoir itself but occur in the surrounding human-impacted areas. These emissions contribute to the overall GHG footprint associated with the reservoir.

The findings presented in Table 7 provide valuable insights into the carbon dynamics of the reservoir. The shift from a carbon sink to a carbon emitter state due to dam construction resulted in substantial emissions, impacting the overall GHG footprint. The calculated net GHG footprint and UAS further highlight the long-term cumulative emissions associated with the reservoir's operation and the additional emissions from external sources.

Table 8 provides a complete overview of the annual distribution of CO_2 and CH_4 emissions within the Granasjøen reservoir.

The total annual emission as already mentioned before, from the reservoir is 841 tCO_2e. Out of this total, CO_2 emissions contribute 761 tCO_2e, while CH_4 emissions account for 82 tCO_2e. Emissions are further broken down into the square meter of the reservoir area. The distribution of emissions per m^2 is the following: CO_2 =

115 $gCO_2e/m^2/yr$, while CH_4 = 13 $gCO_2e/m^2/yr$. CO_2, being the dominant greenhouse gas in terms of total emissions, contributes substantially to the reservoir's overall GHG footprint.

Table 8 Reservoir emissions by pathway

Name of Reservoir	Reservoir Emissions by Pathway				
		Post-Impoundment	Pre-Impoundment	Unrelated Anthropogenic Sources	Net GHG Footprint
Granasjøen	Emission Rate (tCO2e/yr)	376	-481	16	841
	of which CO2	264	-497	0	761
	of which CH4	111	15	14	82
	Emission Rate (gCO2e/m2/yr)	57	-73	2	128
	of which CO2	40	-75	0	115
	of which CH4	17	2	2	13

The power density for both of the studied reservoirs (Mineral only, organic+ mineral soil distribution) is calculated to be 11.3 W/m^2. Both data gives possibility to gain EU green hydropower label from EU taxonomy. (EU Technical Expert Group, 2020)

Furthermore, the allocated greenhouse gas (GHG) emissions intensity for this reservoir is determined to be 2.5 gCO_2e/kWh. This value is lower compared to the national emissions intensity for Norway, which stands at 3.33 gCO_2e/kWh. The remarkably low emissions intensity of the studied reservoir further highlights its environmental superiority in comparison to previous reservoir projects in the Orkla region.

Figure B5 presents a comparison of the emissions from the reservoir with worldwide data. The data presented in Figure B5 shows that the CH_4 diffusive = 15 $gCO_2e/m^2/yr$. This figure is lower than the global mean for CH_4 diffusive emissions, indicating that the reservoir performs favorably in terms of reducing CH_4 emissions. Similarly, the CH_4 bubbling emissions = 2 $gCO_2e/m^2/yr$, which is comparable to the global mean. This suggests that the reservoir's contribution to CH_4 bubbling emissions aligns with the global average. Furthermore, the figure indicates that the reservoir has a CH_4 = 0 $gCO_2e/m^2/yr$. Regarding CO_2 emissions, the reservoir has a CO_2 diffusive = 40 $gCO_2e/m^2/yr$.

Figure B6 provides a graphical representation of the annual net greenhouse gas (GHG) emissions from the Granasjøen reservoir. The data illustrates the emissions pattern over 100 years. In the first year of operation, the emissions were significant, 437 $gCO_2e/m^2/yr$. However, as the years progressed, there has been decreased in emissions. In the second year, emissions decreased to 354 $gCO_2e/m^2/yr$, and this decreasing trend has continued since then. The construction of the dam at Granasjøen took place in 1982, and since then, 41 years have passed. Based on the G-RES forecasting, the projected emission for the year 2023 is 129 $gCO_2e/m^2/yr$. This figure represents a substantial reduction in emissions compared to the initial years of reservoir operation.

Furthermore, the forecasting data suggests that after 100 years of reservoir operation, the emissions will further decline to 77 $gCO_2e/m^2/yr$. This long-term projection signifies the reservoir's potential to continually reduce its environmental impact as it matures and stabilizes.

Figure B6 also presents a visual representation of the annual greenhouse gas (GHG) emissions from the Granasjøen reservoir, focusing on CO_2 and CH emissions. The data shown in the figure provides valuable insights into the emission trends, highlighting the relative magnitudes and the decreasing pattern observed over time.

In the initial year of reservoir operation, the CO_2 diffusive emissions = $311.01gCO_2e/m^2/yr$, while the CH_4 diffusive emissions = $51.368gCO_2e/m^2/yr$ Comparatively, the CH_4 bubbling emissions = $1.821gCO_2e/m^2/yr$. These values demonstrate the varying contributions of different greenhouse gases within the reservoir system.

Importantly Figure B6 emphasizes that all of these emissions are projected to reach zero after 100 years of reservoir operation. CH_4 bubbling will maintain its value at 1.821 $gCO_2e/m^2/yr$ level.

Scenario 2 – With the detailed land coverage information within the reservoir

In this thesis scenario, the results and simulations presented are based on a comprehensive site visit study, which provided valuable insights into the soil composition within the Granasjøen reservoir. This study allowed for a better understanding of the different soil types present, specifically identifying the presence of organic soil alongside minerals. It is important to note that the composition of the soil has a significant influence on greenhouse gas (GHG) emissions within the reservoir. However, it is worth mentioning that the G-RES tool used in this study may not fully account for the emissions associated with organic soil. The tool primarily considers organic soil as a GHG sink after impoundment, meaning tool doesn’t include carbon sequestration in it. As a result, the simulation results presented in this thesis may not be precise compared to scenarios that consider the emissions from mineral soil.

As already mentioned before the focus of this analysis was to assess how the transition from mineral soil to organic soil influenced the emissions intensity. The results obtained from this analysis revealed significant differences in emissions intensity when comparing the emissions from mineral soil alone to the combined emissions from mineral and organic soil. Prior to the transition, the emissions intensity ranged from 2.7-2.5 (gCO_2e/kWh), indicating relatively higher emissions. However, after the land type changed from mineral to organic, the emissions intensity showed a notable decrease. The emissions intensity in the combined scenario ranged from 0-0.2(gCO_2e/kWh), reflecting a considerably lower intensity compared to the previous mineral soil scenario. (Figure 16)

These findings raise important questions regarding the role of organic soil in GHG emissions. It is commonly understood that flooded organic soil tends to be a source of GHG emissions rather than a sink. However, the emissions intensity results obtained using the G-RES tool with organic soil do not align with this expectation, as they indicate minimal emissions or even a sinking effect.

This discrepancy between the G-RES tool results and the anticipated behaviour of organic soil suggests that further investigation and refinement of the tool may be necessary. It is crucial to ensure that the emissions intensity results obtained from the tool accurately reflect the reality of organic soil emissions.

The GIS map made based on NINA data can be found here Figure C1

Volume		Emissions intensity (gCO2e/kWh)
Initial Volume	0.144	0.2
Volume +10%	0.1584	0.2
Volume +15%	0.1656	0.2
Volume +20%	0.1728	0.2
Volume +50%	0.216	0
Volume +100%	0.288	0

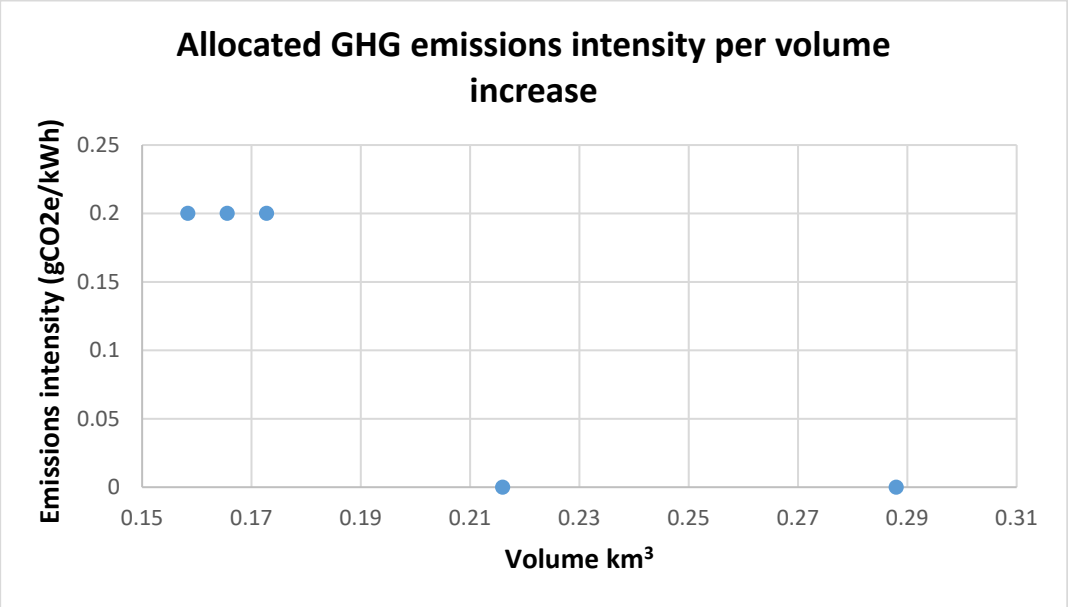

Figure 16 Reservoir volume vs Emissions intensity

The tool results are following:

The analysis of the reservoir with a mix of organic and mineral soil yielded contrasting results compared to the previous analysis focused solely on mineral soil. The total GHG emissions, as indicated in Table 9, decreased significantly from 84,335 tCO_2e to 222 tCO_2e when organic soil was introduced into the simulation.

Table 9 Total footprint Organic + Mineral soil

Name of Reservoir	Total Footprint					
		Post Impoundment	Pre Impoundment	Unrelated Anthropogenic Sources	Construcition (Reservoir)	Net GHG Footprint
Granasjøen	Emission Rate (gCO2e/m2/yr)	56	54	2	0	0.00
	Emission Rate (tCO2e/m2/yr)	375	359	14	0	2.00
	Total Lifetime Emissions (tC02e)	37466	35862	1382	0	222.00

Moreover, the emissions rates for CO_2 and CH_4 showed distinct changes in Table 10. If before when it was only mineral soil there were the following results: CO_2 emissions = 115($gCO_2e/m^2/yr$) and CH_4 =13($gCO_2e/m^2/yr$), now with organic soil the results are the following: CO_2= 14($gCO_2e/m^2/yr$), CH_4= -113($gCO_2e/m^2/yr$) Table 10. Interestingly, the CH_4 emissions rate shifted from a positive value in the mineral case case to a negative value in the organic + mineral soil one: CH_4 = 13 ($gCO_2e/m^2/yr$) CH_4 = value of -113 ($gCO_2e/m^2/yr$).

This unexpected negative value for CH_4 emissions indicates that CH_4 was sunk rather than emitted when organic soil was present. However, this finding contradicts the general understanding that flooded organic land tends to have higher methane emissions rather than sink properties. Consequently, these results from the G-RES tool with organic soil raise concerns regarding their reliability and their alignment with real-world observations.

The discrepancy between the G-RES tool's results and the expected behaviour of organic soil highlights the need for further investigation and improvement. Future research should aim to refine the emissions models and parameters used within the tool to better reflect the actual emissions dynamics of organic soil. This will contribute to more accurate assessments of GHG emissions and enable the development of more effective mitigation strategies for reservoir operations.

Table 10 Reservoir emissions by pathway Organic+Mineral soil

Name of Reservoir	Reservoir Emissions by Pathway				
		Post-Impoundment	Pre-Impoundment	Unrelated Anthropogenic Sources	Net GHG Footprint
Granasjøen	**Emission Rate (tCO2e/yr)**	375	359	14	2
	of which CO2	263	-489	0	752
	of which CH4	111	848	14	-751
	Emission Rate (gCO2e/m2/yr)	56	54	2	0
	of which CO2	40	-74	0	114
	of which CH4	17	128	2	-113

Furthermore, the allocated greenhouse gas (GHG) emissions intensity for this reservoir is determined to be 0 gCO_2e/kWh. This value is much lower compared to the national emissions intensity for Norway, which stands at 3.33 gCO_2e/kWh.

Comparison of the emissions from the reservoir with worldwide data. In the worldwide data comparison results from mix type soil is the same as it was with only mineral soil, which are the following: CH_4 diffusive = 15 $gCO_2e/m^2/yr$. This figure is lower than the global mean for CH_4 diffusive emissions, indicating that the reservoir performs favorably in terms of reducing CH_4 emissions. Similarly, the CH_4 bubbling emissions = 2 $gCO_2e/m^2/yr$, which is comparable to the global mean. This suggests that the reservoir's contribution to CH_4 bubbling emissions aligns with the global average. Furthermore, the figure indicates that the reservoir has a CH_4 = 0 $gCO_2e/m^2/yr$. Regarding CO_2 emissions, the reservoir has a CO_2 diffusive = 40 $gCO_2e/m^2/yr$.

Figure B7 provides a comprehensive overview of the GHG emissions over a 100-year period. The graph reveals that in the first year of reservoir operation, the GHG emissions amounted to 309$gCO_2/e/m^2/yr$. However, as time progresses, the emissions steadily decrease, reaching a value of -50 $gCO_2/e/m^2/yr$ after 100 years. This negative value indicates that the reservoir transitions from being a source of emissions to acting as a sink, with a capacity to absorb 50$CO_2/e/m^2/yr$. Furthermore, it is noteworthy that the project achieves carbon neutrality after 32 years, marking a significant milestone in its environmental performance

The same Figure B7 presents a visual representation of the annual greenhouse gas (GHG) emissions from the Granasjøen reservoir, focusing on CO_2 and CH_4 emissions. In the initial year of reservoir operation, the CO_2 diffusive emissions = 309.735 $gCO_2/e/m^2/yr$, while the CH_4 diffusive emissions = 51.368 $gCO_2/e/m^2/yr$. Comparatively, the CH_4 bubbling emissions = 1.821$gCO_2/e/m^2/yr$. Even though the previous results were different CH_4 still remained the same for the first year, and after 100 years it became 0.

- Litjfossen (Innerdalsvatnet)

The Litjfossen (Innerdalsvatnet) reservoir is the second case in which we have obtained data from two different sources: a detailed soil type description with the report from "Norwegian University of Science and Technology, Science Museum, Report botanical series" (Norwegian University of Science and Technology, n.d.) and a satellite image description. This provides us with valuable insights into the emissions from both mineral soil and organic soil perspectives. The results of these analyses are presented below.

When comparing the emissions from mineral soil alone to the combined emissions from mineral and organic soil, the findings of this investigation indicated considerable variations in emissions intensity. Prior to the changeover, the intensity of emissions varied between 4.3 - 3.7 (gCO_2e/kWh) Figure 17, suggesting considerably greater emissions. However, when the soil type was changed from mineral to organic, the intensity of the emissions decreased.

Volume		Emissions intensity (gCO2e/kWh)
Initial Volume	0.15	4.3
Volume +10%	0.165	4.2
Volume +15%	0.173	4.2
Volume +20%	0.18	4.1
Volume +50%	0.225	3.9
Volume +100%	0.3	3.7

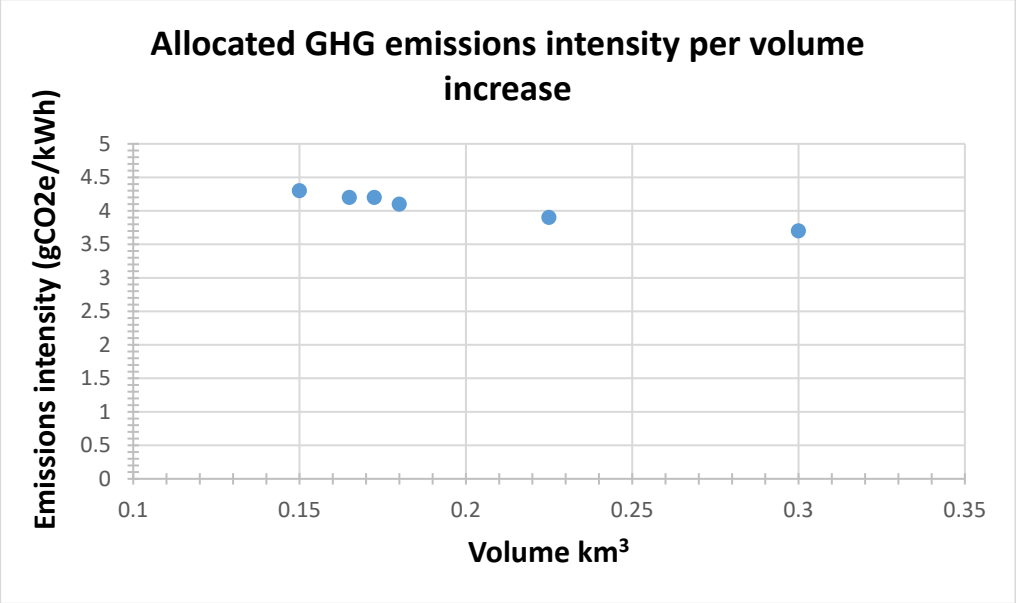

Figure 17 Reservoir volume vs emissions intensity (Mineral scenario)

The results of these analyses are presented below.
From the mineral soil perspective:

- Total GHG emissions: 65932 tCO_2e, from where UAS (Unrelated Anthropogenic Sources) is 630 tCO_2e Table 11

The Table 12 illustrates the following:

- CO_2 emissions rate on per square meter: 89 $gCO_2e/m^2/yr$
- CH_4 emissions rate on per square meter: 13 $gCO_2e/m^2/yr$
- UAS – 2 $gCO_2e/m^2/yr$

Table 11 Total Footprint Mineral soil scenario

Name of Reservoir	Total Footprint					
		Post Impoundment	Pre Impoundment	Unrelated Anthropogenic Sources	Constructio n (Reservoir)	Net GHG Footprint
Litjfossen	Emission Rate (gCO2e/m2/yr)	53	-49	2	0	100.00
	Emission Rate (tCO2e/m2/yr)	343	-323	6	0	660.00
	Total Lifetime Emissions (tC02e)	34297	-32265	630	0	65932.00

Table 12 Reservoir emissions by pathway Mineral soil scenario only

Name of Reservoir	Reservoir Emissions by Pathway				
		Post-Impoundment	Pre-Impoundment	Unrelated Anthropogenic Sources	Net GHG Footprint
Litjfossen	Emission Rate (tCO2e/yr)	343	-323	6	660
	of which CO2	257	-325	0	582
	of which CH4	86	3	6	77
	Emission Rate (gCO2e/m2/yr)	53	-49	2	100
	of which CO2	39	-50	0	89
	of which CH4	13	0	0	13

The combined scenario's emissions intensity varied from 3.7 to 3.1 (gCO_2e/kWh), indicating a much lower intensity than the preceding mineral soil scenario. Figure 18

Volume		Emissions intensity (gCO2e/kWh)
Initial Volume	0.15	3.7
Volume +10%	0.165	3.6
Volume +15%	0.173	3.6
Volume +20%	0.18	3.6
Volume +50%	0.225	3.4
Volume +100%	0.3	3.1

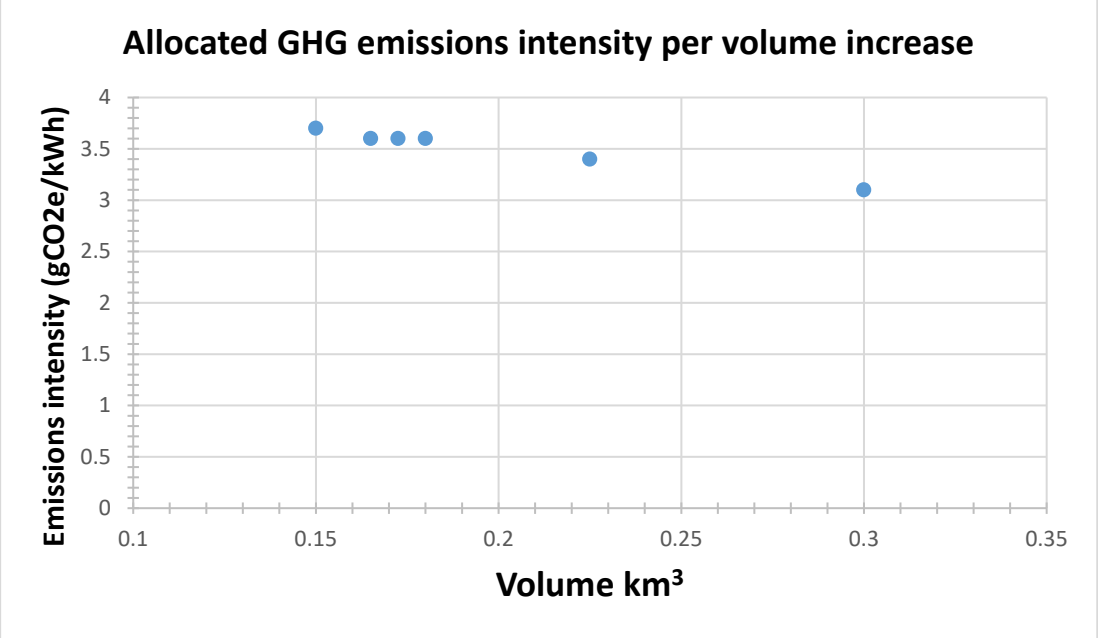

Figure 18 Reservoir volume vs emissoins intensity – Organic + Mineral soil scenario

From the organic soil perspective:

- Total GHG emissions: 55807 tCO_2e, from where UAS (Unrelated Anthropogenic Sources) is 630 tCO_2e Table 13

Table 13 Total footprint Mineral + Organic soil scenario

Name of Reservoir	Total Footprint					
		Post Impoundment	Pre Impoundment	Unrelated Anthropogenic Sources	Construcition (Reservoir)	Net GHG Footprint
Litjfossen	Emission Rate (gCO2e/m2/yr)	53	-34	2	0	85.00
	Emission Rate (tCO2e/m2/yr)	343	-221	6	0	558.00
	Total Lifetime Emissions (tC02e)	34297	-22140	630	0	55807.00

Table 14 represents total and emissions pathway data

- CO_2 emissions rate: 113 $gCO_2e/m^2/yr$
- CH_4 emissions rate: -27 $gCO_2e/m^2/yr$
- UAS – 2 $gCO_2e/m^2/yr$

Table 14 Reservoir emissions by pathway Mineral + Organic soil scenario

Name of Reservoir	Reservoir Emissions by Pathway				
		Post-Impoundment	Pre-Impoundment	Unrelated Anthropogenic Sources	Net GHG Footprint
Litjfossen	**Emission Rate (tCO2e/yr)**	343	-221	6	558
	of which CO2	257	-481	0	738
	of which CH4	86	259	6	-179
	Emission Rate (gCO2e/m2/yr)	53	-34	2	85
	of which CO2	39	-74	0	113
	of which CH4	13	40	0	-27

The case of the Litjfossen (Innerdalsvatnet) reservoir further highlights the contrasting results obtained from the mineral and organic soil perspectives. As observed, the emissions from the reservoir differ significantly depending on the soil type.

When the mineral soil is flooded, the emissions are found to be higher. This aligns with our understanding that mineral soils tend to release greater amounts of greenhouse gases. When the reservoir is inundated with organic soil, however, the emissions are significantly reduced. Organic soils have a higher potential for carbon storage and so contribute less to greenhouse gas emissions.

These disparate results raise serious concerns regarding the G-RES tool's accuracy and usefulness in accounting for the unique properties of various soil types.

The tool's current approach, which treats organic soil as a sink and mineral soil as a source, may not fully capture the complexities of emissions dynamics in reservoirs.

To ensure a more comprehensive and accurate assessment of greenhouse gas emissions, it is crucial to refine the G-RES tool and consider the influence of both mineral and organic soil types. By incorporating the unique properties and emissions patterns associated with each soil type, we can obtain a more realistic representation of the reservoir's environmental impact.

Addressing this discrepancy in results will contribute to improved decision-making processes for reservoir management. It will enable us to develop targeted strategies that mitigate greenhouse gas emissions and enhance the overall sustainability of reservoir projects.

Like the previous case with the Granasjøen reservoir, with Litjfossen (Innerdalsvatnet) as well we read the same case, the power density for both of the studied reservoirs (Mineral only, organic+mineral soil distribution) is calculated to be 11.5 W/m^2.

The allocated greenhouse gas (GHG) emissions intensity for this reservoir is determined to be 3.9 gCO_2e/kWh with the only mineral soil case, and with the organic soil mix the result is 3.3 gCO_2e/kWh. If we consider only the mineral case this value is higher than the national emission intensity for Norway (3.33 gCO_2e/kWh), however, with the mixed soil case it is the same as the national emission intensity 3.33 gCO_2e/kWh.

Figure B8 presents a comparison of the emissions from the reservoir with worldwide data. The data presented in shows that the CH_4 diffusive = 12 $gCO_2e/m^2/yr$. This data is lower than the global mean for CH_4 diffusive emissions, indicating that the reservoir performs favorably in terms of reducing CH_4 emissions. Similarly, the CH_4 bubbling emissions = 1 $gCO_2e/m^2/yr$, which is comparable to the global mean. This suggests that the reservoir's contribution to CH_4 bubbling emissions aligns with the global average. Furthermore, the figure indicates that the reservoir has a CH_4 = 0 $gCO_2e/m^2/yr$. Regarding CO_2 emissions, the reservoir has a CO_2 diffusive = 39 $gCO_2e/m^2/yr$. For the both soil scenarios (Mineral only, mineral+organic soil), the results for the worldwide comparison are the same.

From the GHG emissions over a 100-year period, there are different results, because of the soil type differences. Figure B9
From the mineral soil perspective:
The first-year annual net GHG emissions are 415 $gCO_2e/m^2/yr$, after 100-year annual net GHG emissions = 52 $gCO_2e/m^2/yr$
From the pathway perspective, the results are the following:

- CO_2 diffusive emissions rate in the first year: 307.16 $gCO_2e/m^2/yr$
- CO_2 diffusive emissions rate after 100 years: 0 $gCO_2e/m^2/yr$
- CH_4 diffusive emissions rate in the first year: 57.323 $gCO_2e/m^2/yr$
- CH_4 diffusive emissions rate after 100 years: 0 $gCO_2e/m^2/yr$
- CH_4 bubbling rate in the first year: 0.764 $gCO_2e/m^2/yr$
- CH_4 bubbling rate after 100 years 0.764 $gCO_2e/m^2/yr$

CH_4 bubbling maintained the same numbers over the 100 years.

From the organic soil perspective: Figure B10

- CO_2 diffusive emissions rate in the first year: 397 $gCO_2e/m^2/yr$
- CO_2 diffusive emissions rate after 100 years: 37 $gCO_2e/m^2/yr$
- CH_4 diffusive emissions rate in the first year: 55.01 $gCO_2e/m^2/yr$
- CH_4 diffusive emissions rate after 100 years: 0 $gCO_2e/m^2/yr$
- CH_4 bubbling rate in the first year: 0.889 $gCO_2e/m^2/yr$ yr
- CH_4 bubbling rate after 100 years 0.889 $gCO_2e/m^2/yr$

CH_4 bubbling maintained the same numbers over the 100 years, the same case as it had with mineral soil.

- Falningsjøen

Results from Falningsjøen are below:

Volume		Emissions intensity (gCO2e/kWh)
Initial Volume	0.125	1
Volume +10%	0.1375	0.9
Volume +15%	0.14375	0.9
Volume +20%	0.15	0.9
Volume +50%	0.1875	0.8
Volume +100%	0.25	0.6

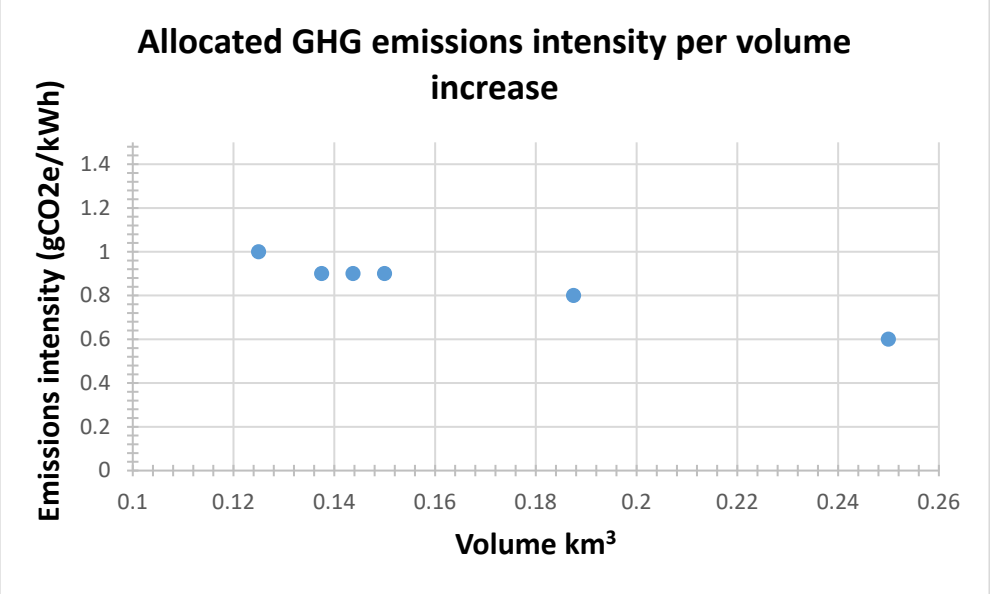

Figure 19 Reservoir volume VS emissions intensity

The figure 19 provides valuable insights, indicating that as the volume increases, emissions result in a noticeable decrease. For simulation reservoir volume is 0.1875 km^3 which has 0.8 (gCO_2e/kWh) intensity which is low for Norway. For Norway the national number as already mentioned before is following: 3.33 gCO_2e/kWh. This reservoir has the same characteristics as the previous.

Power density for this reservoir is 9.2W/m^2, since the number is moderate it means that this project may require the larger areas and larger volumes to generate the energy.

Table 15 presents comprehensive data regarding the overall footprint of the Falningsjøen reservoir. Before the construction of the dam, the location exhibited a carbon sink state, with 3337 tCO_2e stored, indicating its capacity to absorb and store carbon. However, upon the completion of the dam, the increased water level led to a transformation from a carbon sink to a carbon emitter state. The emissions resulting from this shift totalled 9098 tCO_2e.

The outcome revealed a total lifetime GHG footprint of 12435 tCO_2e for the reservoir project. Furthermore, the annual emission rate was estimated to be 124 tCO_2e/yr, reflecting the average emission intensity over the reservoir's lifespan.

Table 15 Falningsjøen Total footprint

Name of Reservoir	Total Footprint					
		Post Impoundment	Pre Impoundment	Unrelated Anthropogenic Sources	Construction (Reservoir)	Net GHG Footprint
Falningsjøen	Emission Rate (gCO2e/m2/yr)	24	-9	0	0	33.00
	Emission Rate (tCO2e/m2/yr)	91	-33	0	0	124.00
	Total Lifetime Emissions (tC02e)	9098	-3337	0	0	12435.00

It is noteworthy that the reservoir has a carbon storage capacity of 0 (UAS).

Table 16 provides a complete overview of the annual distribution of CO_2 and CH_4 emissions within the Falningsjøen reservoir.

The total annual emissions from the reservoir are the following:

The total emission = 124 tCO_2e.

Out of this total on the per square basis, CO_2 = 28 $gCO_2/m^2/yr$, while CH_4 = 5 $gCO_2/m^2/yr$.

Table 16 Reservoir emissions by pathway

Name of Reservoir	Reservoir Emissions by Pathway				
		Post-Impoundment	Pre-Impoundment	Unrelated Anthropogenic Sources	Net GHG Footprint
Granasjøen	Emission Rate (tCO2e/yr)	91	-33	0	124
	of which CO2	55	-50	0	105
	of which CH4	36	17	0	19
	Emission Rate (gCO2e/m2/yr)	24	-9	0	33
	of which CO2	15	-13	0	28
	of which CH4	9	4	0	5

CO_2, being the dominant greenhouse gas in terms of total emissions, contributes substantially to the reservoir's overall GHG footprint.

Figure B11 represents a comparison of the emissions from the reservoir with worldwide data. The data presented in shows that the CH_4 diffusive = 9 $gCO_2e/m^2/yr$. This data is lower than the global mean for CH_4 diffusive emissions, indicating that the reservoir performs favorably in terms of reducing CH_4 emissions. Similarly, the CH_4 bubbling emissions = 0 $gCO_2e/m^2/yr$, which is comparable to the global mean. This suggests that the reservoir's contribution to CH_4 bubbling emissions aligns with the global average. Furthermore, the figure indicates that the reservoir has a CH_4 = 0 $gCO_2e/m^2/yr$. Regarding CO_2 emissions, the reservoir has a CO_2 diffusive = 15 $gCO_2e/m^2/yr$.

The Figure B12 illustrates the emissions pattern over 100 years. In the first year of operation, the emissions were following, 149 $gCO_2e/m^2/yr$. However, as the

years progressed, there has been decreased in emissions. In the second year, emissions decreased to 118 $gCO_2e/m^2/yr.$, and this decreasing trend has continued since then. After 100 years since the construction the emissions will be 10 $gCO_2e/m^2/yr$. Today in 2023 after 39 the emissions are 28 $gCO_2e/m^2/yr$. The same Figure B11 presents a visual representation of the annual greenhouse gas (GHG) emissions from the Falningsjøen reservoir, focusing on CO_2 and CH_4 emissions. In the initial year of reservoir operation, the CO_2 diffusive emissions = 113.388 $gCO_2e/m^2/yr$, while the CH_4 diffusive emissions = 26.26 $gCO_2e/m^2/yr$. Comparatively, the CH_4 bubbling emissions = 0.497 $gCO_2e/m^2/yr$. Even though the previous results were different CH_4 still remained the same for the first year, and after 100 years it became 0.

- Sverjesjøen

The results for Sverjesjøen are below:

Volume		Emissions intensity (gCO2e/kWh)
Initial Volume	0.007	1
Volume +10%	0.0077	1
Volume +15%	0.00805	1
Volume +20%	0.0084	0.9
Volume +50%	0.0105	0.9
Volume +100%	0.0175	0.7

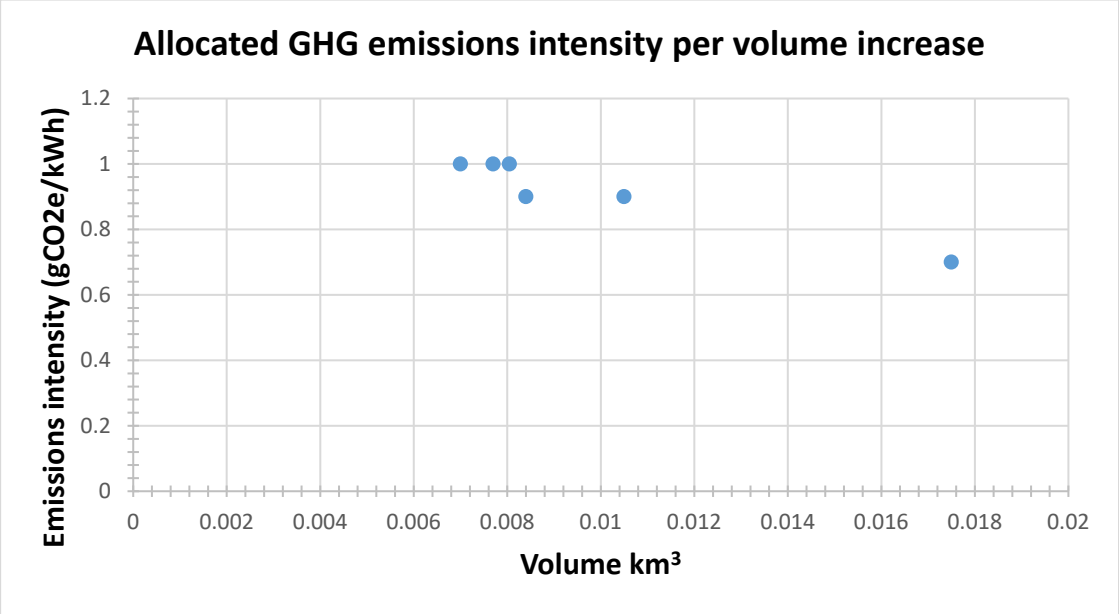

Figure 20 Reservoir volume vs Emissions intensity

Since Sverjesjøen was not built and it was expanded, it didn't have major emissions intensity. However, the first year of production was thought for the environment since the annual emissions were high. All of this information will be discussed below.

Power density for this reservoir is 21.3W/m^2, allocated GHG emissions intensity is 0.9 gCO_2e/kWh which is low for Norway. For Norway the national number as already mentioned before is following: 3.33 gCO_2e/kWh. This reservoir has the same characteristics as the previous.

Table 17 represents the total footprint from Sverjesjøen.

- Total GHG emissions = 13380 tCO_2e. It is important to note that 79 tCO_2e of this total can be attributed to UAS (Unrelated Anthropogenic Sources).

Table 17 Total footprint Sverjesjøen

Name of Reservoir	Total Footprint					
		Post Impoundment	Pre Impoundment	Unrelated Anthropogenic Sources	Construction (Reservoir)	Net GHG Footprint
Sverjesjøen	Emission Rate (gCO2e/m2/yr)	82	0	0	0	82.00
	Emission Rate (tCO2e/m2/yr)	135	0	0	0	135.00
	Total Lifetime Emissions (tC02e)	13459	0	79	0	13380.00

The Table 18 present total and reservoir emissions by pathway.

- The CO_2 emissions = 42 $gCO_2e/m^2/yr$. This figure represents the amount of CO_2 emitted per square meter annually.
- CH_4 emissions rate = 40 $gCO_2e/m^2/yr$, implying that the reservoir expansion had minimal to no influence on CH_4 emissions. Total footprint Sverjesjøen

Table 18 Sverjesjøen emissions by pathway

Name of Reservoir	Reservoir Emissions by Pathway				
		Post-Impoundment	Pre-Impoundment	Unrelated Anthropogenic Sources	Net GHG Footprint
Sverjesjøen	Emission Rate (tCO2e/yr)	135	0	0	135
	of which CO2	69	0	0	69
	of which CH4	66	0	0	66
	Emission Rate (gCO2e/m2/yr)	82	0	0	82
	of which CO2	42	0	0	42
	of which CH4	40	0	0	40

Figure B13 represents a comparison of the emissions from the reservoir with worldwide data. The data presented in shows that the CH_4 diffusive = 34 $gCO_2e/m^2/yr$. This data is closer to the global mean for CH_4 diffusive emissions. The CH_4 bubbling emissions = 6 $gCO_2e/m^2/yr$, which is comparable to the global mean. This suggests that the reservoir's contribution to CH_4 bubbling emissions aligns with the global average. Furthermore, the figure indicates that the reservoir has a CH_4 = 0 $gCO_2e/m^2/yr$. Regarding CO_2 emissions, the reservoir has a CO_2 diffusive = 42 $gCO_2e/m^2/yr$ which is also closer to the global mean.

Emissions pattern over 100 years are following: Figure B14

The first-year net GHG emission was 467 $gCO_2e/m^2/yr$, and after 100 years since the lake expansion, it will be 13 $gCO_2e/m^2/yr$. On the detailed data level, the first year after expansion, CO_2 diffusive = 335.881 $gCO_2e/m^2/yr$, CH_4 diffusive = 123.043 $gCO_2e/m^2/yr$, and CH_4 bubbling = 7.695 $gCO_2e/m^2/yr$. After 100 years all GHG emissions will be 0, and only CH_4 bubbling will be the same value as the first year of the expansion. Figure B 13

It is clear through detailed calculations and research that soil type has a substantial impact on greenhouse gas (GHG) emissions, especially when contemplating reservoir building or enlargement. It emphasizes the need of gathering correct and relevant data and information related to each project in order to get exact results.

Examining the Orkla scheme, it is observed that Falningsjøen and Sverjesjøen are expanded reservoirs, while Granasjøen and Litjfossen - Innerdalsvatnet are built reservoirs. Consequently, the latter two reservoirs exhibit higher GHG emissions compared to the former two.

These findings highlight the contrasting emissions patterns between expanded and built reservoirs, further emphasizing the crucial role of soil type. It reinforces the significance of understanding the environmental characteristics and conditions unique to each project, as they directly impact GHG emissions.

Figure 21 represents the emission rate distributions in the reservoirs, in the Orkla Scheme.

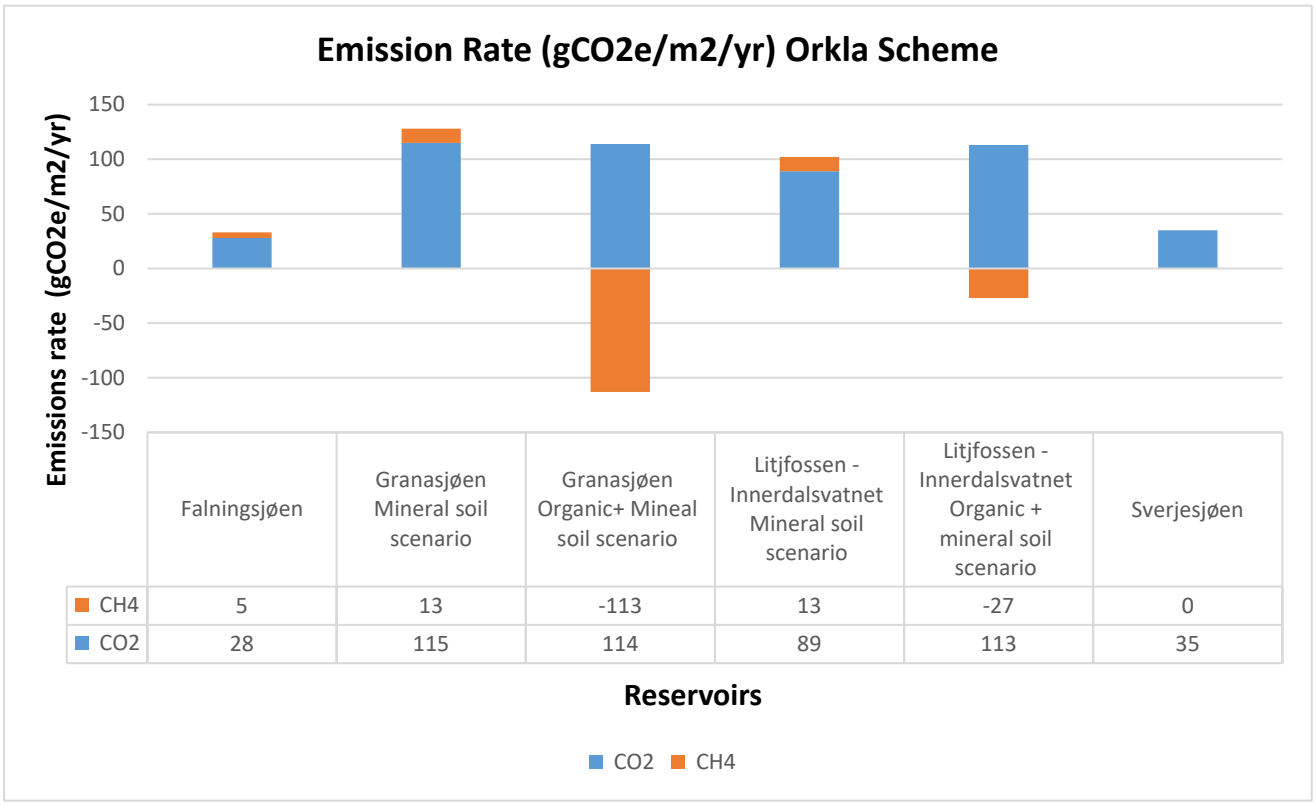

Figure 21 Emissions rate Orkla Scheme

7.1.3 Results from Sira-Kvina Scheme

The results from Sira-Kvina Scheme are represented below.

- Flothølen

Flothølen is the expanded reservoir, and because of that the emissions intensity is not too high, and also didn't change on the lower or higher volume of the reservoir. For this reservoir the annual wind speed is retrived from (Seklima.met.no, n.d.) since the station was close to the reservoir elevation. The elevation of the reservois is 672 m.a.s.l, and the station elevation is 560m/s m.a.s.l

Volume		Emissions intensity (gCO2e/kWh)
Initial Volume	0.317	0.4
Volume +10%	0.3487	0.4
Volume +15%	0.365	0.4
Volume +20%	0.3804	0.4
Volume +50%	0.4755	0.4
Volume +100%	0.634	0.4

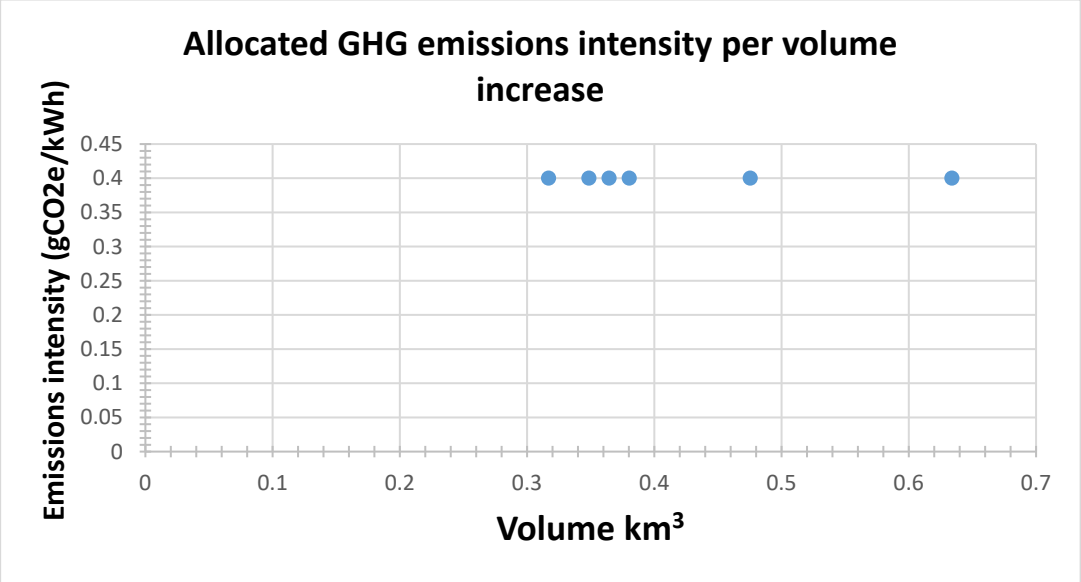

Figure 22 Reservoir volume and Emission intensity

The Flothølen reservoir, as described earlier, is an expanded lake, which has resulted in lower emissions compared to constructing a reservoir from scratch. The table provided presents the total footprint of the reservoir, indicating the quantity of greenhouse gas emissions associated with it.

Based on the data provided, the total footprint of the reservoir is recorded as 22376 tCO_2e Table 19. This value is derived from a CO_2 emission = 115 gCO_2-$e/m^2/yr$ and an ineresting result for CH_4 emissions = -25 $gCO_2e/m^2/yr$ Table 20. The negative value for CH_4 emissions implies that methane emissions might have stopped after the expansion of the lake. It is noteworthy that approximately 25% (0.656 km^2) of the reservoir's land cover is characterized by forested areas.

These findings raise considerable doubts regarding the reliability of the reservoir's emission data. The significant reduction in CH_4 emissions after the lake expansion, coupled with the presence of a substantial forested land cover, casts doubt on the accuracy and validity of the reported emission figures for this particular reservoir. Further investigation and scrutiny are necessary to validate the results and assess the true environmental impact of the reservoir.

Table 19 Total footprint

Name of Reservoir	Total Footprint					
		Post Impoundment	Pre Impoundment	Unrelated Anthropogenic Sources	Construction (Reservoir)	Net GHG Footprint
Flothølen	Emission Rate (gCO2e/m2/yr)	68	-21	0	0	89.00
	Emission Rate (tCO2e/m2/yr)	170	-54	0	0	224.00
	Total Lifetime Emissions (tC02e)	17013	-5363	0	0	22376.00

The power density for this reservoir is 48W/m^2, since the number is high it means that this project doesn't require larger areas and larger volumes to generate the energy, which also means that less area is necessary to be flooded. The allocated GHG emissions intensity is 0.4 gCO_2e/kWh which is low for Norway. For Norway the national number as already mentioned before is the following: 3.33 gCO_2e/kWh

Table 20 Reservoir emissions pathway

Name of Reservoir	Reservoir Emissions by Pathway				
		Post-Impoundment	Pre-Impoundment	Unrelated Anthropogenic Sources	Net GHG Footprint
Flothølen	Emission Rate (tCO2e/yr)	170	-54	0	224
	of which CO2	170	-117	0	287
	of which CH4	0	64	0	-64
	Emission Rate (gCO2e/m2/yr)	68	-21	0	89
	of which CO2	68	-47	0	115
	of which CH4	0	25	0	-25

For Flothølen there is no data for the worldwide data comparison, which means that it is unknown for us CH_4 and CO_2 comparison worldwide.

However, it is possible to check the emission pathway and distribution in the reservoir over 100 years.

In the first year of expansion, the net greenhouse gas (GHG) emissions were relatively high - 696 gCO_2e/m^2/yr. However, in the following year, it decreased significantly - 549 gCO_2e/m^2/yr. Projections indicate that, based on the expansion, the emissions are expected to further decline to 30 gCO_2e/m^2/yr over the course of 100 years.

Considering the emission pathway, the following results are obtained:

CO_2 diffusive: 546.56 $gCO_2e/m^2/yr$

CH_4 diffusive: 123.37 $gCO_2e/m^2/yr$

CH_4 bubbling: 4.14 $gCO_2e/m^2/yr$

Over the 100 years, it is expected that the CO_2 diffusive and CH4 diffusive emissions will gradually decrease, eventually reaching zero. However, the CH_4 bubbling emission is anticipated to persist at a constant rate of 4.14 $gCO_2e/m^2/yr$ throughout the entire period. Figure B15

These findings highlight the evolving emission patterns within the reservoir over an extended timeframe. The analysis suggests a significant reduction in emissions, particularly in terms of CO_2 and diffusive CH_4, while emphasizing the consistent contribution of CH_4 bubbling emissions over the 100-year period.

- Valevatn

The results for reservoir volume and emissions intensity from Valevatn are given below

Volume		Emissions intensity (gCO2e/kWh)
Initial Volume	0.267	2.6
Volume +10%	0.2937	2.5
Volume +15%	0.307	2.4
Volume +20%	0.3204	2.4
Volume +50%	0.4005	2.1
Volume +100%	0.534	1.8

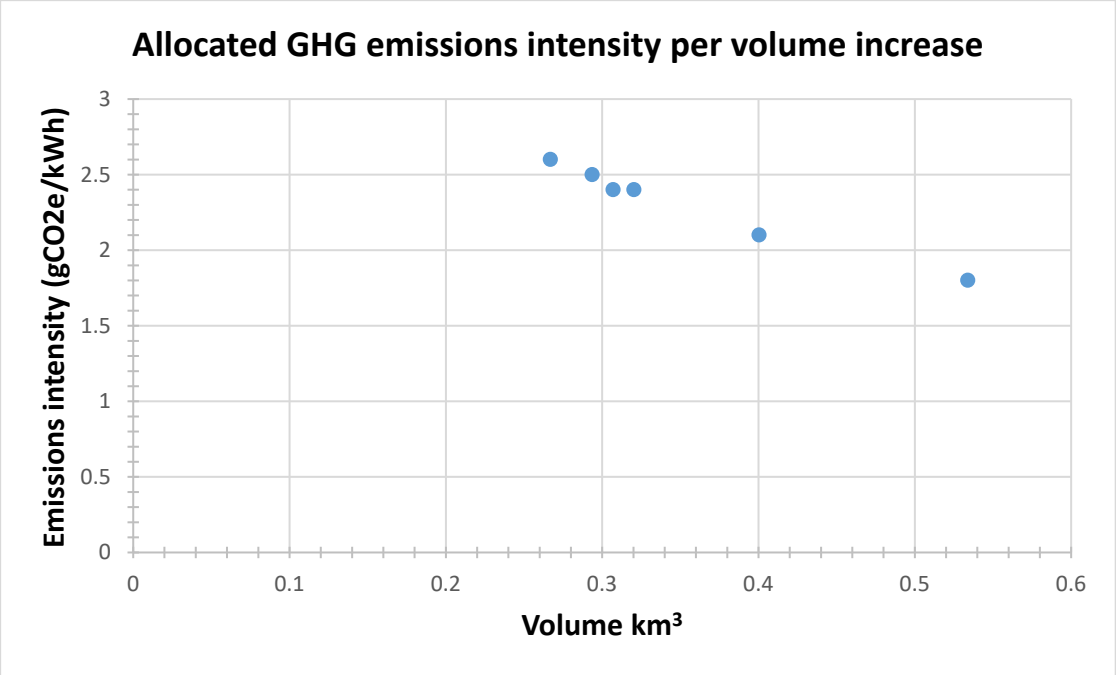

Figure 23 Reservoir volume vs Emissions intensity

The emissions associated with the Valevatn reservoir are as follows:

Total lifetime emissions: 12,684 tCO_2e Table 21

Table 21 Total footprint

Name of Reservoir	Total Footprint					
		Post Impoundment	Pre Impoundment	Unrelated Anthropogenic Sources	Constructio n (Reservoir)	Net GHG Footprint
Valevatn	Emission Rate (gCO2e/m2/yr)	104	-8	0	0	112.00
	Emission Rate (tCO2e/m2/yr)	1152	-85	0	0	1237.00
	Total Lifetime Emissions (tC02e)	115152	-8532	0	0	123684.00

From the total emissions the results are following: CO_2 emissions: 89 $gCO_2e/m^2/yr$ CH_4 emissions: 23 $gCO_2e/m^2/yr$. Table 22

Table 22 Reservoir emissions by pathway

Name of Reservoir	Reservoir Emissions by Pathway				
		Post-Impoundment	Pre-Impoundment	Unrelated Anthropogenic Sources	Net GHG Footprint
Valevatn	Emission Rate (tCO2e/yr)	1152	-85	0	1237
	of which CO2	471	-511	0	982
	of which CH4	680	425	0	255
	Emission Rate (gCO2e/m2/yr)	104	-8	0	112
	of which CO2	43	-46	0	89
	of which CH4	62	39	0	23

Despite being an expanded reservoir, Valevatn exhibits a moderate emission rate. The provided data indicates that before the expansion, the lake served as a sink for CO_2, absorbing more carbon dioxide than it emitted. However, following the expansion, CO_2 emissions were observed, making Valevatn a greenhouse gas emitter, particularly CH_4.

This information highlights the shift in the reservoir's emissions profile after its expansion. While it previously acted as a carbon sink, absorbing CO_2, the expansion resulted in increased CO_2 emissions and the emergence of CH_4 emissions. This transformation makes Valevatn a reservoir that contributes to greenhouse gas emissions.

Understanding the emissions profile of Valevatn provides valuable insights into the environmental impact of the reservoir expansion. It underscores the importance of considering the emissions dynamics when evaluating the overall greenhouse gas footprint of hydroelectric projects.

The power density of this reservoir is recorded at $10.9W/m^2$, representing a moderate value. This indicates that to generate the desired energy output, larger

areas and volumes may be required compared to reservoirs with higher power densities.

Furthermore, the allocated greenhouse gas (GHG) emissions intensity for this reservoir is 2.1 gCO_2e/kWh, which is relatively low for Norway. As previously mentioned, the national average for Norway is 3.33 gCO_2e/kWh. The lower emissions intensity of this reservoir indicates a favorable environmental performance in terms of GHG emissions per unit of electricity generated.

However, it is essential to investigate the reasons behind the moderate emissions intensity of expanded reservoirs. Further analysis and examination are needed to understand the factors contributing to the observed emissions levels. By delving into the specific characteristics and operational aspects of expanded reservoirs, it is possible to gain insights into their emissions profiles and identify opportunities for further improvements.

Understanding the emissions intensity of expanded reservoirs is crucial for assessing their environmental impact and optimizing their performance. By addressing and investigating the factors behind the moderate emissions intensity, it becomes possible to develop strategies and measures to minimize the ecological footprint associated with such reservoirs

In a global context, Valevatn demonstrates results that align closely with the average emissions levels. Figure B16 The specific emissions breakdown for the reservoir is as follows:

- CH_4 diffusive: 41 $gCO_2e/m^2/yr$
- CH_4 bubbling: 12 $gCO_2e/m^2/yr$
- CO_2 diffusive: 43 $gCO_2e/m^2/yr$

The emissions pathway and distribution within the Valevatn reservoir over a span of 100 years are outlined below.

In the first year of expansion, the net greenhouse gas (GHG) emissions were relatively high - 528 $gCO_2e/m^2/yr$. However, in the following year, it decreased significantly - 433 $gCO_2e/m^2/yr$. Projections indicate that, based on the expansion, the emissions are expected to further decline to 33 $gCO_2e/m^2/yr$ over the course of 100 years. Figure B17

Analyzing the emission pathway within the reservoir, the following results were obtained:

CO_2 diffusive: 343.791 $gCO_2e/m^2/yr$

CH_4 diffusive: 157.204 $gCO_2e/m^2/yr$

CH_4 bubbling: 18.812 $gCO_2e/m^2/yr$

It is noteworthy that Valevatn exhibits the highest CH_4 bubbling result among all the reservoirs studied in this thesis. This finding can potentially be attributed to sedimentation within the lake. However, considering that sedimentation is not

prevalent on a large scale in Norway, further investigation and reassessment are required to obtain more precise calculations and understanding.

Over 100 years, it is anticipated that the emissions from CO_2-diffusive and CH_4-diffusive pathways will gradually decrease until reaching zero. However, the CH_4 bubbling emission is expected to persist at a constant rate of 18.812 $gCO_2e/m^2/yr$ throughout the entire duration.

The analysis provides valuable insights into the emissions dynamics and long-term trajectory of the Valevatn reservoir. By identifying the dominant emission pathways and their behaviour over time, it becomes possible to develop strategies for managing and mitigating the environmental impact associated with the reservoir's GHG emissions.

- Gravatn

The results for volume vs emissions intensity from Gravatn are given below.

Volume		Emissions intensity (gCO2e/kWh)
Initial Volume	0.34	0
Volume +10%	0.374	0
Volume +15%	0.391	0
Volume +20%	0.408	0
Volume +50%	0.51	0
Volume +100%	0.68	0

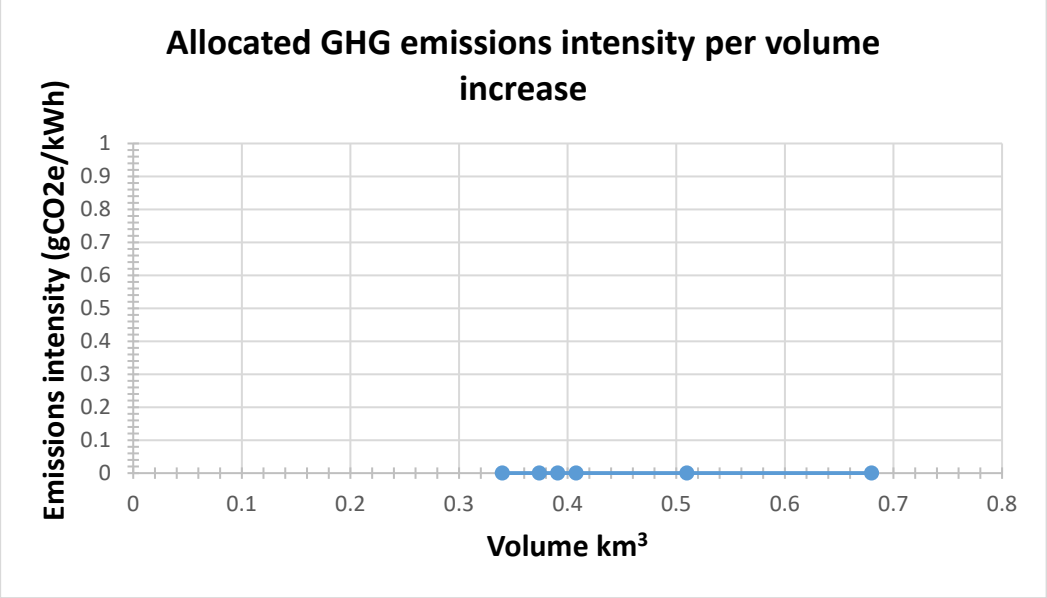

Figure 24 Reservoir Volume VS emissions intensity

The results obtained from Gravatn reservoir are truly remarkable, as they demonstrate its role as a significant greenhouse gas (GHG) sink. This is particularly beneficial considering the current climate situation. The data from the G-RES analysis, which focuses on this reservoir, are outlined below:

The Gravatn reservoir delivers exceptional results, as indicated by a total footprint of

-1852 tCO_2e. This negative value signifies that over the lifespan of the reservoir, it will act as a carbon sink, effectively will sink 1852 tCO_2e. Table 23

Table 23 Total footprint

Name of Reservoir	Total Footprint					
		Post Impoundment	Pre Impoundment	Unrelated Anthropogenic Sources	Construction (Reservoir)	Net GHG Footprint
Gravatn	Emission Rate (gCO2e/m2/yr)	52	55	0	0	-3.00
	Emission Rate (tCO2e/m2/yr)	275	294	0	0	-19.00
	Total Lifetime Emissions (tC02e)	27507	29359	0	0	-1852.00

CH_4 will be sunk 31 ($gCO_2e/m^2/yr$), and as the Net GHG emissions are calculated based on Equation 2 Net GHG Footprint, the Net GHG emissions will be -3 ($gCO_2e/m^2/yr$), which means that Gravatn will sink 3 ($gCO_2e/m^2/yr$), every year. Table 24

Table 24 Reservoir emissions by pathway

Name of Reservoir	Reservoir Emissions by Pathway				
		Post-Impoundment	Pre-Impoundment	Unrelated Anthropogenic Sources	Net GHG Footprint
Gravatn	Emission Rate (tCO2e/yr)	275	294	0	-19
	of which CO2	99	-50	0	149
	of which CH4	176	343	0	-167
	Emission Rate (gCO2e/m2/yr)	52	55	0	-3
	of which CO2	18	-9	0	27
	of which CH4	33	64	0	-31

These findings highlight the significant carbon sequestration potential of the Gravatn reservoir. By sinking a substantial amount of CO_2 and effectively managing methane emissions, it plays a crucial role in mitigating greenhouse gas emissions and combating climate change. The negative Net GHG emissions underscore the reservoir's capacity to act as an ongoing carbon sink, further contributing to the reduction of atmospheric carbon dioxide levels. Such results showcase the importance of reservoirs in climate change mitigation strategies and emphasize the positive environmental impact of the Gravatn reservoir.

Power density for this reservoir is 22.5W/m^2, since the number is high it means that this project doesn’t require the larger areas and larger volumes to generate

the energy, which also means that less area is necessary to be flooded. Allocated GHG emissions intensity is 0gCO_2e/kWh which is low since the reservoir is expanded and not build, which caused lower intensity. For Norway the national number as already mentioned before is following: 3.33 gCO_2e/kWh

Figure B18 describes the Worldwide comparison. From where we can read that CH_4 diffusive is 27 ($gCO_2e/m^2/yr$), CH_4 bubbling=5($gCO_2e/m^2/yr$), CH_4 degassing =($gCO_2e/m^2/yr$), and CO_2 diffusive = 18($gCO_2e/m^2/yr$).

The 100-year distribution of Gravatn is described by Figure B19. As we can see from the first year of operation the reservoir has emissions, which is 185 ($gCO_2e/m^2/yr$). However 33 years the emissions are 0($gCO_2e/m^2/yr$) and 34 years later the reservoir started to sink the emissions. Since its expansion is 53 years(it was expanded in 1970), and nowadays data reservoir has already sunk 24($gCO_2e/m^2/yr$). After 100 years of operation since the expansion reservoir will be able to sink 46($gCO_2e/m^2/yr$).

By the annual total GHG emissions by emission pathway, the first-year reservoir emitted CO_2 diffusive = 144.531($gCO_2e/m^2/yr$). CH_4 diffusive = 90.844 ($gCO_2e/m^2/yr$). and CH_4 bubbling = 5.144 ($gCO_2e/m^2/yr$)., after 100 years these numbers are 0 ($gCO_2e/m^2/yr$).

- Roskreppfjord- Kverevatn

In contrast to the previously expanded reservoirs, Roskreppfjord-Kverevatn presents different results that distinguish it from its counterparts. Despite being an expanded reservoir, it deviates from the trend observed in other reservoirs. While some reservoirs showcased lower emissions and even the potential for carbon sinking, Roskreppfjord-Kverevatn exhibits higher emissions and a substantial intensity rate.

It is worth noting that a common pattern emerges in this reservoir, similar to others, where increased volume correlates with decreased emissions. This observation suggests that reservoir volume plays a significant role in influencing emissions levels.

However, it is crucial to acknowledge that the accuracy of the provided data should be verified through real-life measurements. Conducting calculations based on real-time data will enable a more precise assessment of the reservoir's emissions profile. Only through such rigorous analysis can the validity of the reported results be confirmed.

Therefore, it is recommended to validate the data through field measurements and ensure that the calculations accurately represent the emissions and intensity of Roskreppfjord-Kverevatn. This verification process is essential to ascertain the

accuracy and reliability of the results presented and to provide a more comprehensive understanding of the reservoir's environmental impact.

The intensity rate associated with this project is relatively high, at 5.7 gCO_2e/kWh Figure 25. This value exceeds the national average for Norway, which stands at 3.33 gCO_2e/kWh. The disparity in intensity rates calls for an in-depth analysis to identify the specific factors or operational practices contributing to the higher emissions associated with this project. Understanding these factors is crucial for developing strategies to mitigate and reduce the emissions intensity, aligning it with national sustainability goals.

Volume		Emissions intensity (gCO2e/kWh)
Initial Volume	0.695	7.3
Volume +10%	0.7645	6.9
Volume +15%	0.799	6.7
Volume +20%	0.834	6.6
Volume +50%	1.0425	5.7
Volume +100%	1.39	4.5

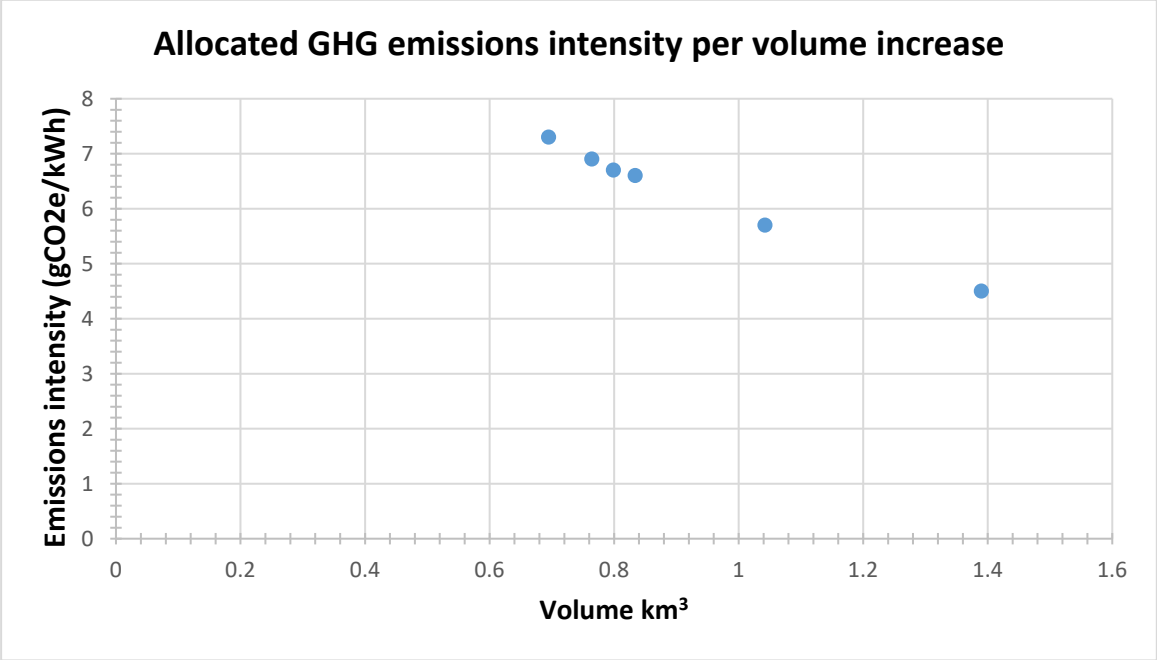

Figure 25 Reservoir volume vs emissions intensity

The power density of this particular project is remarkably low, measuring at 1.7 W/m^2. This figure raises significant questions because such a low power density suggests that a substantial volume of water is required for power production. It prompts further investigation to confirm the accuracy of this data and understand the factors contributing to this low power density. This number is also lower than the threshold given by the EU Taxonomy for Sustainable Finance, which means that this project can't have a green hydropower certificate.

The data provided in Table 25 reveals that the total footprint of the Kvifjorden reservoir is 77087 tCO_2e. We can read from the table below that this reservoir pre-impoundment had high emissions.

Table 25 Total footprint

Name of Reservoir	Total Footprint					
		Post Impoundment	Pre Impoundment	Unrelated Anthropogenic Sources	Construcitio n (Reservoir)	Net GHG Footprint
Roskreppfjord-Kverevatn	Emission Rate (gCO2e/m2/yr)	37	11	0	0	26.00
	Emission Rate (tCO2e/m2/yr)	1095	324	0	0	771.00
	Total Lifetime Emissions (tC02e)	109487	32400	0	0	77087.00

This footprint is calculated based on CO_2 emissions of 23 $gCO_2e/m^2/yr$ and CH_4 emissions of 3 $gCO_2e/m^2/yr$. Table 26

Table 26 Reservoir emissions by pathway

Name of Reservoir	Reservoir Emissions by Pathway				
		Post-Impoundment	Pre-Impoundment	Unrelated Anthropogenic Sources	Net GHG Footprint
Roskreppfjord-Kverevatn	Emission Rate (tCO2e/yr)	1095	324	0	771
	of which CO2	694	0	0	694
	of which CH4	401	324	0	77
	Emission Rate (gCO2e/m2/yr)	37	11	0	26
	of which CO2	23	0	0	23
	of which CH4	14	11	0	3

The higher emissions observed in the Kvifjorden reservoir can be attributed to the construction process and subsequent changes in the ecosystem. The conversion from a natural state to a reservoir often leads to the release of previously sequestered carbon and the disturbance of methane-emitting organic matter.

These results highlight the importance of considering the specific characteristics of each reservoir within a scheme. The Kvifjorden reservoir's emissions profile indicates a need for further analysis and potential mitigation strategies to minimize its environmental impact.

In a worldwide comparison, the CH_4 diffusive emission of this reservoir is recorded at 13 $gCO_2e/m^2/yr$, which falls below the global average. Similarly, the CH_4 bubbling emission is at 1 $gCO_2e/m^2/yr$, aligning with the average value. Additionally, the CO_2 diffusive emission is measured at 23 $gCO_2e/m^2/yr$, also lower than the global mean. Results can be seen on Figure B20

Despite this reservoir having a high-intensity value and relatively higher emissions on a global scale, it still maintains a low overall impact. These

emission values indicate that the reservoir's emissions are comparatively moderate when considering global standards and benchmarks.

It is worth noting that these findings provide insight into the reservoir's performance relative to worldwide emissions levels. By comparing these results to global averages, we can evaluate the reservoir's environmental impact on a broader scale. These lower emission values, particularly for CH_4 and CO_2 diffusive emissions, highlight the reservoir's relatively lower contribution to global greenhouse gas emissions.

However, it is crucial to conduct further analysis and consider local and regional factors to gain a comprehensive understanding of the reservoir's impact within its specific context. Evaluating the reservoir's performance against both global and local benchmarks will facilitate a more accurate assessment of its environmental implications and inform appropriate mitigation strategies.

The 100-year distribution of the Roskreppfjord-Kverevatn reservoir is represented below. Analyzing these figures reveals several notable trends. In the first year of operation, the reservoir exhibited emissions totalling 199.6 $gCO_2e/m^2/yr$. However, after 68 years, since the expansion the emissions reached zero (0 $gCO_2e/m^2/yr$). Remarkably, 69 years later, the reservoir transitioned into a carbon sink, actively sequestering emissions.

Forecasts for the next 100 years, based on the reservoir's expansion, suggest it will be capable to sink 9 $gCO_2e/m^2/yr$. Figure B21

Examining the annual total GHG emissions by emission pathway, we can read the following data:

CO_2 diffusive = 182.359 $gCO_2e/m^2/yr$

CH_4 diffusive = 27.32 $gCO_2e/m^2/yr$

CH_4 bubbling = 0.794 $gCO_2e/m^2/yr$

However, over the course of 100 years, these emission figures steadily decline to zero.

These findings provide valuable insights into the long-term emission patterns and carbon sequestration potential of the Roskreppfjord-Kverevatn reservoir. The data highlights a significant reduction in emissions over time and reinforces the reservoir's capacity to serve as a carbon sink.

- Øysteinevja

The results regarding volume vs intensity from Øysteinevja, are given below. Since the reservoir is expanded, the emission intensity at any volume value is 0.1. Figure 26

Volume		Emissions intensity (gCO2e/kWh)
Initial Volume	0.104	0.1
Volume +10%	0.1144	0.1
Volume +15%	0.120	0.1
Volume +20%	0.1248	0.1
Volume +50%	0.156	0.1
Volume +100%	0.208	0.1

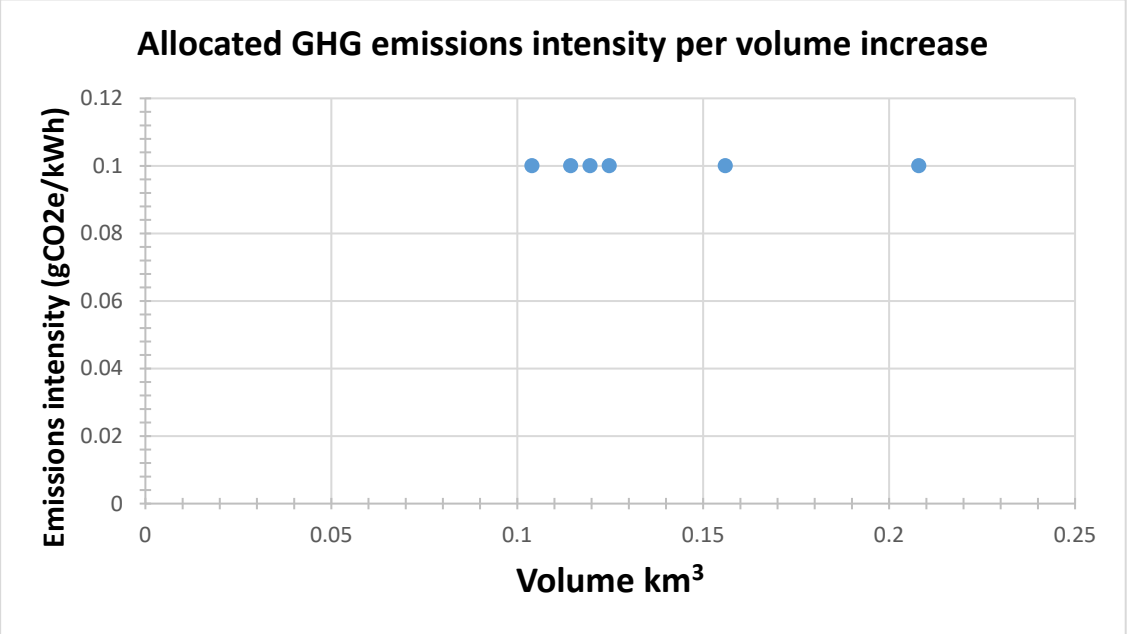

Figure 26 Reservoir volume vs emissions intensity

The Øysteinevja reservoir the following results, evident through its total footprint of 23343 tCO_2e Table 27.

Table 27 Total footprint

Name of Reservoir	Total Footprint					
		Post Impoundment	Pre Impoundment	Unrelated Anthropogenic Sources	Construction (Reservoir)	Net GHG Footprint
Øyarvatn	Emission Rate (gCO2e/m2/yr)	43	14	0	0	29.00
	Emission Rate (tCO2e/m2/yr)	344	111	0	0	233.00
	Total Lifetime Emissions (tC02e)	34446	11103	0	0	23343.00

The reservoir emits CO_2 at a rate of 25 $gCO_2e/m^2/yr$. This signifies the amount of CO_2 released per square meter annually. CH_4 emissions:CH_4 = 2 $gCO_2e/m^2/yr$

By employing Equation 2 Net GHG Footprint to calculate the results, it is determined that the Øysteinevja reservoir has a net emission rate of 29 $gCO_2e/m^2/yr$. Table 28

Table 28 Reservoir emissions by pathway

Name of Reservoir	Reservoir Emissions by Pathway				
		Post-Impoundment	Pre-Impoundment	Unrelated Anthropogenic Sources	Net GHG Footprint
Øyarvatn	Emission Rate (tCO2e/yr)	344	111	0	233
	of which CO2	204	-12	0	216
	of which CH4	140	123	0	17
	Emission Rate (gCO2e/m2/yr)	43	14	0	29
	of which CO2	25	0	0	25
	of which CH4	17	15	0	2

Overall, the Øysteinevja reservoir demonstrates a positive environmental performance, with low net GHG emissions and a capacity to effectively mitigate methane emissions. Its ability to sequester methane contributes to the larger efforts in combating climate change and establishes the reservoir as an environmentally responsible source of energy.
The power density of this particular project is remarkably too high, measuring 118.8 W/m^2. This reservoir has possibility to gain green hydropower certificaty under EU taxonomy. Allocated GHG emissions intensity is 0 gCO_2e/kWh which is low for Norway. For Norway the national number as already mentioned before is the following: 3.33 gCO_2e/kW

In a worldwide comparison, the CH_4 diffusive emission of this reservoir is recorded at 15 $gCO_2e/m^2/yr$, which falls below the global average. Similarly, the CH_4 bubbling emission is at 2 $gCO_2e/m^2/yr$, aligning with the average value. Additionally, the CO_2 diffusive emission is measured at 25 $gCO_2e/m^2/yr$, also lower than the global mean. Figure B22

The 100-year distribution of Øysteinevja is described by As we can see from the first year of operation the reservoir has emissions, which is 254.3 ($gCO_2e/m^2/yr$). However 75 years the emissions are 0($gCO_2e/m^2/yr$) and 77 years later the reservoir started to sink the emissions. After 100 years of operation since the expansion reservoir will be able to sink 9 ($gCO_2e/m^2/yr$).

By the annual total GHG emissions by emission pathway, the first-year reservoir emitted CO_2 diffusive = 197.59 ($gCO_2e/m^2/yr$). CH_4 diffusive = 67.92 ($gCO_2e/m^2/yr$) and CH_4 bubbling = 2.11 ($gCO_2e/m^2/yr$)., after 100 years these numbers are 0 ($gCO_2e/m^2/yr$). Figure B23

- Kvifjorden (Nesjen)

The Figure 27 exhibits a consistent pattern observed in previous reservoirs, wherein an increase in volume coincides with a decrease in emissions intensity. This trend underscores the notion that as the reservoir volume expands, the emissions intensity diminishes accordingly.

Volume		Emissions intensity (gCO2e/kWh)
Initial Volume	0.275	1
Volume +10%	0.3025	0.9
Volume +15%	0.316	0.9
Volume +20%	0.33	0.9
Volume +50%	0.4125	0.8
Volume +100%	0.55	0.7

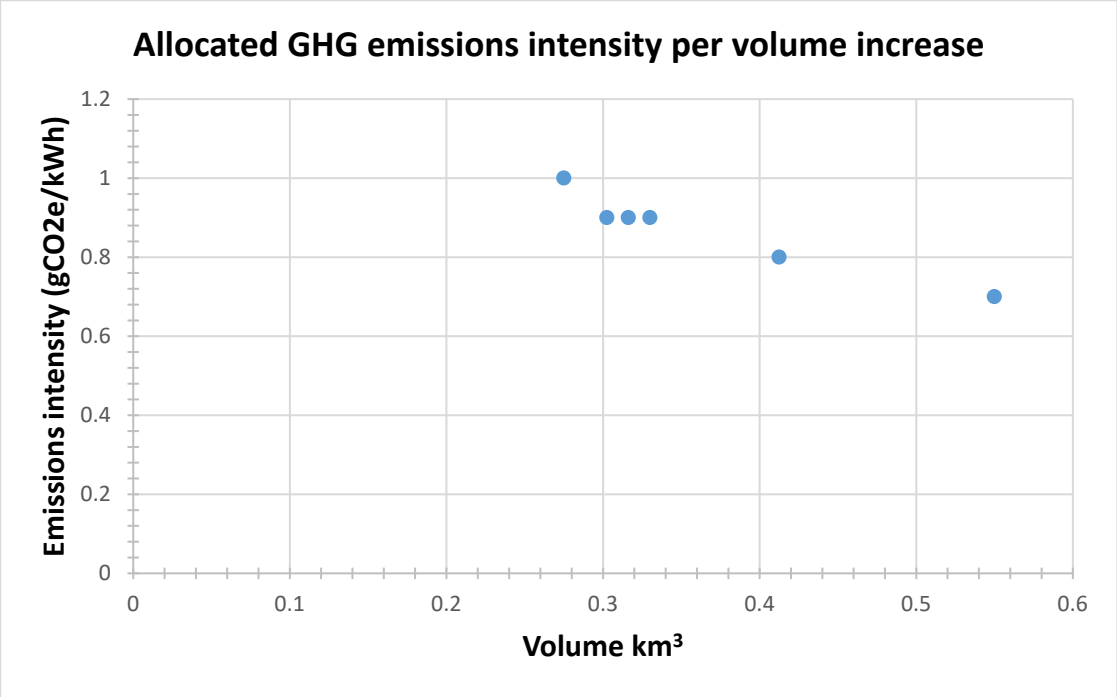

Figure 27 Reservoirs volume vs emissions intensity

The Kvifjorden-Nesjen reservoir showcases the following results, with a total footprint of 63990 tCO_2e. Table 29

Table 29 Total footprint

Name of Reservoir	Total Footprint					
		Post Impoundment	Pre Impoundment	Unrelated Anthropogenic Sources	Constructio n (Reservoir)	Net GHG Footprint
Kvifjorden-nesjen	Emission Rate (gCO2e/m2/yr)	48	7	0	0	41.00
	Emission Rate (tCO2e/m2/yr)	743	103	0	0	640.00
	Total Lifetime Emissions (tC02e)	74265	10275	0	0	63990.00

CO_2 emissions: The reservoir emits CO_2 at a rate of 31 $gCO_2e/m^2/yr$. This indicates the amount of CO_2 released per square meter annually, reflecting its carbon footprint. CH_4 emissions: The reservoir exhibits CH_4 emissions of 10 $gCO_2e/m^2/yr$. This signifies the methane emissions per square meter annually. Table 30

Table 30 Reservoir emissions pathway

Name of Reservoir	Reservoir Emissions by Pathway				
		Post-Impoundment	Pre-Impoundment	Unrelated Anthropogenic Sources	Net GHG Footprint
Kvifjorden-nesjen	Emission Rate (tCO2e/yr)	743	103	0	640
	of which CO2	415	-68	0	483
	of which CH4	328	170	0	158
	Emission Rate (gCO2e/m2/yr)	48	7	0	41
	of which CO2	27	-4	0	31
	of which CH4	21	11	0	10

Despite being a built reservoir, it is noteworthy that Kvifjorden-Nesjen exhibits low emissions. This represents a positive characteristic of the hydropower project, emphasizing its favorable environmental performance. The ability to maintain low emissions despite being a built reservoir underscores the project's commitment to sustainability and highlights its effectiveness in minimizing greenhouse gas emissions.

These findings further contribute to positioning Kvifjorden-Nesjen as an environmentally friendly hydropower project, aligning with the broader goals of reducing carbon footprints and mitigating climate change impacts.

Power density for this reservoir is $13W/m^2$, since the number is not too high, it means that this project maybe requires the larger areas and larger volumes to generate the energy. Allocated GHG emissions intensity is 0.8 gCO_2e/kWh which is low for Norway. For Norway the national number as already mentioned before is following: 3.33 gCO_2e/kWh

In terms of global comparison, this reservoir's CH_4 diffusive emission is 18 $gCO_2e/m^2/yr$, which is lower than the global average. Similarly, the CH_4 bubbling emission is 3 $gCO_2e/m^2/yr$, which is in line with the average. Furthermore, the CO_2 diffusive emission is measured at 27 $gCO_2e/m^2/yr$, which is lower than the world average.

Despite the fact that it is a build reservir on a global scale, this reservoir has a modest overall impact. When compared to worldwide norms and benchmarks, these emission figures suggest that the reservoir's emissions are quite low. Figure B24

The reservoir's 100-year distribution is shown here for Kvifjorden (Nesjen). The examination of these numbers reveals numerous interesting tendencies. The

reservoir produced 277 $gCO_2e/m^2/yr$ of emissions in its first year of operation. Figure B25

We may read the following statistics by examining annual total GHG emissions by emission pathway:

CO_2 diffusive = 215.288 $gCO_2e/m^2/yr$

CH_4 diffusive = 63.58g $gCO_2e/m^2/yr$

CH_4 bubbling = 4.957 $gCO_2e/m^2/yr$

However, over the course of a century, these emission levels gradually drop to zero, CH_4 will maintain its value of 4.957 $gCO_2e/m^2/yr$.

- Homstølvatnet

Homstølvatnet is the next expanded reservoir in the Sira-Kvina scheme. It is an expanded reservoir with very low emissions.

The volume emissions intensity can be found below.

Volume		Emissions intensity (gCO2e/kWh)
Initial Volume	0.055	0
Volume +10%	0.0605	0
Volume +15%	0.063	0
Volume +20%	0.066	0
Volume +50%	0.0825	0
Volume +100%	0.11	0

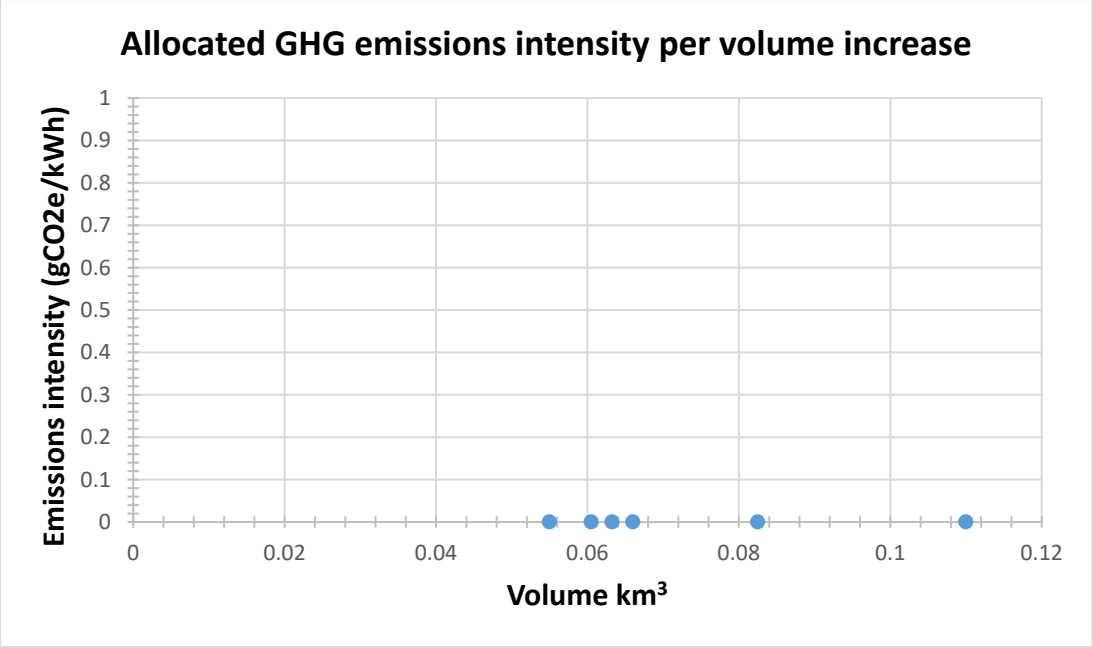

Figure 28 Reservoir volume vs emissions intensity

Based on the available data, the reservoir exhibits a total footprint of 11,919 tCO_2e. Table 31

Table 31 Total footprint

Name of Reservoir	Total Footprint					
		Post Impoundment	Pre Impoundment	Unrelated Anthropogenic Sources	Construcitio n (Reservoir)	Net GHG Footprint
Homstølvatnet	Emission Rate (gCO2e/m2/yr)	36	-5	0	0	41.00
	Emission Rate (tCO2e/m2/yr)	105	-14	0	0	119.00
	Total Lifetime Emissions (tC02e)	10548	-1371	0	0	11919.00

This calculation takes into account the following emission values: CO_2 emissions of 48 $gCO_2e/m^2/yr$ and notably, negative CH_4 emissions of -7 $gCO_2e/m^2/yr$. Table 32 . The negative value assigned to CH_4 emissions indicates that methane emissions may have sunk following the expansion of the lake. This implies that per square meter, 7g of CH_4 will sink yearly. Such a significant reduction in CH_4 emissions can have a substantial impact on overall greenhouse gas (GHG) emissions. The sinking of 7g of CH_4 per square meter each year signifies an effective mitigation strategy, as the reservoir actively removes methane from the atmosphere. This accomplishment holds particular significance, as methane is a potent GHG with a greater warming potential compared to CO_2.

Table 32 Reservoir emissions by pathway

Name of Reservoir	Reservoir Emissions by Pathway				
		Post-Impoundment	Pre-Impoundment	Unrelated Anthropogenic Sources	Net GHG Footprint
Homstølvatnet	Emission Rate (tCO2e/yr)	105	-14	0	119
	of which CO2	50	-89	0	139
	of which CH4	55	75	0	-20
	Emission Rate (gCO2e/m2/yr)	36	-5	0	41
	of which CO2	17	-31	0	48
	of which CH4	19	26	0	-7

These findings highlight the reservoir's ability to contribute to GHG reduction efforts through the suppression of methane emissions. The substantial decrease in CH_4 emissions after the lake expansion is a positive outcome, demonstrating the project's success in mitigating its environmental impact.

The power density is $332.2W/m^2$, which is a very good result and indicates that larger areas do not need to be flooded in order to have energy. Furthermore, the assigned greenhouse gas (GHG) emissions intensity for this reservoir is 0 gCO_2e/kWh. This figure is much lower than Norway's national emissions intensity, which is 3.33 gCO_2e/kWh. The analyzed reservoir's exceptionally low emissions intensity emphasizes its environmental superiority over past reservoir constructions.

In terms of worldwide comparison, the CH_4 diffusive emission from this reservoir is 16 $gCO_2e/m^2/yr$, which is lower than the global average. Similarly, the CH_4 bubbling emission is 2 $gCO_2e/m^2/yr$, which is comparable to the national average. Furthermore, the CO_2 diffusive emission is 17 $gCO_2e/m^2/yr$, which is lower than the global average. Figure B26

The reservoir's 100-year distribution is depicted. Figure for Homstlvatnet An analysis of these figures reveals following results. In its first year of operation, the reservoir emitted 224 $gCO_2e/m^2/yr$.

Forecasts for the next 100 years based on reservoir expansion imply that it will be 10$gCO_2e/m^2/yr$. Figure B27

By studying annual total GHG emissions by emission route, we may deduce the following statistics:

CO_2 diffusive = 137.987 $gCO_2e/m^2/yr$.

CH_4 diffusive = 78.847 $gCO_2e/m^2/yr$.

CH_4 bubbling = 2.248 $gCO_2e/m^2/yr$.

Over the course of a century, these emission levels progressively decline to zero, however, CH_4 bubbling will maintain its result (2.248 $gCO_2e/m^2/yr$)

In the Sira-Kvina scheme, a single reservoir, Kvifjorden, is constructed, while the others undergo expansion or regulation. Surprisingly, despite their similar volume and area, Kvifjorden does not emerge as the primary greenhouse gas (GHG) emitter within the scheme. Instead, the expanded reservoir consistently exhibits higher emissions. This discrepancy raises concerns as the expected emission pattern suggests that the constructed reservoir should have lower emissions. Therefore, it is crucial to conduct real-life assessments of these reservoirs and gather precise data. Only then can we accurately calculate the exact GHG emissions associated with each reservoir, allowing for a comprehensive evaluation of their environmental impact.

The Figure 29 presents the emissions rate in Sira-Kvina scheme.

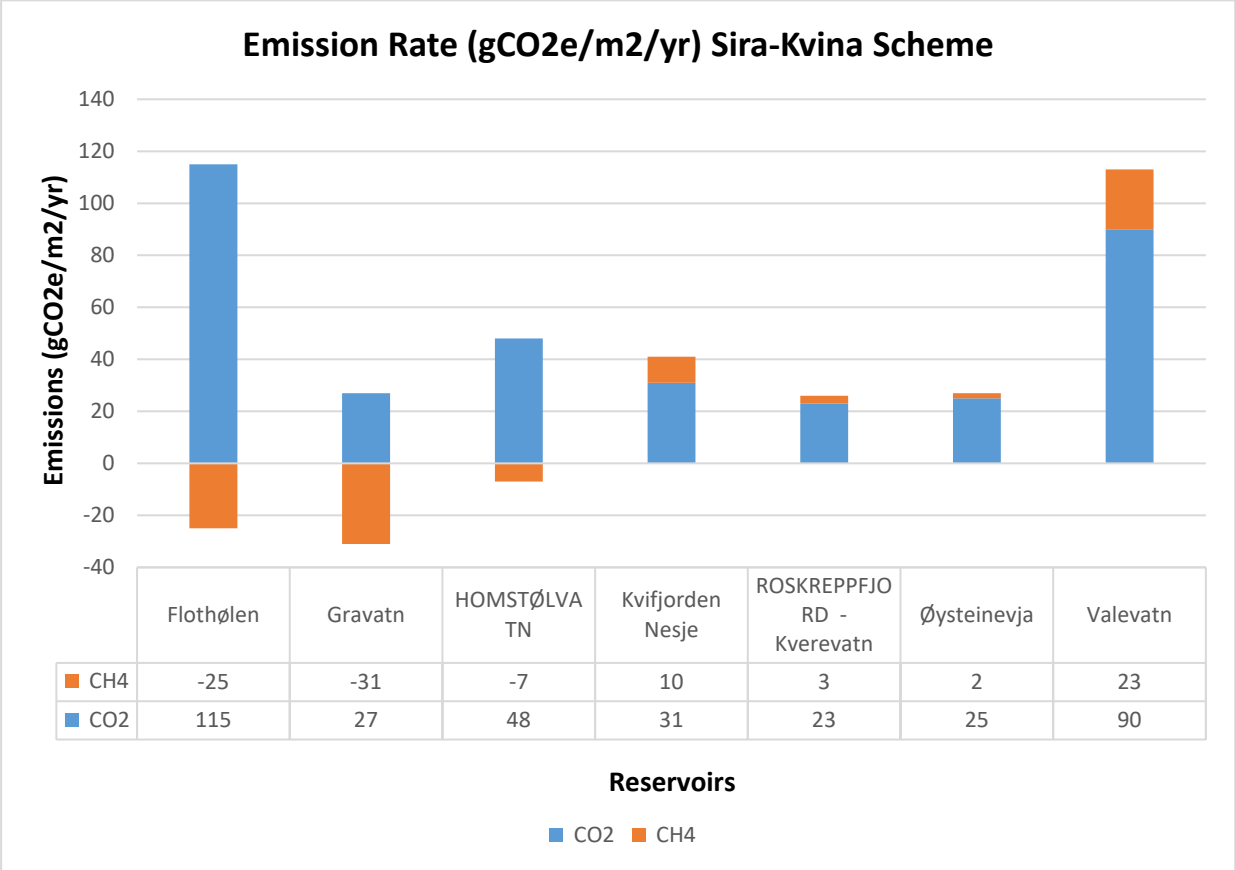

Figure 29 Emissions rate Sira-Kvina scheme

After conducting simulations and calculations, a thorough examination of emission intensities for Norway was carried out based on the obtained data. The analysis focused on 15 reservoirs, specifically those with mineral soil, excluding mixed soil types. The average emission number from these selected reservoirs was found to be 1.37($gCO_2e/m^2/yr$). This number is lower than the national number for Norway, which is 3.33($gCO_2e/m^2/yr$), it also indicates that the reservoirs in Norway have the potential to generate environmentally friendly or "green" electricity.

Figure 30 illustrates the emissions intensity numbers of the studied reservoirs. Notably, Kverevatn in the Sira-Kvina scheme shows the highest intensity at 5.7($gCO_2e/m^2/yr$). However, this exceptionally high figure raises doubts about its accuracy. On the other hand, the Orkla and Sira-Kvina schemes demonstrate the lowest intensity figures, with a 0($gCO_2e/m^2/yr$) intensity. It is important to note that the 0($gCO_2e/m^2/yr$) value attributed to the Orkla scheme originates from Granasjøen, where the scenario involves mineral and organic soil. In this case, the analysis tool considers the impoundment of organic soil as a potential sink, raising concerns about the accuracy of this particular result. Consequently, only two reservoirs, Gravatn and Homstølvatn, exhibit 0($gCO_2e/m^2/yr$) emissions, which are likely the most reliable values in this context.

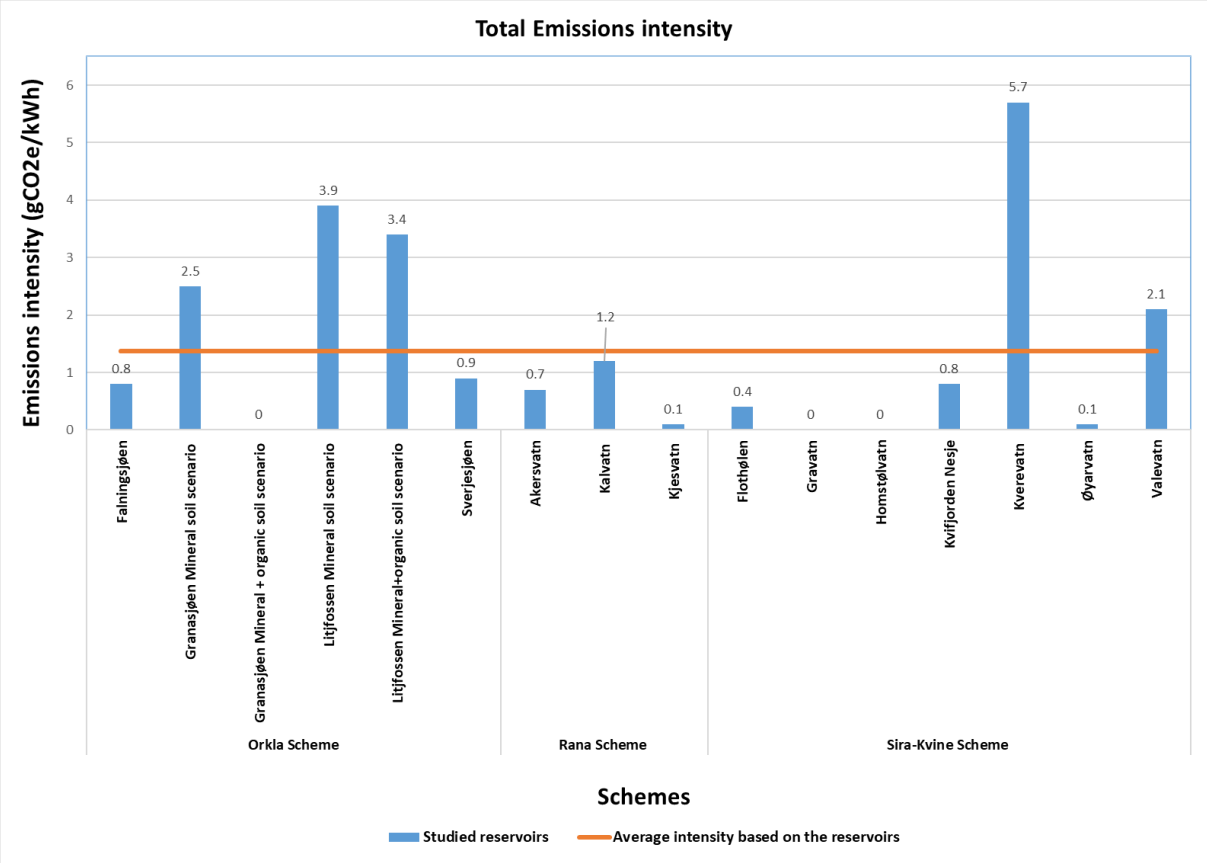

Figure 30 Emissions intensity from studied reservoirs

8 Discussion and Recommendations

8.1 Emissions from other renewable energies

8.1.1 Onshore Wind

The importance of land coverage and soil type in assessing the greenhouse gas (GHG) emissions associated with energy production becomes evident when considering the case of hydropower. In hydropower projects, if the land that was flooded during dam construction consisted of highly vegetated areas or had organic soil, the resulting emissions were found to be significantly higher. However, it should be noted that the G-RES tool, previously mentioned, inaccurately accounted for emissions from organic soil by treating it as an emission sink after impoundment, which is not correct.

Similarly, in the context of wind power production, land plays a crucial role, although it does not involve flooding. If a suitable location for a wind farm happens to be a highly forested area, the unfortunate consequence is the clearance of those trees. Deforestation is a significant contributor to the chain of GHG emissions, as trees act as important stores and sink for these emissions, actively sequestering carbon dioxide.

However, it's not just the loss of trees that can impact emissions in wind power projects. The process of constructing a wind farm itself involves land disturbance, which can result in the release of previously sunk GHG emissions. Additionally, the change in land coverage from a forested area to agricultural land or bare land, among other possibilities, further influences the overall emissions trajectory.

Thus, it becomes crucial to consider the multifaceted effects of land use and land cover alterations in the context of wind power generation. By recognizing the potential consequences such as deforestation, land disturbance, and changes in land coverage, we can gain a more comprehensive understanding of the increased emissions associated with wind power projects and develop strategies to mitigate their environmental impact.

In this section, the following will be presented.

- The examination of greenhouse gas (GHG) emissions resulting from land-based opportunity changes associated with wind farms.
- Results regarding how the establishment of wind farms effects on soil organic carbon and how land changes
- The emissions intensity derived from the life cycle assessment (LCA) of wind farms, in Norway.

The examination of greenhouse gas (GHG) emissions resulting from land-based opportunity changes associated with wind farms.

All the results are which are presented in this section are taken from the report (Quantifying the land-based opportunity carbon costs of onshore wind farms (Fabrizio Albanito, 2022)) which is based on the results from a study in Scotland. Unfortunately, there is no other detailed study done yet regarding how much CO_2 will be produced after the soil disturbance during the wind farm construction. The study was conducted in Scotland, based on 3348 wind turbines. The analysis indicated that the wind farms analysed in the study generated 4.9 million tonnes of CO_2 from land use changes.

CO_2 emissions from wind farms constructed in peatlands:

60 wind plants were examined to check CO_2 emissions from wind farms constructed in peatlands, from where we have the following data:

The total emissions: 4013230 tCO_2

CO_2 emissions from wind farms constructed in forest:

34 wind plants were examined to check CO_2 emissions from wind farms constructed in forest. Based on the premise that each turbine required 1 hectare of forest to be removed for construction, the total amount of forest directly displaced by wind turbines was roughly 783 ha. The amounts removed varied among the five forest types as follows: felled > conifer > broadleaved > mixed mostly broadleaved > shrub. The results are following:

The total emissions from direct emissions (DE): 367400 tCO_2

The total emissions from indirect emissions (IE): 139904 tCO_2

CO_2 emissions from wind farms constructed in croplands and other land use type:

Results are based on the 68 wind farms constructed or under construction in cropland and distributed across 45 agricultural parishes. Also 137 wind farms on the “other land uses” comprises nardus - molinia grasslands, dry and wet heather moor, montane vegetation, undefined mixed woodland, pasture land, low scrubland, and smooth grasslands. The results are following:

The total emissions from arable land: 37858 tCO_2

The total emissions from other land uses: 312844 tCO_2

Results regarding how the establishment of wind farms effects on soil organic carbon and how land changes

All the results are which are presented in this section are taken from the report (Assessing the effects of wind farms on soil organic carbon (Ozge Isik Pekkan, 2021))

The purpose of this study is to estimate the change in soil organic carbon (SOC) stock induced by land cover changes produced by wind farm setups in the Karaburun peninsula.

Land-use change caused by the loss of forests and grasslands can result in considerable carbon emissions that contribute to the greenhouse effect. From the report we can read that wind farm installations modified an area of 466.39 ha, of which 330.19 ha were bare fields and 136.20 ha were artificial surfaces. According to the assessments, the installation of wind farms on the Karaburun Peninsula resulted in a total decrease in SOC of 18,330.57 tC Table 27.

Table 33 provides important insights into the profound impact of wind farms on land coverage. As already mentioned, land coverage changes for wind farm infrastructure have a huge influence on climate change, since it may lead to chopping down healthy trees, or even it can destroy carbon storage and lead to the emissions released into the atmosphere. A careful examination of the table reveals a striking transformation: the forest land coverage area has decreased by nearly sixfold, giving way to bare land. This alteration has worrisome implications for climate change mitigation efforts. More can be found in Figure B1.1

Table 33 Soil organic carbon change depending on land cover change due to wind farm establishment (Ozge Isik Pekkan, 2021)

From	To	Amount (ha)	Change (t C per ha)	Total change (t C)
Forest	Bare land	280.36	-42.91	-12030.25
Forest	Artificial surfaces	125.58	-39.56	-4967.94
Bare land	Artificial surfaces	1.04	3.34	3.47
Agriculture	Bare land	49.28	-23.18	-1142.31
Agriculture	Artificial surfaces	9.58	-19.84	-190.07
Total				-18327.1

The location of wind power stations, which are considered renewable and clean energy sources, is critical for soil organic carbon stock. This decrease in the quantity of soil organic carbon store will surely have physical, chemical, and biological effects. At the same time, a reduction in soil organic carbon store corresponds to an increase in atmospheric carbon. Each ton of SOC is comparable to 3.67 tons of CO_2 in the atmosphere. The SOC reduction of 18,330.57 t found in this investigation is comparable to 67,273.20 tons of atmospheric carbon at this time. As a result, it should be considered that, in addition to numerous other harmful impacts (effects on human health, effects on the ecology, etc.), As a result, in addition to many other negative impacts (effects on human health, affects on the ecology, effects on animals, and so on),

land cover changes generated by wind farms may indirectly create major problems such as climate change.

The emissions intensity derived from the life cycle assessment (LCA) of wind farms, both on a global scale and with a specific focus on Norway.

In this section, we will review the outcomes of two Norwegian onshore wind farms, Kjllefjord and Fjeldskr, based on LCA (Life Cycle Assessments). Findings are retrieved from *The Norwegian Research Council and partner consortium in the Energy Trading and Environment 2020 project* -GHG emissions and energy performance of wind power by Hanne Lerche Raadal and Bjørn Ivar Vold (The Norwegian Research Council, 2020)

According to the findings, the overall GHG emissions for wind power generation from Kjllefjord and Fjeldskr are 11.0 and 15.1 g CO_2-equivalents/kWh, respectively, with the wind farm with its largest turbines emitting the least Figure B1.2. Consequently, it becomes imperative to prioritize the utilization of steel produced through renewable energy sources.

To assess the environmental impact of different energy mixes used in steel manufacturing, which is a major contributor to overall greenhouse gas (GHG) emissions, specific scenarios have been developed for each wind farm. These scenarios primarily focus on the European average electricity consumption mix (Centre for Life cycle inventories, n.d.). Additionally, two additional scenarios have been created to represent a "worst case" and "best case" situation.

Considering that the project is owned by Statkraft, an evaluation of the impact of a gravitation foundation compared to the base case's solid rock foundation was also conducted.

Based on the information presented in Figure B1.3 it is evident that the steel manufacturing process powered by hydroelectricity has the lowest (aCO_2-eqv./kWh) for both wind farms. Furthermore, with regard to the foundation type, the rock foundation exhibited the lowest emissions at the foundation level.

In conclusion, the findings emphasize the significance of employing renewable energy sources, in the steel manufacturing process for this wind farms. Additionally, they highlight the benefits of utilizing a solid rock foundation to minimize emissions at the foundation level.

On a world basis, wind energy has the lowest carbon footprint of any source of energy. On a life-cycle basis, onshore wind emits 11 grams of CO_2 equivalent to every kWh of energy generated, whereas offshore wind emits 12 grams. Wind energy aids in the fight against climate change and offers several other environmental advantages. Figure B1.4

8.1.2 Offshore wind

In this section we will review the report which presents a comprehensive analysis of six distinct offshore conceptual designs, focusing primarily on evaluating their respective emissions Table 34. The main objective was to assess and compare the environmental impact of these designs. The study encompassed five floating concepts and one bottom-fixed concept, thoroughly examining the emissions associated with each model. Findings are retrieved from *The Norwegian Research Council and partner consortium in the Energy Trading and Environment 2020 project* -GHG emissions and energy performance of wind power by Hanne Lerche Raadal and Bjørn Ivar Vold (The Norwegian Research Council, 2020)

Table 34 Short description of analysed concepts (The Norwegian Research Council, 2020)

Concept	Name	General Description
Floating	Sway	Tension-Leg Spar (TLS) similar to the SWAY concept
	Umaine Semi-s	Umaine Semi-Submersible
	Umaine Spar	Umaine Spar-Buoy (same as OC3-Hywing, at water depth of 200m)
	Umaine TLP	Tension-Leg Platfrom with vertical tendons
	MIT TLB	MIT Tension-Leg Buoy (TLB)
Bottom-Fixed	OC4 Jacket	IEA OC4 Jacket

The default wind farm has a lifespan of 20 years and a capacity factor of 46%. The Capacity Factor (CF) is calculated by dividing the actual yearly electricity output by the maximum feasible annual electricity generation (at full power). It is given as a fraction or as a percentage. The functional unit for the analysis in this study was 1 kWh of onshore energy generated and supplied into the system. As a result, the GHG emissions and energy performance described in this study correspond to 1 kWh of onshore wind power transmitted to the grid. The system limits contain all key life cycle stages, such as raw material manufacturing, transportation, installation, and decommissioning, among others. This is in conformity with the International EPD System's Product Category Rules for energy generation. (The International EPD system, 2011). Grid losses through cables from offshore to onshore have not been included

The outcomes of GHG emissions are divided into life cycle stages. Table 35

Table 35 Short description of the life cycle stages being included in the analyses. (The Norwegian Research Council, 2020)

Life cycle stage	Description
Installation (fuel)	Fuel consumption related to the transportation of all the equipment from shore to offshore site in order to install the wind farm.
Turbine materials	Production, processing and transport of all the infrastructure material related to the turbine production. Disposal of materials is also included (credits from material to recycling are not included).
Platform materials	Production, processing and transport of all the infrastructure material related the platform production, including production of internal and external (from offshore to shore) cables. Disposal of materials is also included (credits from material to recycling are not included).
Maintenance (fuel)	Fuel consumption related to the transportation from shore to offshore site due to maintenance.
Maintenance (infrastructure/ reinvestment)	Production, processing and transport of all the material used for maintenance during the lifetime of the wind farm. The reinvestments needed are given annually and multiplied with the lifetime. Disposal of materials used for maintenance is included in this life stage.
Maintenance (others)	Production, processing and transport of support materials used for maintenance (oil, cotton etc.) and treatment of waste.
Decommissioning (fuel)	Fuel consumed for decommissioning the wind farm. For simplification the decommissioning is assumed equal to the installation (fuel) and operation (reversed). Disposal of materials is included in the life cycle stages Turbine and platform materials, respectively.

The overall GHG emissions from the analyzed offshore ideas range between 18.0 (MIT TLB) and 31.4 (Umaine Semi-S) g CO_2-equivalents/kWh, indicating a 75% increase over the MIT TLB concept (representing the lowest GHG emissions).

Furthermore, Figure B1.10 clearly demonstrates that the turbine and foundation/platform materials contribute the most to total GHG emissions. The platform contribution ranges from 6.3 (MIT TLB) to 19.7 g CO_2-equivalents/kWh, equating to 35% and 63% of total GHG emissions from each installation, respectively. Since the tower and RNA are identical, the changes between the ideas are classified as equivalent. Several platform ideas are further investigated in order to identify the most significant factors influencing these GHG emissions. Figure B1.11

As shown in Figure B1.11, steel manufacturing is the largest contributor to overall platform GHG emissions for all designs (divided into steel linked to the platform and anchor/cables, respectively). Depending on the idea, steel manufacturing produces 50% to 89% of total platform GHG emissions. Apart from the MIT TLB, the production of aluminum in conjunction with internal and external connections is the second greatest platform contributor. External cables provide 1.95 g CO_2-equivalents/kWh in total.

As indicated in Figure B1.11, the GHG emissions from turbine materials (assumed to be the same for all concepts) are 4.7 g CO_2-equivalents/kWh, accounting for 15% (Umaine Semi-S) to 26% (MIT TLB) of total GHG emissions.

Figure B1.12 introduces the major parameters influencing turbine GHG emissions.

The Figure B1.12 illustrates that steel and glass fiber has the greatest impact on turbine GHG emissions, accounting for 55% and 27%, respectively. Furthermore, the primary turbine components (tower, rotor, and nacelle) each generate around one-third of total turbine GHG emissions.

Figure B1.10 further shows that the installation and decommissioning life cycle activities produce 6.2 and 5.8 g CO_2-equivalents/kWh for the bottom fixed and floating concepts, respectively. This indicates a range of 18% to 33% of total GHG emissions associated with each installation.

8.1.3 Solar

As mentioned earlier in the wind section, determining the specific CO_2 emissions associated with solar farms, excluding those derived from life cycle assessments (LCAs), presents a significant challenge. Such emissions would provide valuable insights into the release of CO_2 when we "emit" stored emissions from the ground. Nevertheless, it is feasible to assess the impact of solar farm construction on land transformation, including changes in land type and the resulting usable land area.

While quantifying CO_2 emissions directly from solar farms without considering LCAs is difficult, we can analyze the effects of solar farm development on land usage. This analysis allows us to determine how land types will be altered and the extent to which various land areas will be converted. Additionally, we can evaluate the amount of land that will remain usable after the construction of solar farms.

In this section, we will discuss the potential land use change emissions of solar energy from the case study in the EU, India, Japan and South Korea, after this, about the CO_2 emissions based on the LCA study around the world.

Potential land use change emissions of solar energy

Results are based on the scientific report – *The potential land requirements and related land use change emissions of solar energy.* (Dirk-Jan van de Ven, 2021)

Solar energy may occupy 0.5-5% of total land at 25-80% penetration in the areas' electricity mix by 2050. The ensuing changes in land cover, including indirect consequences, will most likely result in a net carbon release ranging from 0 to 50 gCO_2/kWh, depending on the location, scale of development, solar technology efficiency, and land management methods in solar parks. As a result, new solar energy infrastructure should be planned and regulated in a coordinated manner to avoid a major rise in their life cycle emissions due to terrestrial carbon losses.

Figure B1.5 presents the results obtained for the absolute and relative land requirements of solar energy. These results are based on land suitable for commercial production, excluding rooftops, deserts, and dry scrublands. The table showcases data from simulated scenarios with penetration rates ranging from 26% to 79% of the electricity mix, considering various future solar PV module efficiencies.

Europe, due to its lower irradiance and higher latitude, exhibits nearly double the absolute land use per unit of solar output compared to Japan and South Korea, and three times higher than India. This disparity becomes more pronounced as penetration rates increase. It occurs as the potential for solar energy generation on rooftops becomes saturated, coupled with diminishing returns for land-based solar energy.

With solar energy accounting for 25–80% of the power mix, land usage by USSE is expected to be considerable, the results are following:

EU - 0.5–2.8% of the total area

India - 0.3–1.4%

Japan and South Korea - 1.2–5.2%

Because highly attractive solar energy locations, such as southern Europe, northwestern India, southern Japan, and South Korea, are picked in each region, this occupation is unequally distributed over the world. Figure B1.6

The future land requirements of solar energy for each scenario and region can be better understood by comparing them to the existing levels of built-up areas and agricultural cropland. Solar PV panels or CSP heliostats are expected to occupy a significant fraction of the total built-up area, including urban areas and solar land, in all three regions by 2050 assuming solar power accounts for at least half of the energy generated. In particular, solar energy land would exceed 50% of present urban land in the EU, 85% in India, and 75% in Japan and South Korea.

From a contrary perspective, a large quantity of sunlight that might be used for agricultural crop development would instead be used to generate power, notably in Japan and South Korea (29-39%) and the EU (8-10%). The relative allocation of land between crops and solar energy shows notable variations within each region, potentially leading to local ecosystem and landscape implications.

Currently, solar energy infrastructure has a minimal land footprint on a global scale. However, as the goal is to achieve net-zero emissions by 2050, an expansion of solar farms will be necessary, leading to increased land coverage and changes. The magnitude of this indirect influence on land covering is determined by agricultural and forest productivity in areas where solar energy penetration occurs. Cropland would be displaced from regions with higher agricultural productivity, such as the EU, Japan, and South Korea, to places with lower crop output. This shift would indirectly contribute to an increase in

worldwide agricultural coverage, increasing by up to 22% the impact of solar energy growth in these locations on global land competition.

This effect is less pronounced at lower levels of solar energy penetration (even negative in the EU), because solar energy is expected to displace the most marginal farmland first. The influence of solar growth on global land competition is less substantial in India, where present and predicted agricultural productivity is lower than the world average. Figure B1.7 shows that the expansion of solar energy, either directly or indirectly, reduces noncommercial land cover on a global scale: for every 100 hectares of solar land in the EU, we find that, depending on the solar penetration level, 31 to 43 hectares of unmanaged forest may be cleared globally. In India, the same amount of solar land would remove 27 to 30 hectares of unmanaged forest, whereas, in Japan and South Korea, the ratio is 49 to 54 hectares.

The changes in land cover in Figure B1.7 imply that solar expansion causes LUC(Land use change) emissions, such as iLUC (indirect land use change) emissions from increased global land competition, emissions from vegetation loss if forest and scrubland are cleared to make way for solar land (either directly through deforestation or indirectly by avoiding future afforestation), and carbon release from soil and vegetation directly below the installed panels, where sunlight is greatly reduced. However, the land management regime used in solar land is responsible for a significant portion of the emission balance. If all vegetation is destroyed and not allowed to recover through the use of herbicides, as is customary in many countries, LUC emissions from solar expansion are exacerbated. In contrast, converting arable land plots to solar parks whose surface is managed as pastures will result in net carbon sequestration in vegetation and soil in the decades following the conversion (except for the land directly beneath the panels, where photosynthesis is largely blocked), offsetting some or all of the unavoidable LUC emissions caused by land competition. In actuality, the use of a certain land management strategy is determined by a variety of local conditions (policy, climate, etc.).

Figure B1.8 and Figure B1.9 show the derived LUC emissions per unit of solar energy installed from 2020 to 2050 for various simulated solar penetration and module efficiency scenarios, as well as for various land management regimes in solar parks. They show that solar development scenarios until 2050 would almost certainly result in net LUC emissions, however, there may be net carbon sequestration in India if solar parks are managed as pastures. When delayed post-2050 impacts on local carbon cycles are considered (Figure B1.9), the sequestration effect is increased. The change in land cover induced by the increase of solar energy in the EU would release 13 to 53 g of CO_2 per kWh of electricity produced, accounting for 4 to 16% of CO_2 emissions from natural gas-fired power. Solar energy requires far less land cover change per unit of output in India (Figure B1.7), and LUC emissions per kWh are expected to be less than 12 g of CO_2 in all scenarios. LUC emissions from solar energy expansion range from 11 to 35 g of CO_2 per kWh in Japan and South Korea. The results show that

LUC emissions are comparable to about 10 to 50% of current non-land life cycle emissions when using relatively efficient PV technologies such as monocrystalline and multi-crystalline silicon. Instead, they estimated that LUC emissions in the range of 50 to 150% of non-land life cycle emissions when using less space-efficient but more resource-efficient PV technologies such as thin-film Cadmium telluride (CdTe) made by depositing one or more thin layers of photovoltaic material on a glass, plastic, or metal substrate (higher range of LUC emissions, lower range of non-land life cycle emissions). In most situations, seeding solar land with herbs and managing it as pasture reduces net LUC emissions by more than 50%.

CO_2 emissions based on the LCA study around the world.

Concentrated solar energy emits 38 grams of CO_2 equivalent every kWh of electricity generated, PV roof solar energy emits 41 grams, and PV utility solar energy emits 48 grams. To comprehend the carbon footprint of solar energy, we must examine its life cycle and the carbon impact of each stage. Since the CO_2 emissions happen when the factory is constructing the solar panels. After the construction of panels little or no emissions is occurring, however, after the lifetime of panels if the decision is made to build back the panel CO_2 is emitted from decommissioning the solar farms and land restoration. A solar power plant has several components, and producing these components necessitates the use of machinery that releases CO_2. Mirrors, heat exchange fluid, receivers, engines, turbines, and generators, as well as transmission lines, transformers, and substations, all have a carbon footprint while providing power to customers. The carbon footprint of this phase is relatively low since there are very little CO_2 emissions or waste products connected with running PV and concentrating solar energy. CO_2 emissions are related with the functioning of mechanical equipment (e.g., receivers, engines, turbines, generators, substations, and transformers) at power plants during this stage. Overall, solar energy is sustainable since it emits no greenhouse gases, and hazards to land usage, water consumption, and hazardous materials may be managed by proper disposal procedures and solar power plant siting. However, solar still can have a negative influence on the environment, it effects to the land use, water use and it uses the hazardous materials. While constructing the huge solar farm it can impact the land use with the extent of land degradation and habitat loss is determined by technology, site topography, and solar resource intensity. Large-scale solar farms on abandoned land, as well as small-scale farms on top of buildings or residences, can help to reduce negative environmental consequences.

Despite the fact that solar energy is green and CO_2 emission free, it still can have a negative influence on the environment, it affects land use, water use and it uses hazardous materials. While constructing the huge solar farm it can impact the land use with the extent of land degradation and habitat loss determined by technology, site topography, and solar resource intensity. Large-scale solar farms on abandoned land, as well as small-scale farms on top of buildings or residences, can help to reduce negative environmental consequences. Water is

used to build PV components, while CSPs (How it Works: Water for Power Plant Cooling, n.d.) need water to cool, this is one of the reasons why floating solar panels have high efficiency, since the water which is already in nature can cool down the panel and it can produce more energy. Hydropower and solar panels can make an amazing mix with the fight against GHG, while "helping" each other in the production of electricity. Lastly, PV cells are made from hydrochloric acid, sulfuric acid, nitric acid, hydrogen fluoride, 1,1,1-trichloroethane, and acetone. They may constitute major harm to the environment and public health if not handled and disposed of correctly. Strict restrictions are in place to limit the possibility of this happening.

8.2 Comparison of renewable energies

In order to compare the emissions intensity of different energy sources, the data obtained from G-RES and other studies have been analysed. First, focusing on hydropower, the average intensity based on the results from 15 reservoirs in Norway has been calculated.

The findings revealed an emissions intensity of 1.37 gCO_2e/kWh, which is lower than the national average of 3.33 gCO_2e/kWh mentioned earlier. It indicates that hydropower derived from these reservoirs contributes to lower greenhouse gas emissions.

Next, the emissions intensity for wind energy in Norway, utilizing data from both offshore and onshore wind farms has been examined. The average intensity for onshore wind farms was calculated to be 13.05 gCO_2e/kWh, while for offshore wind concepts, it was determined to be 22.28 gCO_2e/kWh. These values illustrate the emissions associated with generating wind energy in the country.

Additionally, the emissions intensity for solar farms, considering global data on concentrated, roof, and utility solar energy have been analyzed. The calculations revealed a solar intensity of 42.33 gCO_2e/kWh. This indicates that solar energy, while considered a clean energy source, still has a higher emissions intensity compared to hydropower and wind energy.

Figure 31 illustrates these results, with the emissions intensity based on G-RES calculations indicating the lowest value, while solar energy demonstrates the highest emissions intensity. It is important to note that for a more accurate assessment of hydropower, a study based on life cycle analysis (LCA) and reservoir emissions should be conducted to obtain the final emissions intensity figure.

Overall, these findings suggest that hydropower, based on the analysis of reservoir emissions without an LCA study, appears to be the cleanest energy source among the examined options. However, a comprehensive study incorporating LCA and reservoir emissions is necessary to derive a more precise emissions intensity for hydropower.

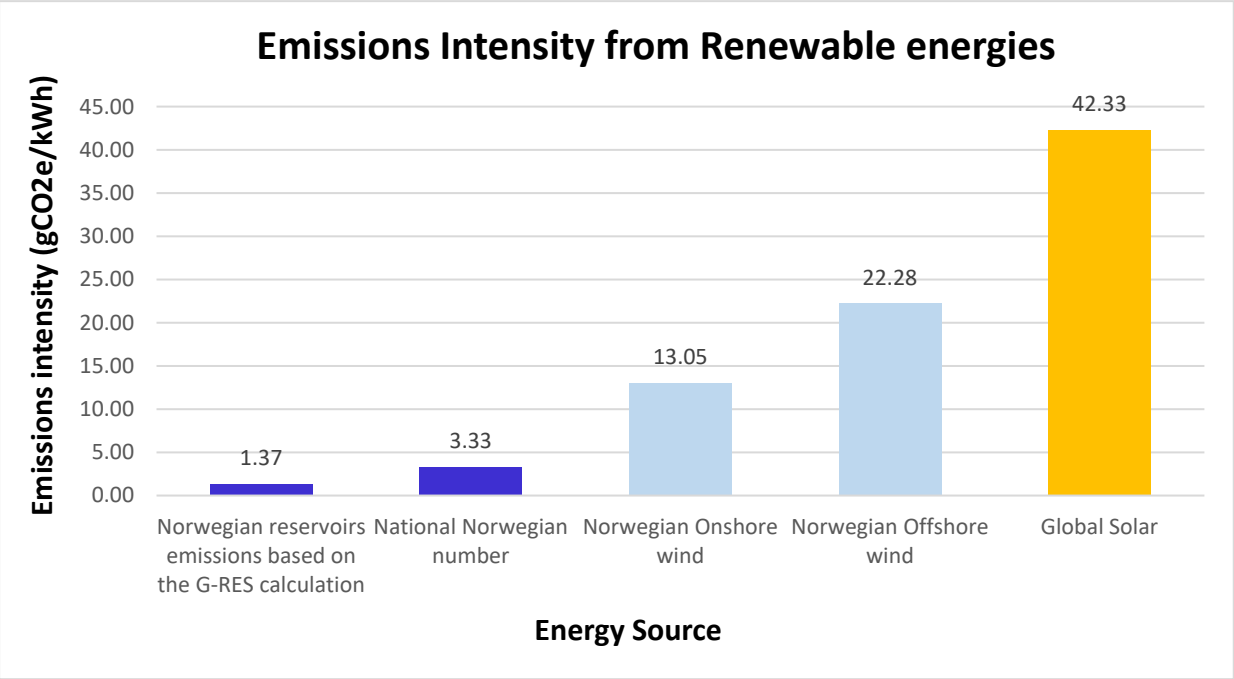

Figure 31 Emissions intensity from renewable energies

8.3 Issues with G-RES tool

While working on the G-RES tool, some difficulties arose, particularly related to the tool itself and Earth Engine. Despite the tool's potential for accurately assessing GHG emissions and providing reservoir information, it is prone to inaccuracies in crucial data.

Let's first address the issues with the tool:

One significant problem with the G-RES tool is related to changes in soil types. When transitioning from mineral to organic soil, the tool incorrectly treats it as a sink. This miscalculation arises because the tool fails to account for the impact of adding organic soil after impoundment. To accurately determine GHG emissions from the reservoir, it is crucial to consider the emissions resulting from flooding land with substantial organic soil. Merely assessing emissions before impoundment is insufficient.

The tool currently offers only four climate zones (Boreal, temperate, tropical, subtropical), which limits its precision, especially in countries like Norway. In areas with higher elevations, an arctic climate zone is more appropriate. Adding an arctic climate zone to the tool would enable more accurate calculations. In the case of Norway, where some reservoirs are located in the arctic climate zone, selecting the boreal climate zone for all cases may lead to inaccuracies.

Despite providing all the necessary information for the tool, the calculation of thermocline depth is not consistently performed. While it occasionally calculates this parameter, in most cases, the cell remains empty.

If the selected sites are the cascade system, the tool is not developed for the cascade system.

The tool does not account for N_2O emissions in its analysis and calculations.

Furthermore, there are several issues with Earth Engine presented below:

The provided maximum and minimum reservoir depth information in Earth Engine was consistently incorrect for all the reservoirs which have been studied. The maximum depth was always lower than the minimum depth. Attempting to interchange the data did not yield accurate results, as the values were either extremely low or, in some cases, reported as zero depth.

A bug exists in Earth Engine's code, specifically in line 116. When the latitude of the dam exceeds 60 degrees, Earth Engine fails to navigate, calculate elevation, or provide dam geometry information. Consequently, no data is obtained in these cases. Please refer to Figure 32 to check the results before and after.

Another problem has been found in the land cover information for the reservoir. By comparing the data from Earth Engine with precise data provided by the co-supervisor, it has been found that the information from Earth Engine was often incorrect. This inconsistency frequently led to inaccurate GHG emission calculations for the reservoir.

Addressing these issues with the G-RES tool and resolving the inaccuracies in Earth Engine's data and functionalities is crucial for ensuring reliable assessments of GHG emissions and improving the overall effectiveness of the tool.

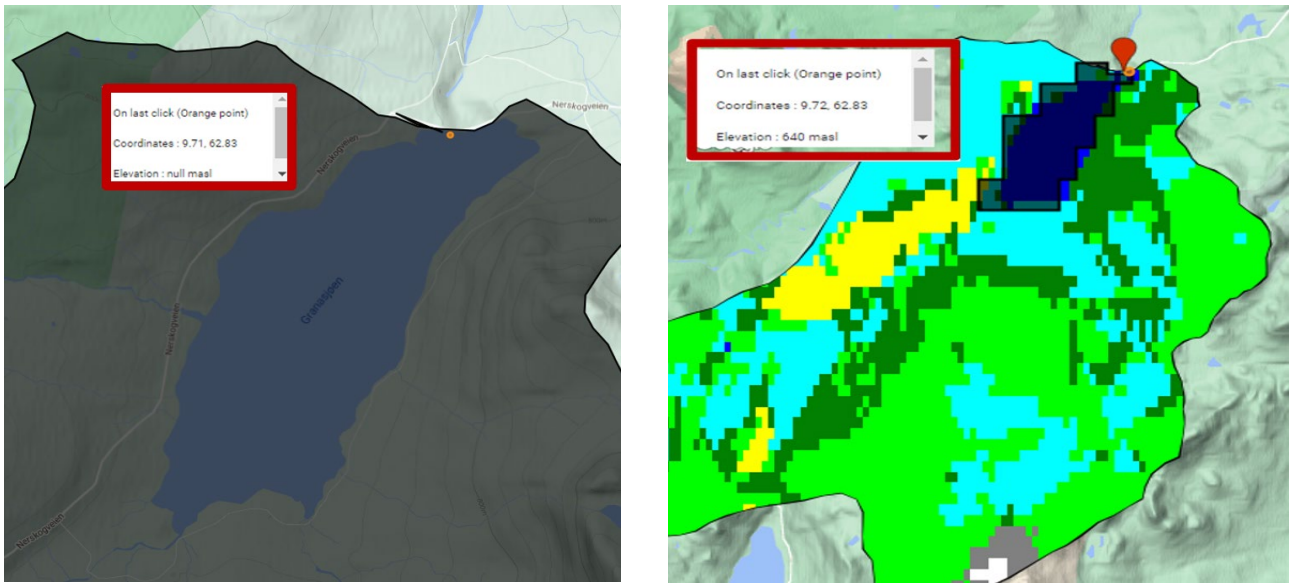

Figure 32 The results from EE before and after the bug correction in the code

8.4 Solution for G-RES tool / Potential fixes

One possibility that has been found which allowed me to continue working with the tool, was that the bug has been fixed in the EE (Earth Engine). With the assistance of the remarkable G-RES team, although the code they provided did not function properly, the location has been identified. By making necessary adjustments to the code, it was possible to successfully utilize the tool. To view the corrected code, please refer to Figure 33. This needs to be checked and changed by the G-RES team, to avoid future issues caused by the incorrect code.

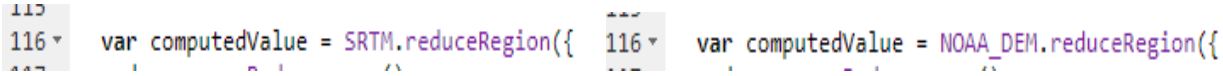

Figure 33 Corrected bug in the code, before and after

9 Conclusion

The research aimed to investigate and analyze greenhouse gas (GHG) emissions from reservoirs using the G-RES tool which is led by International Hydropower Association and the UNESCO Chair in Global Environmental Change, The G-res Tool was developed using a conceptual framework created with scientists from the University of Quebec at Montreal (UQAM), the Norwegian Foundation for Scientific and Industrial Research (SINTEF) and the Natural Resources Institute of Finland (LUKE), with assistance from the World Bank.. Through simulations and calculations, it was observed that the G-RES tool has the potential to calculate GHG emissions from reservoirs. However, due to its novelty, further development and upgrades are necessary to ensure accurate results. The findings indicated that although reservoirs do emit GHGs, the emission levels are relatively lower compared to wind and solar power generation. This is primarily due to the fact that reservoirs are typically already built, and the emission rate from water bodies alone is minimal, especially in cases where reservoirs are expanded rather than newly constructed.

The simulations highlighted the significance of land cover and soil type within reservoirs, as they determine the number of emissions released into the atmosphere. Therefore, it is crucial to thoroughly study these factors prior to the impoundment of land for reservoir construction.

The study showed that the lowest emissions intensity from reservoirs can be $0gCO_2e/kWh$, while the highest is $5.7gCO_2e/kWh$, in a comparison from Norwegian onshore wind the lowest emissions rate is $11gCO_2e/kWh$, and from the offshore wind concepts the lowest 18 gCO_2e/kWh, and the highest $31.4gCO_2e/kWh$, while the lowest global solar emissions rate is $38gCO_2e/kWh$, while the highest is $48gCO_2e/kWh$.

To further development in this field, it is crucial to conduct comprehensive studies and calculations, as there is currently limited documentation or calculations available regarding GHG emissions from reservoirs without life cycle assessment (LCA).

Additionally, for wind and solar projects, it is crucial to calculate GHG emissions resulting from land-based changes and evaluate how the soil responds to these alterations. Most GHG emissions studies rely on LCA, which assesses the CO_2 emissions associated with the production of essential components of wind turbines and solar panels. This alone is insufficient to determine the overall environmental friendliness of these renewable energy sources.

Further examination and improvement of the G-RES tool are necessary, ensuring that all requirements are met. The proper utilization of this tool can save considerable time, expenses, and resources, enabling hydropower project owners to attain certification and generate green electricity.

References

Innerdalsvatnen , Wikipedia . (u.d.). Hentet fra https://no.wikipedia.org/wiki/Innerdalsvatnet

Sira Kvina Scheme, Skagerakkraft . (u.d.). Hentet fra Skagerakkraft: https://www.skagerakkraft.no/vassdrag_2/our-watercourses/sira-kvina/

CEDREN, H. A. (2023). *Greenhouse gas status of hydro reservoirs.* Center for Environmental Design of Renewable Energy (CEDREN).

Centre for Life cycle inventories, 2. (u.d.). *The EcoInvent database for processes, products and transport. Integrated in the life cycle software tool SimaPro (Pré).,*. Hentet fra http://www.ecoinvent.ch/

Dirk-Jan van de Ven, I. C.-P.-E. (2021). *The potential land requirements and related land use change emissions of solar energy.*

EEA - European Environment Agency, Climate change mitigation : reducing emissions. (u.d.). Hentet fra EEA - European Environment Agency: https://www.eea.europa.eu/en/topics/in-depth/climate-change-mitigation-reducing-emissions#:~:text=Mitigating%20climate%20change%20means%20reducing,important%20part%20of%20the%20solution.

Energy Efficiency and renewable enegy, Types of hydropower plants . (u.d.). Hentet fra https://www.energy.gov/eere/water/types-hydropower-plants

EU Technical Expert Group, O. S. (2020). *Taxonomy: Final report of the Technical Expert.*

Fabrizio Albanito, S. R. (2022). Quantifying the land-based opportunity carbon costs of onshore wind farms. *Journal of cleaner production*, 10.

Global Wind Energy Council, Global Wind Report. (u.d.). Hentet fra Global Wind Energy Council: https://gwec.net/global-wind-report-2019/

Granasjøen. (u.d.). Hentet fra Wikipedia: https://no.wikipedia.org/wiki/Granasj%C3%B8en

How it Works: Water for Power Plant Cooling. (u.d.). Hentet fra Union of concerned scientist : How it Works: Water for Power Plant Cooling

Hydroelectricity . (IEA). Hentet fra https://www.iea.org/reports/hydroelectricity

IEA, Solar PV . (u.d.). Hentet fra IEA: https://www.iea.org/reports/solar-pv

IEA, Wind Electricity. (u.d.). Hentet fra IEA: https://www.iea.org/reports/wind-electricity

IHA - International Hydropower Assosication . (u.d.). Hentet fra https://www.hydropower.org/iha/discover-types-of-hydropower

IPCC. (u.d.). Hentet fra https://www.world-nuclear.org/information-library/energy-and-the-environment/carbon-dioxide-emissions-from-electricity.aspx

IPCC Glossary . (u.d.). Hentet fra https://www.ipcc.ch/sr15/chapter/glossary/

IRENA, Solar Energy . (u.d.). Hentet fra IRENA: https://www.irena.org/Energy-Transition/Technology/Solar-energy#:~:text=Solar%20energy%20is%20used%20worldwide,convert%20sunlight%20directly%20into%20electricity.

Jonkman, J. e. (2009). *Definition of a 5-MW Reference Wind Turbine for Offshore System Development.*

Modahl, M. S. (2019). *The inventory and life cycle data for Norwegian hydroelectricity.*

Nevina . (u.d.). Hentet fra https://nevina.nve.no/

NINA . (u.d.). Hentet fra https://www.nina.no/

Norge i Bilder. (u.d.). Hentet fra https://norgeibilder.no/

Norwegian University of Science and Technology, S. M. (u.d.). *Norwegian University of Science and Technology, Science Museum, Report botanical serie*. Hentet fra https://www.ntnu.no/museum/botaniske-og-zoologiske-rapporter

NVE - Grana . (u.d.). Hentet fra https://www.nve.no/om-nve/nves-utvalgte-kulturminner/dammer/nerskogen/

NVE - Granasjøen. (u.d.). Hentet fra NVE.no: https://www.nve.no/om-nve/nves-utvalgte-kulturminner/dammer/nerskogen/

NVE - Manøvreringsreglement . (u.d.). Hentet fra https://www.nve.no/kdb/sc7384.pdf

NVE - Norway's hydroelectric development, T. J. (2021). *Norway's hydroelectric development.* NVE.

NVE Atlas. (u.d.). Hentet fra https://atlas.nve.no/Html5Viewer/index.html?viewer=nveatlas&layerTheme=null&scale=40000&basemap=&center=264786.2000000002%2C6950598.2650000015&layers=

Nve Atlas . (u.d.). Hentet fra https://atlas.nve.no/Html5Viewer/index.html?viewer=nveatlas#

Nve Atlas - Flothølen (Dam Kilen) . (u.d.). Hentet fra https://atlas.nve.no/Html5Viewer/index.html?viewer=nveatlas&layerTheme=null&scale=10000&basemap=&center=34839.203386250214%2C6568367.917971381&layers=

NVE Atlas - Gravatn. (u.d.). Hentet fra https://atlas.nve.no/Html5Viewer/index.html?viewer=nveatlas&layerTheme=null&scale=80000&basemap=&center=30841.34122385923%2C6558626.436248833&layers=3BHcOm

Nve Atlas - Tjorhomvatn. (u.d.). Hentet fra https://atlas.nve.no/Html5Viewer/index.html?viewer=nveatlas&layerTheme=null&scale=20000&basemap=&center=30485.119377616324%2C6554444.569705645&layers=

NVE atlas Homstvolvatnet. (u.d.). Hentet fra https://atlas.nve.no/Html5Viewer/index.html?viewer=nveatlas&layerTheme=null&scale=80000&basemap=&center=40726.083589266585%2C6539994.968067669&layers=3BHcOm

Nve Atlas Nesjen. (u.d.). Hentet fra https://atlas.nve.no/Html5Viewer/index.html?viewer=nveatlas&layerTheme=null&scale=160000&basemap=&center=49679.601496302406%2C6556744.4494833&layers=3BHcOm

NVE -Litjjfossen . (u.d.). Hentet fra https://www.nve.no/energi/energisystem/vannkraft/vannkraftdatabase/vannkraftverk/?id=247

Ozge Isik Pekkan, M. A. (2021). *Assessing the effects of wind farms on soil organic carbon.*

Rudd, J. R. (1993). *Are hydroelectric reservoirs significant sources of greenhouse gases?*

Seklima.met.no. (u.d.). Hentet fra https://seklima.met.no/

Sira Kvina Oyarvatn. (u.d.). Hentet fra https://www.sirakvina.no/oyarvatn/oyarvatn-article316-928.html

Sira-Kvina. (u.d.). Hentet fra https://www.sirakvina.no/anlegg/category858.html

Statkraft/Rana. (u.d.). Hentet fra https://www.statkraft.com/about-statkraft/where-we-operate/norway/rana-hydropower-plant/

(u.d.). *The GHG Reservoir Tool (G-RES) Technical Document.*

The International EPD system, T. I. (2011, 04 11). *Product Category Rules CPC 171 Electrical Energy CPC 173 Steam And Hot Water PCR 2007:08 Version 2.01*. Hentet fra http://www.environdec.com/en/Product-Category-Rules/Detail/?Pcr=5802.

The Norwegian Research Council, V. H. (2020). *GHG emissions and energy performance of wind power.* The Norwegian Research Council and partner consortium in the Energy Trading and Environment 2020 project.

United Nations - Renewable energy - Powering a safer future. (u.d.). Hentet fra United Nations: https://www.un.org/en/climatechange/raising-ambition/renewable-energy

What is the wind energy . (u.d.). Hentet fra Power and beyond : https://www.power-and-beyond.com/what-is-wind-energy-definition-types-and-more-a-e95f3c16c898e889f0757f62ee91038d/

Wind Energy. (u.d.). Hentet fra IRENA - International Renewable Energy Agency: https://www.irena.org/Energy-Transition/Technology/Wind-energy#:~:text=The%20amount%20of%20power%20that,by%20a%20factor%20of%20eight.

Appendices

This section will present the figures, calculation tables, and results used in this study.

Appendix A - Reservoirs overview

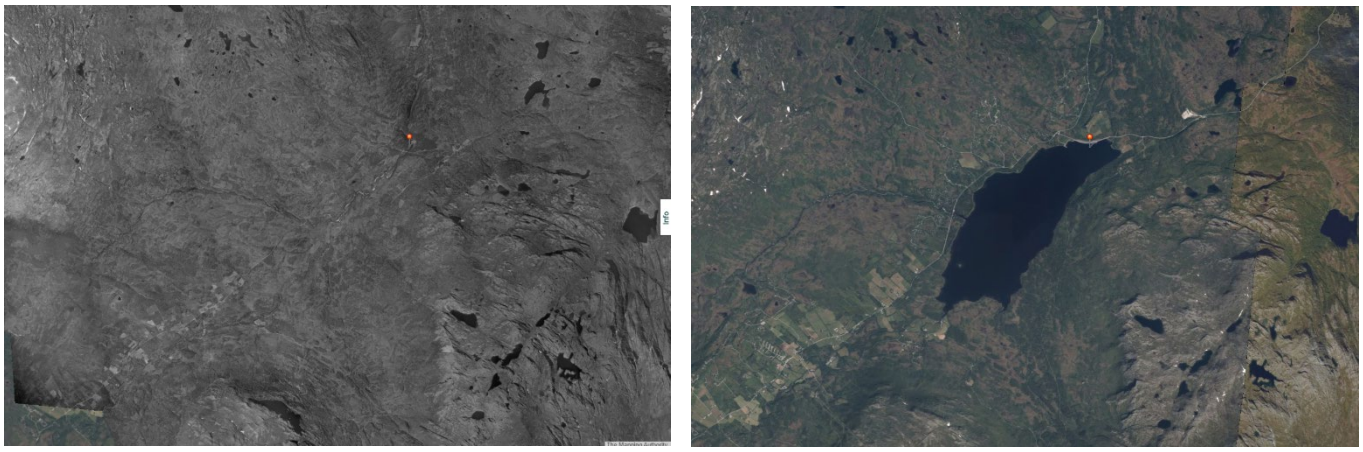

Figure A 1 Granasjøen before and impoundment (Norge i Bilder, n.d.)

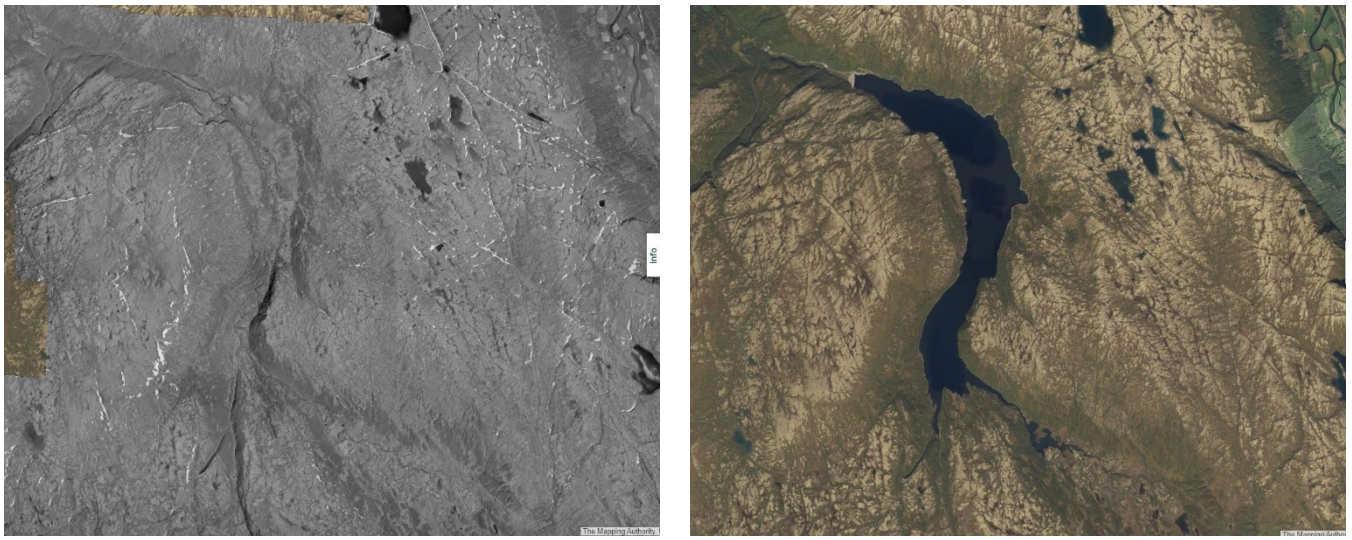

Figure A 2 Litjfossen (Innerdalsvatnet) before and after impoundment (Norge i Bilder, n.d.)

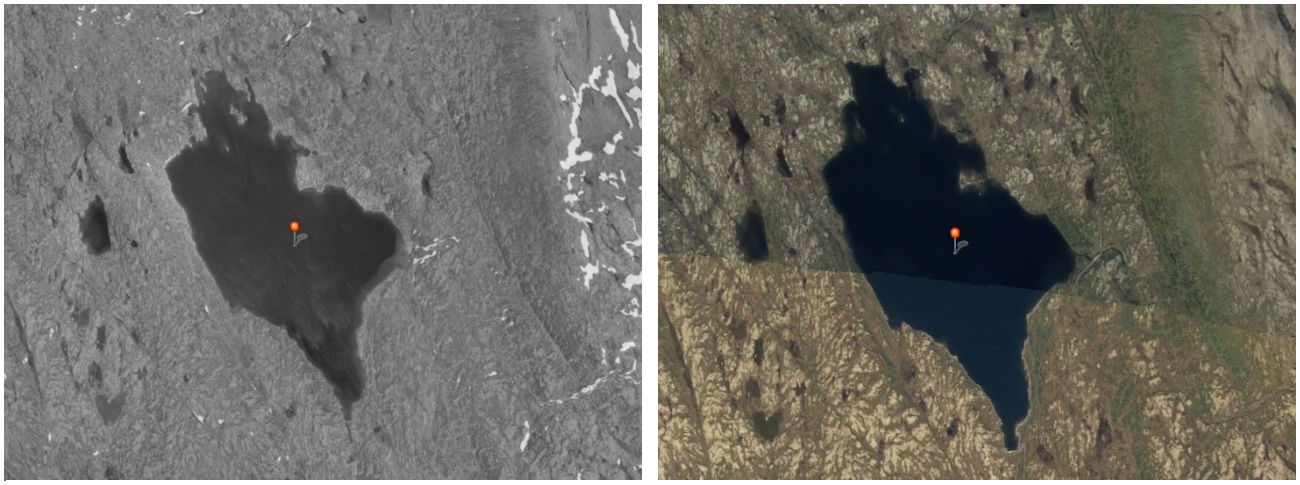

Figure A 3 Sverjesjøen before and impoundment (Norge i Bilder, n.d.)

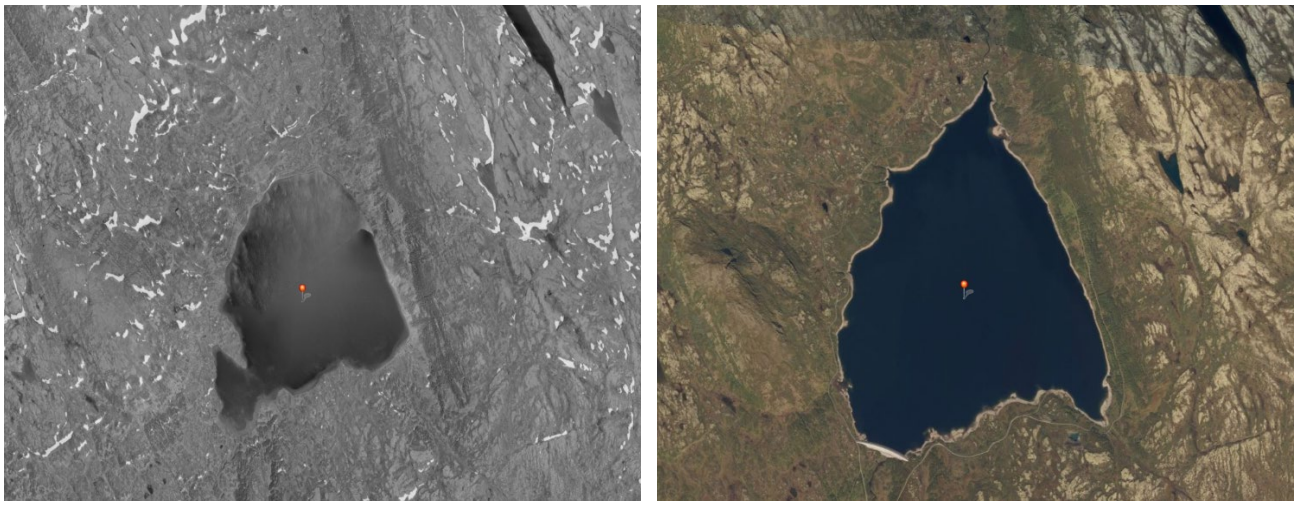

Figure A 4 Falningsjøen before and after impoundment (Norge i Bilder, n.d.)

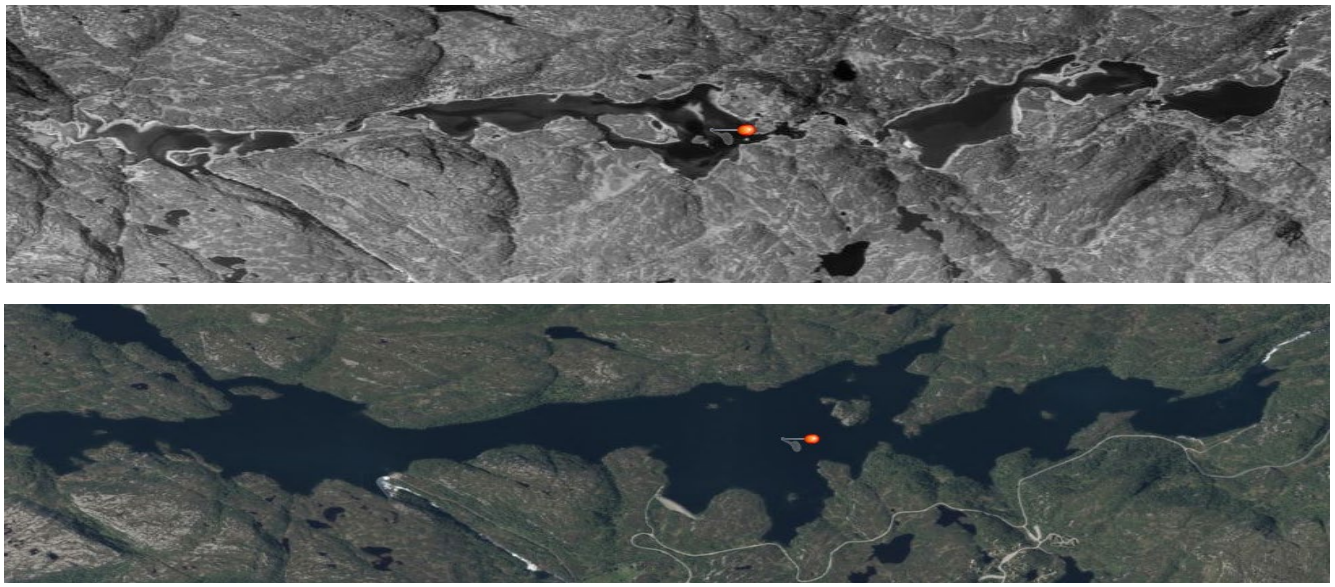

Figure A 5 Flothølen before and after impoundment (Norge i Bilder, n.d.)

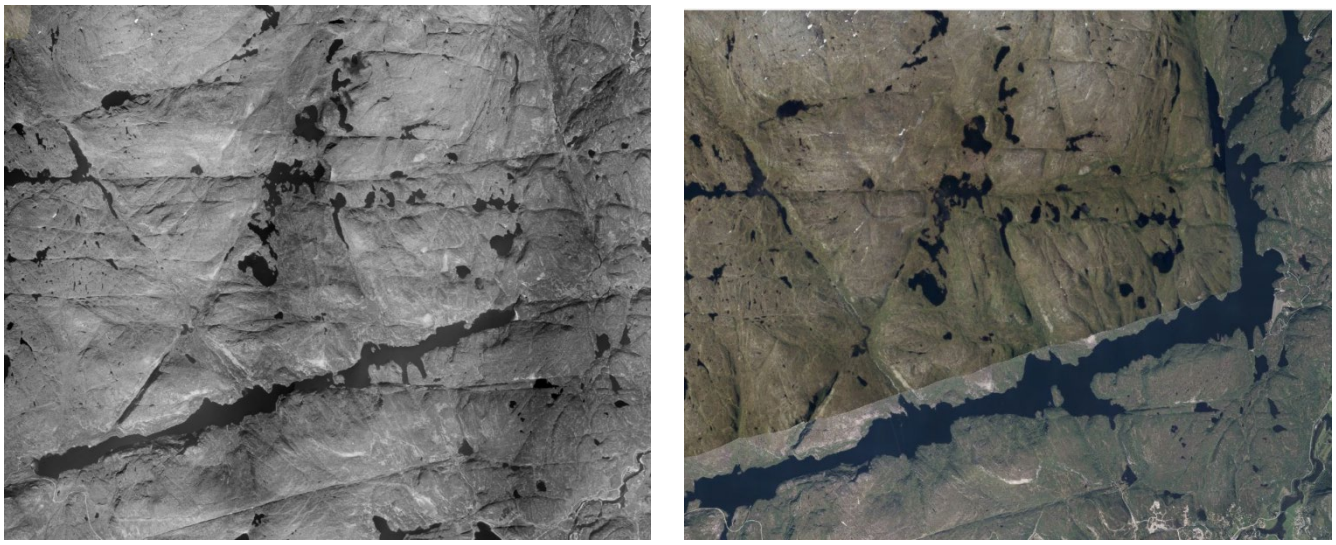

Figure A 6 Valevatn before and after impoundment (Norge i Bilder, n.d.)

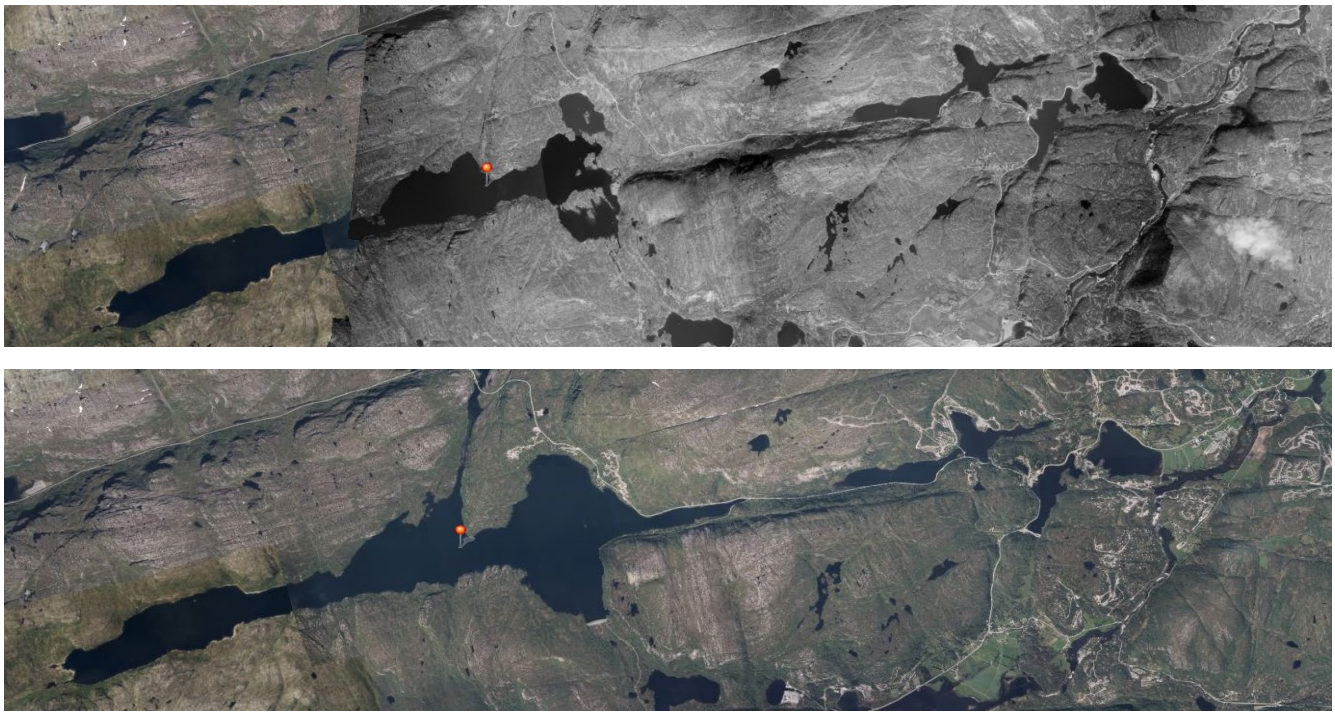

Figure A 7 Gravatn before and after impoundment (Norge i Bilder, n.d.)

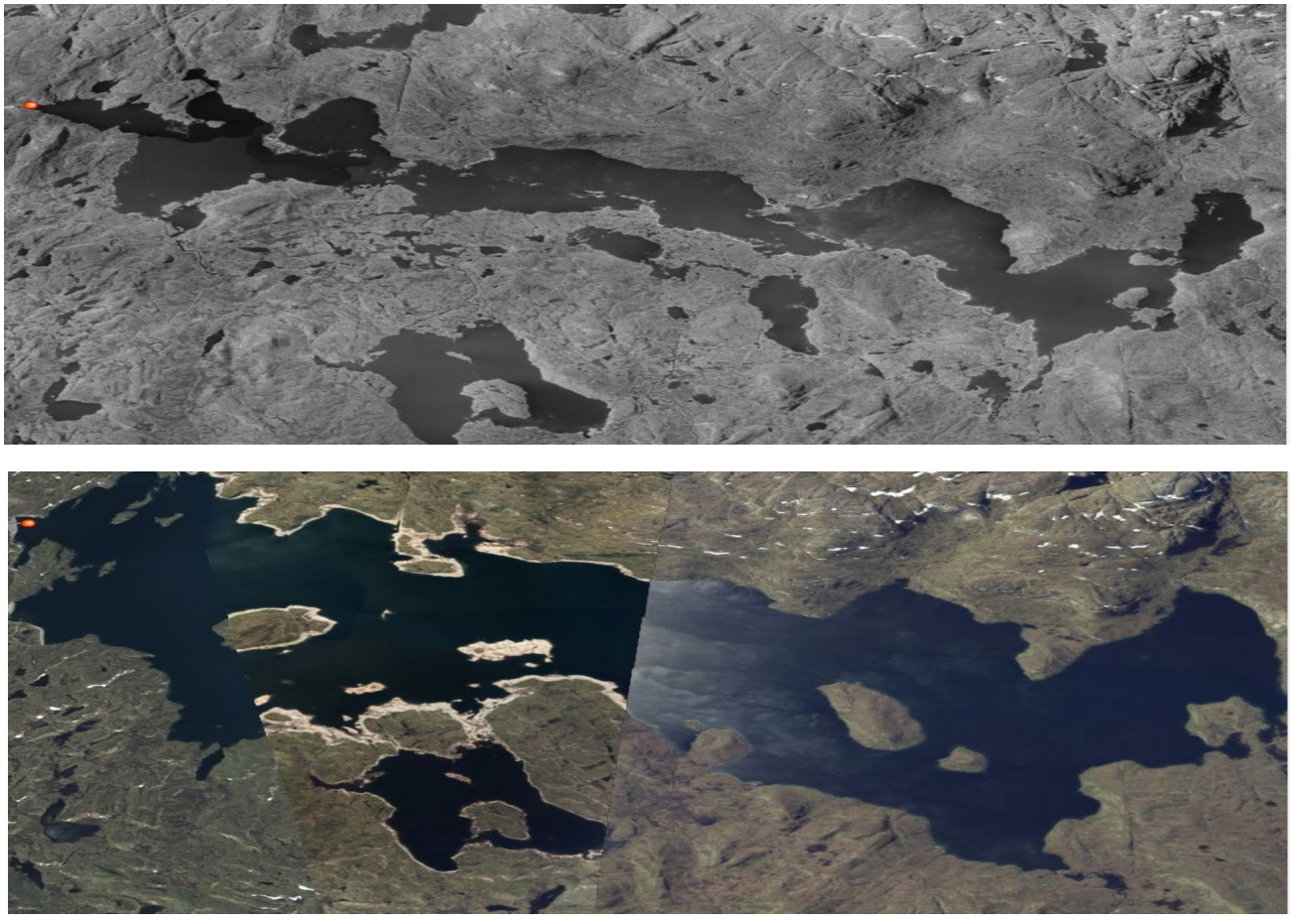

Figure A 8 Kverevatn Rosskreppfjorden before and after impoundment (Norge i Bilder, n.d.)

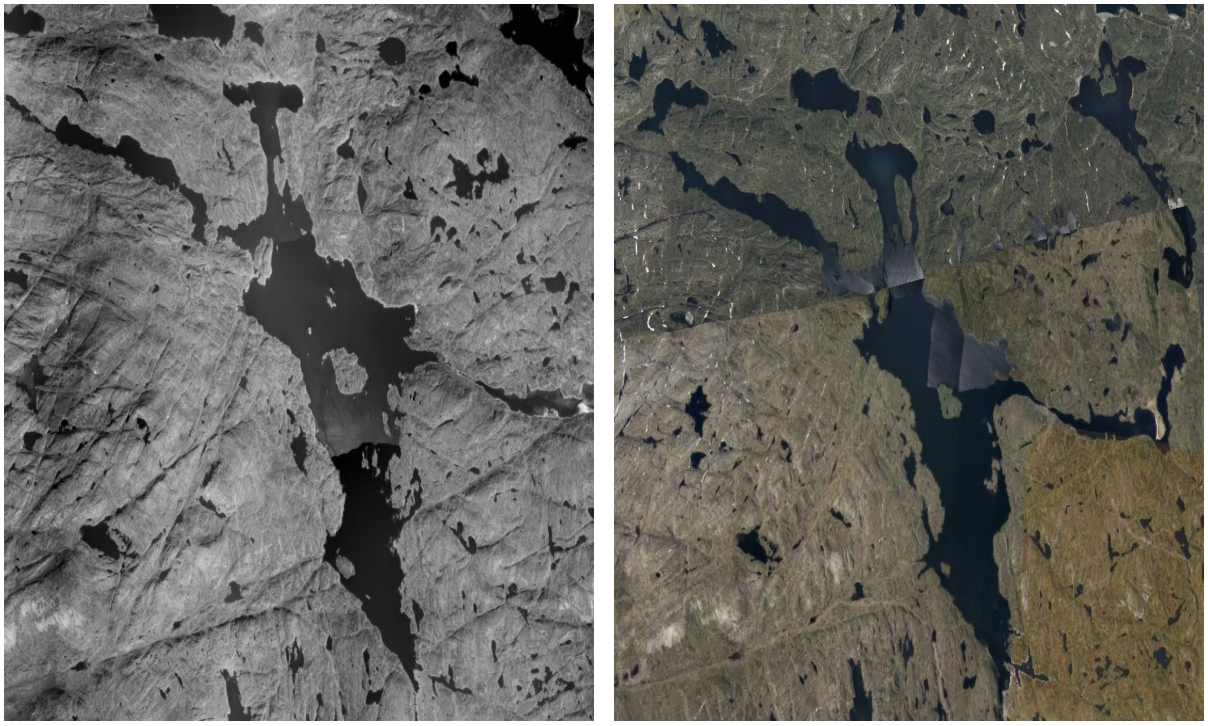

Figure A 9 Øyarvatnet before and after impoundment (Norge i Bilder, n.d.)

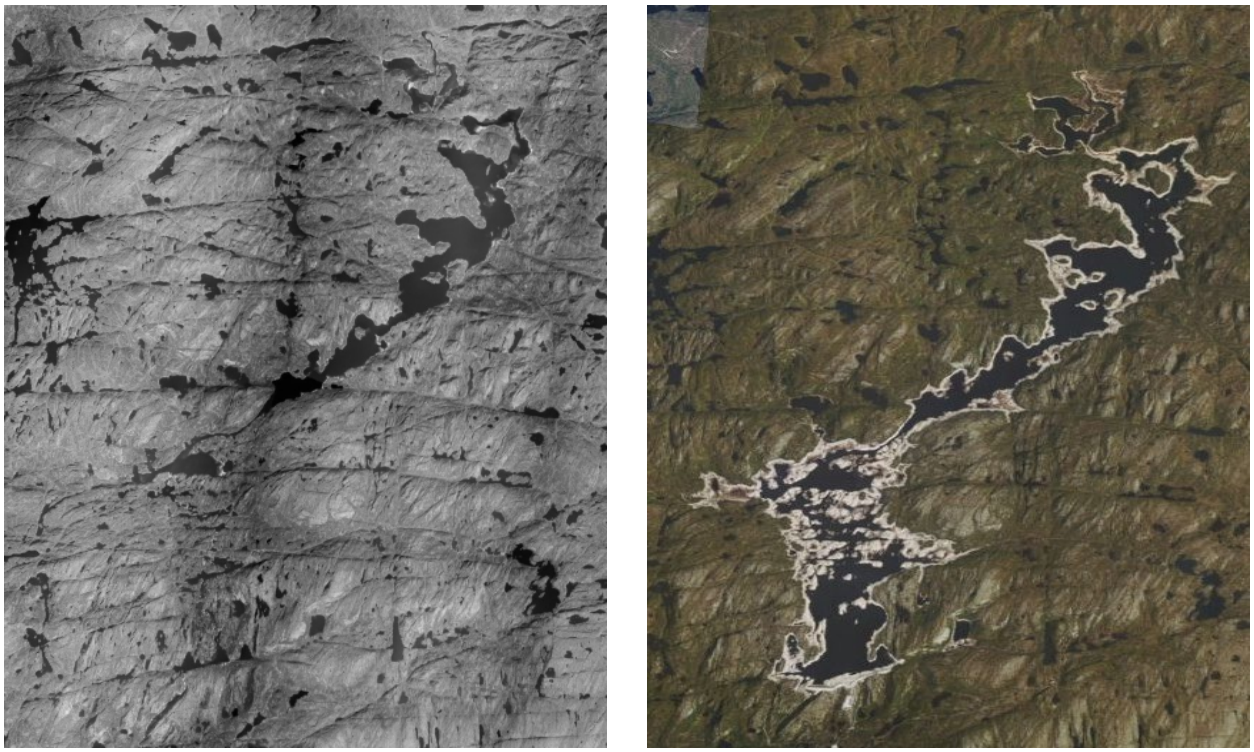

Figure A 10 Kvifjorden -Nesjen before and after impoundment (Norge i Bilder, n.d.)

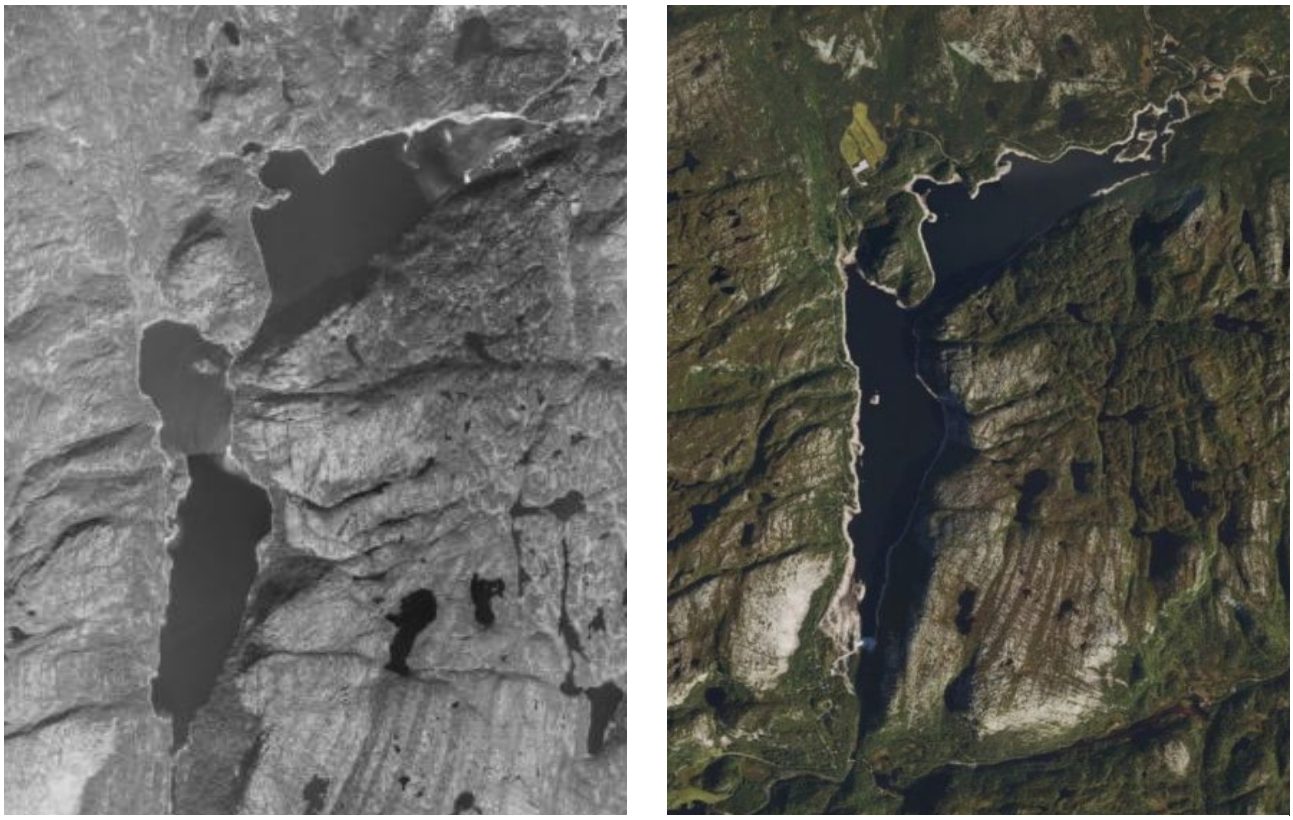

Figure A 11 Homstølvatnet before and after impoundment (Norge i Bilder, n.d.)

Appendix B – Hydropower Results overview

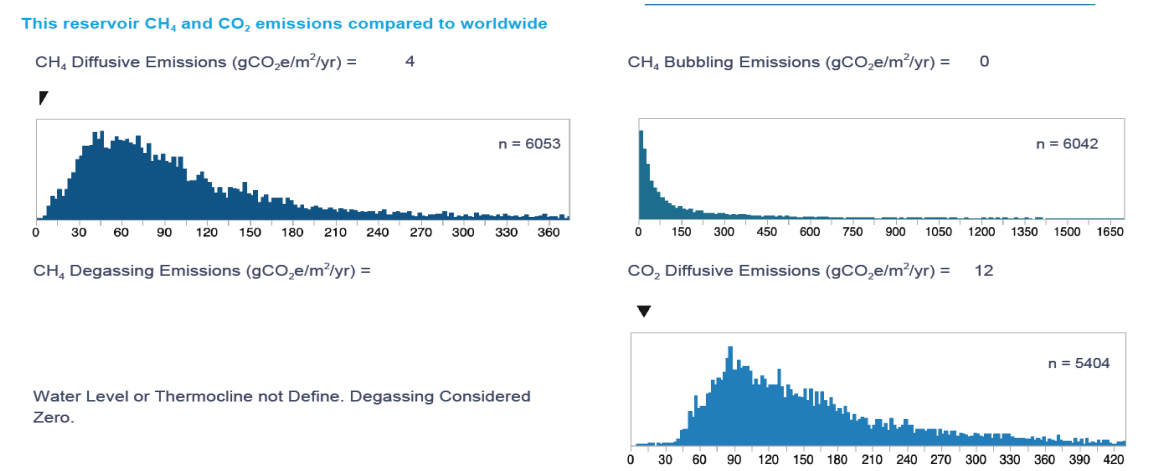

Figure B 1 Results from Akersvatn compared to worldwide data

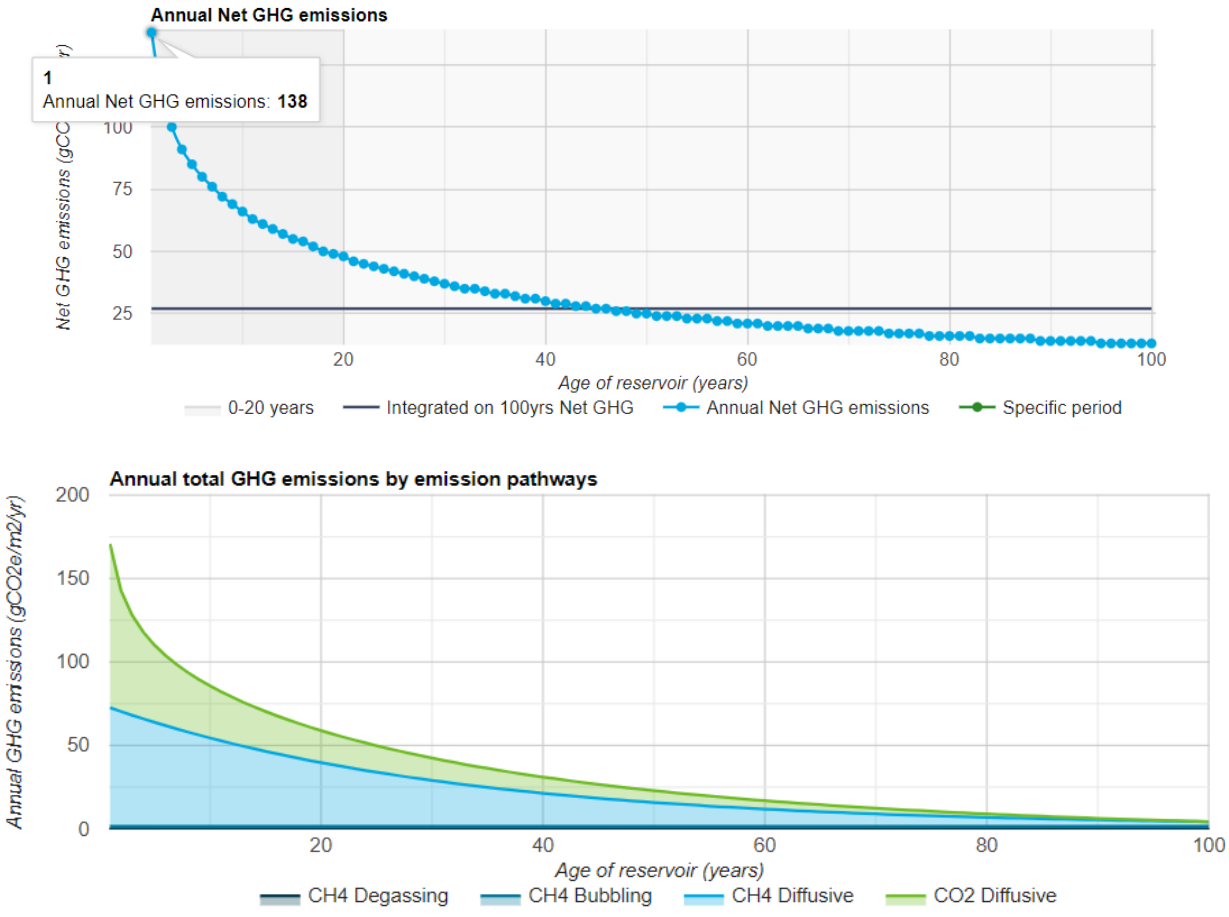

Figure B 2 Akersvatn annual GHG emissions and total GHG emissions by pathway

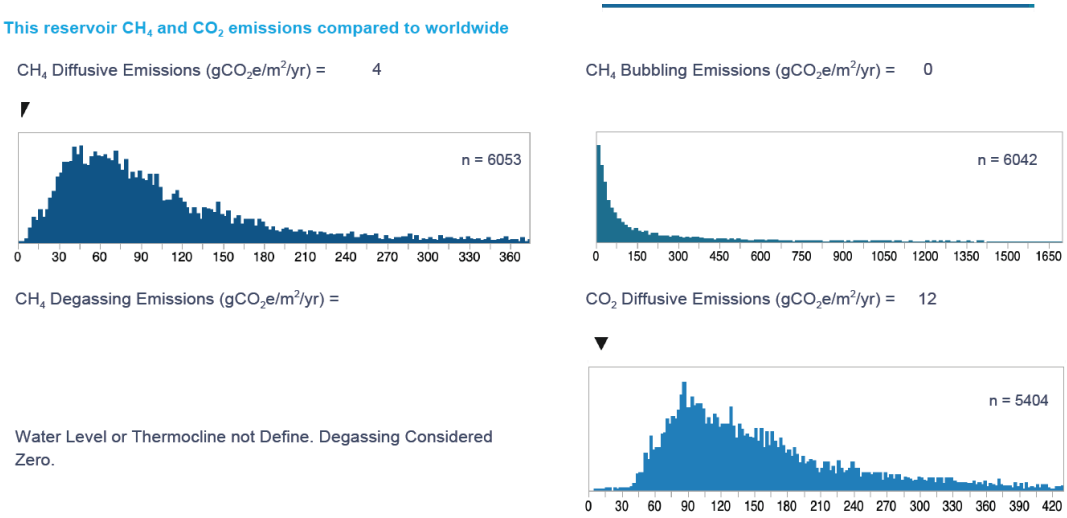

Figure B 3 Results from Kjensvatn compared to worldwide data

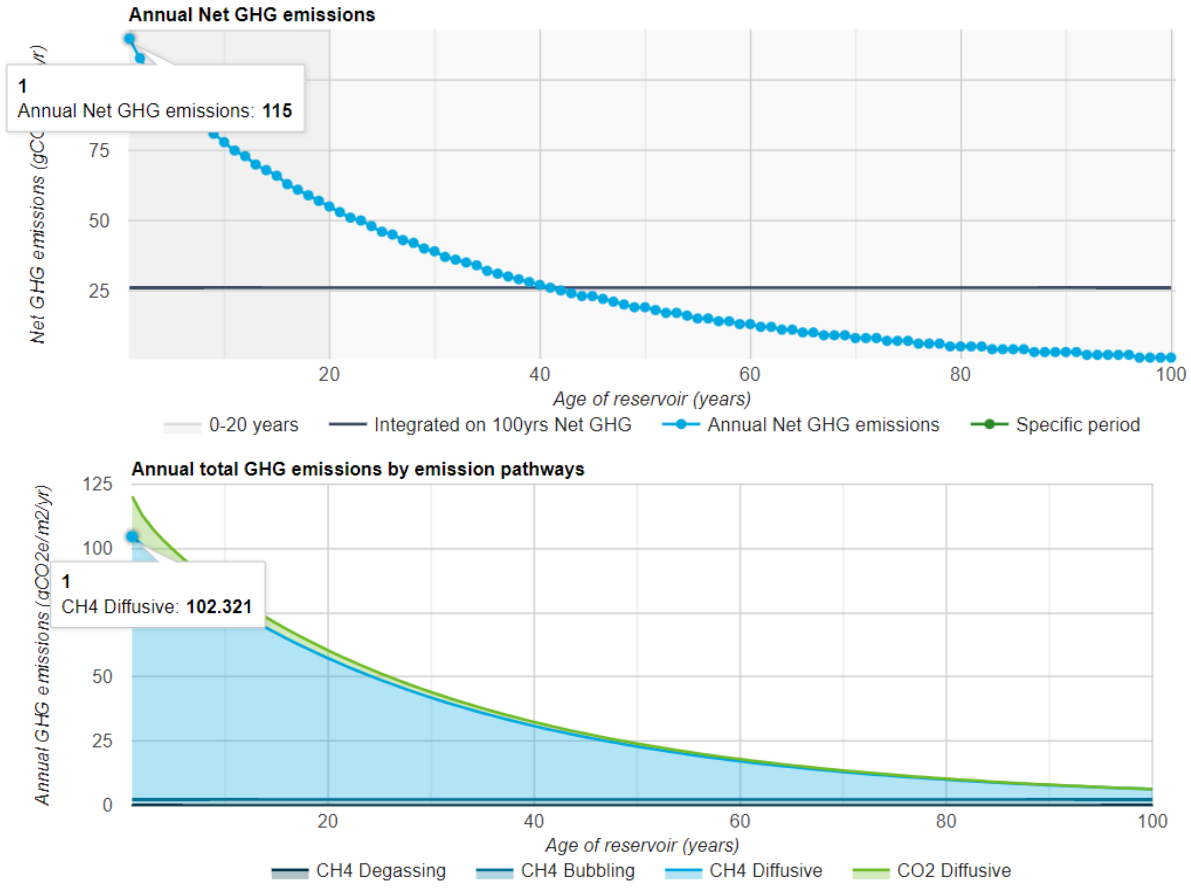

Figure B 4 Kjensvatn annual GHG emissions and total GHG emissions by pathway

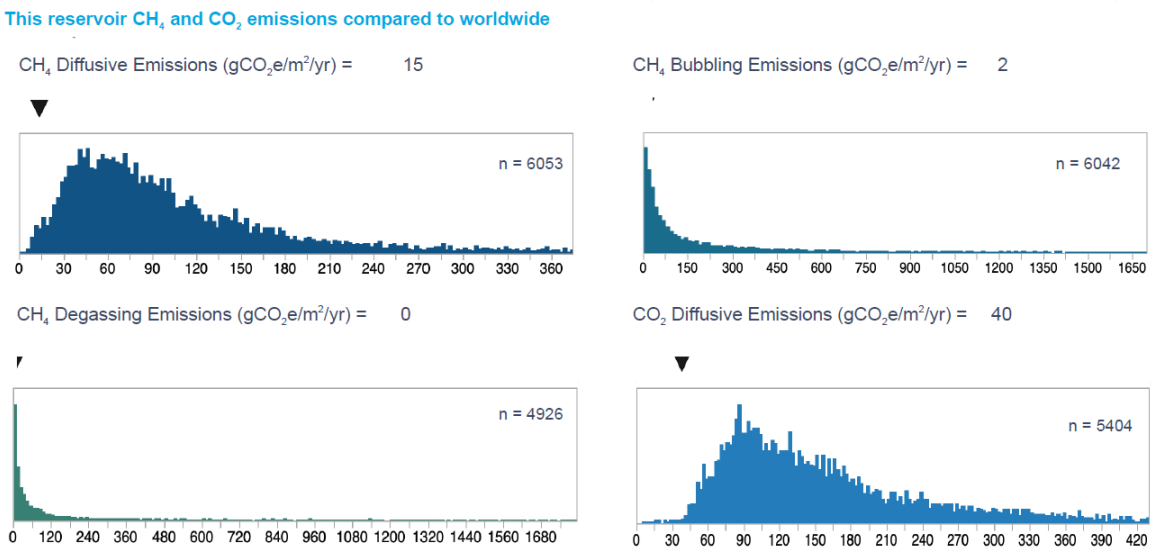

Figure B 5 Results from Granasjøen compared to worldwide data (Mineral soil scenario)

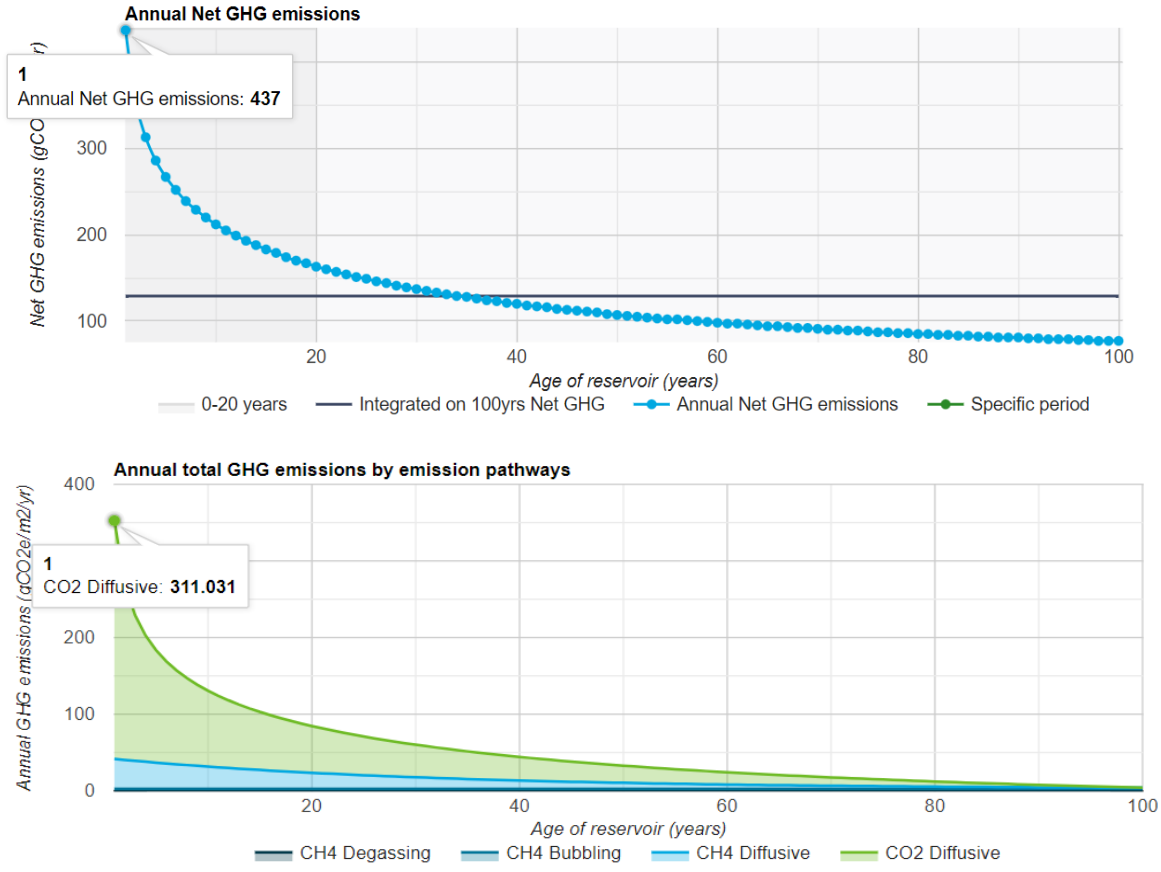

Figure B 6 Granasjøen annual GHG emissions and total GHG emissions by pathway (Mineral soil scenario)

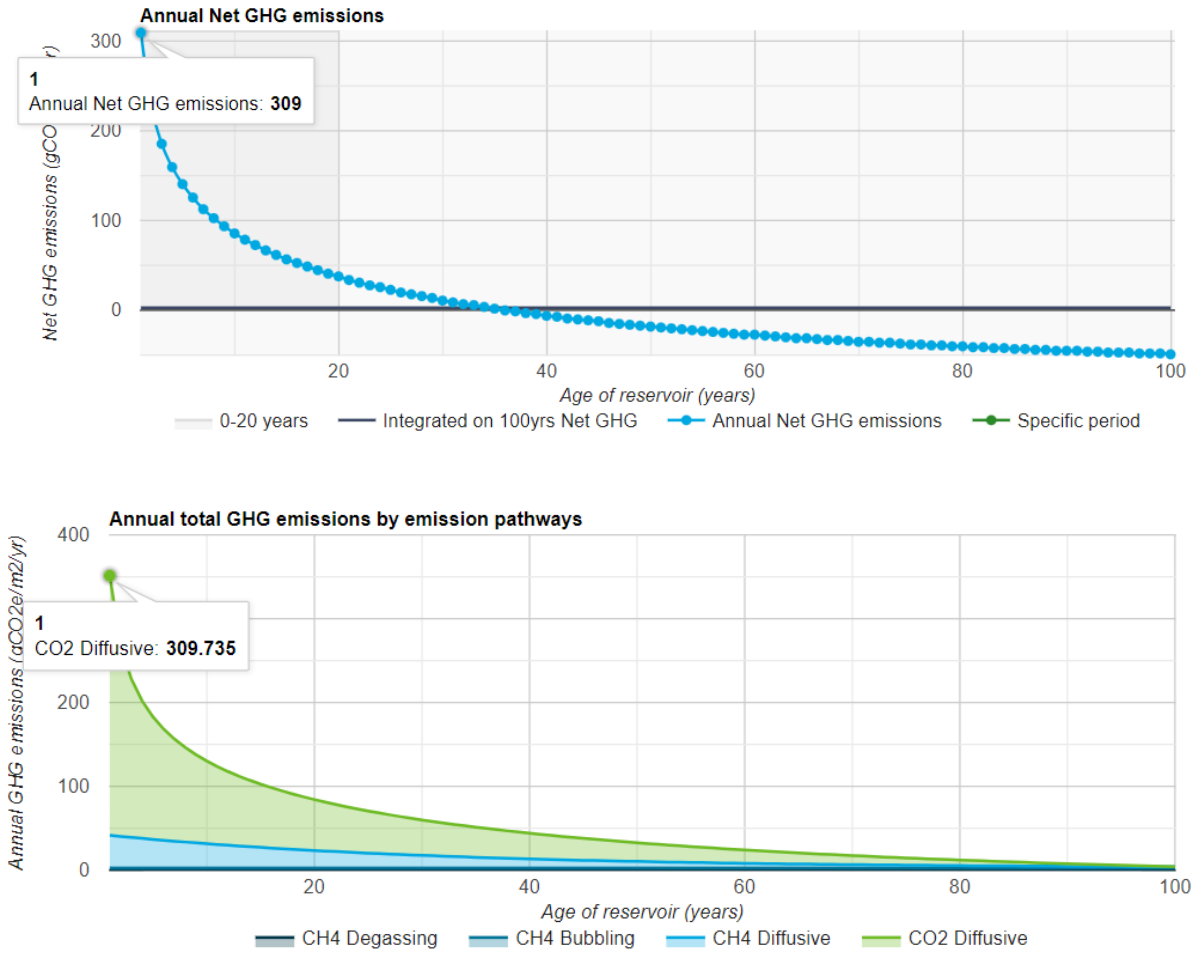

Figure B 7 Granasjøen annual GHG emissions and total GHG emissions by pathway (Mineral + Organic soil scenario)

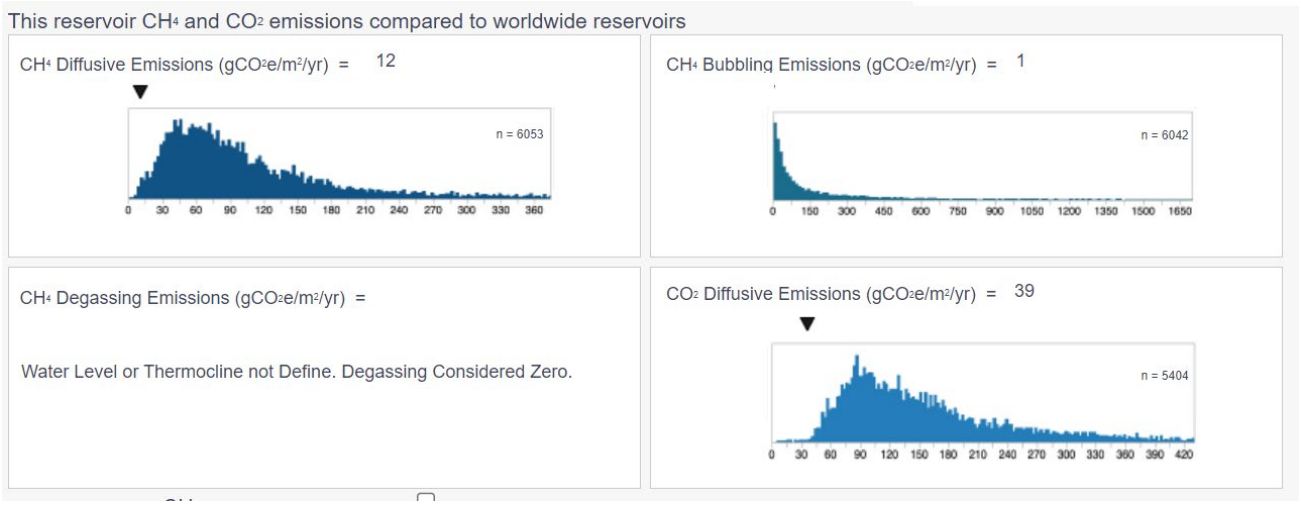

Figure B 8 Results from Litjfossen (Innerdalsvatnet) compared to worldwide data (Both soil scenarios)

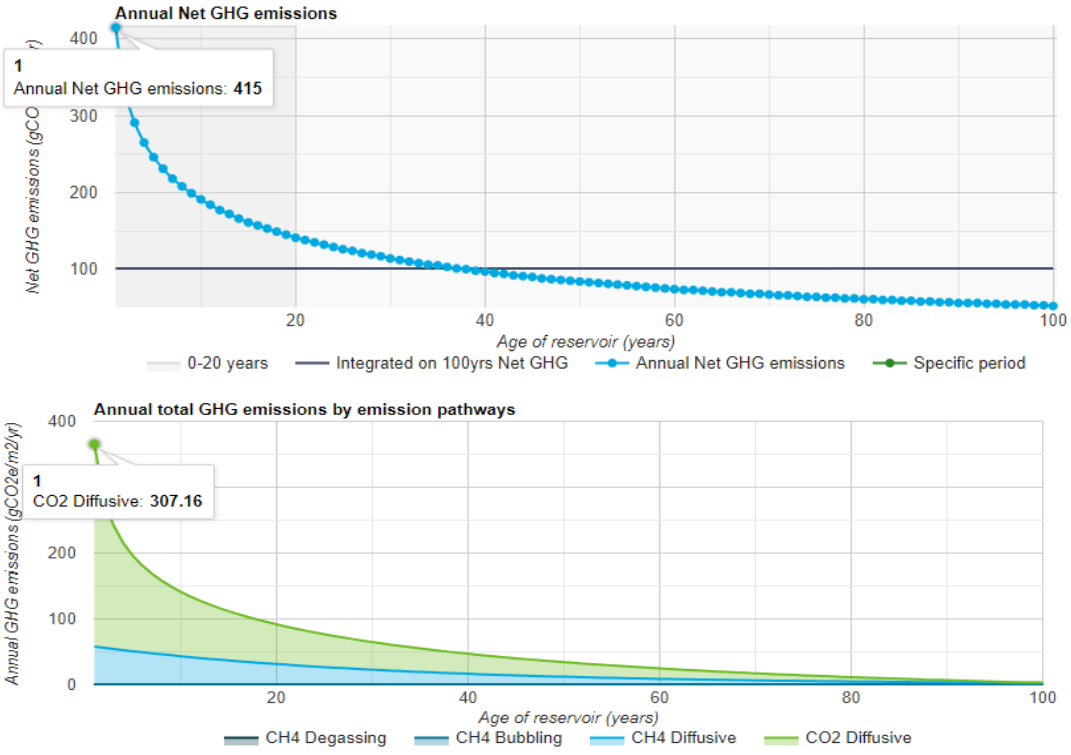

Figure B 9 Litjfossen (Innerdalsvatnet) annual GHG emissions and total GHG emissions by pathway (Mineral soil scenario)

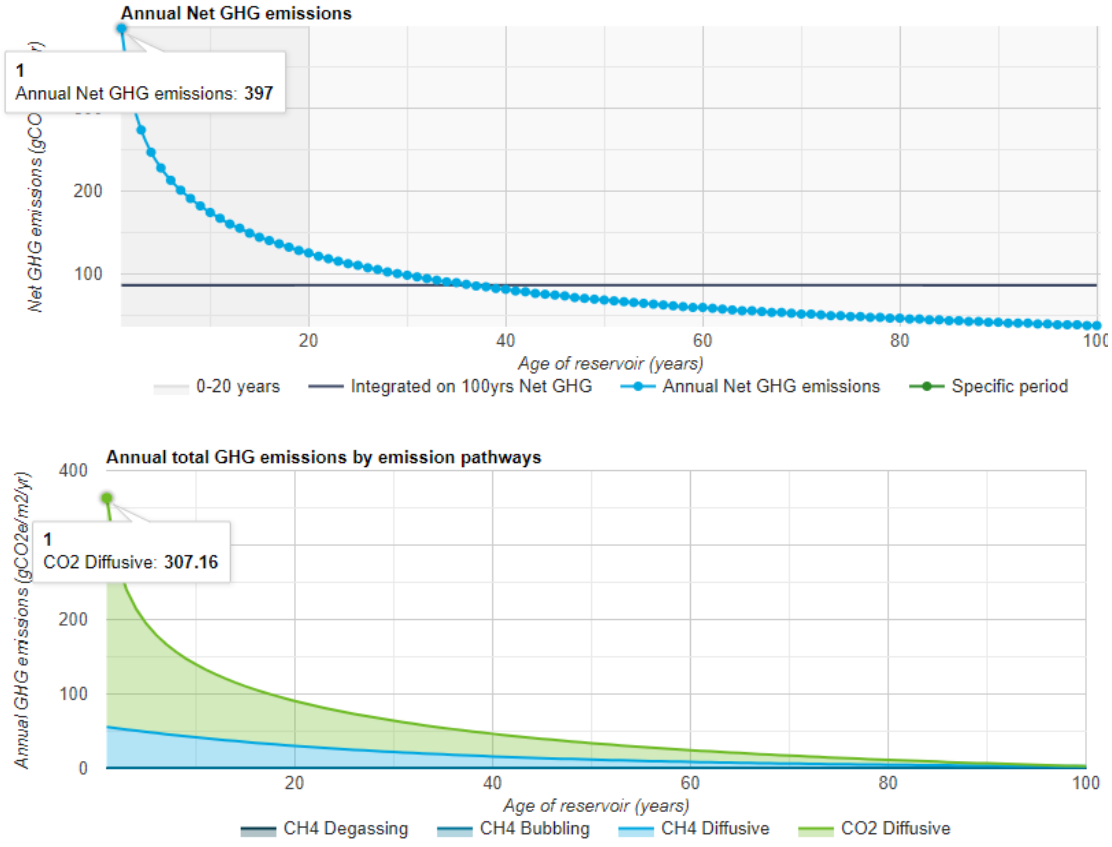

Figure B 10 Litjfossen (Innerdalsvatnet) annual GHG emissions and total GHG emissions by pathway (Mineral + Organic soil scenario)

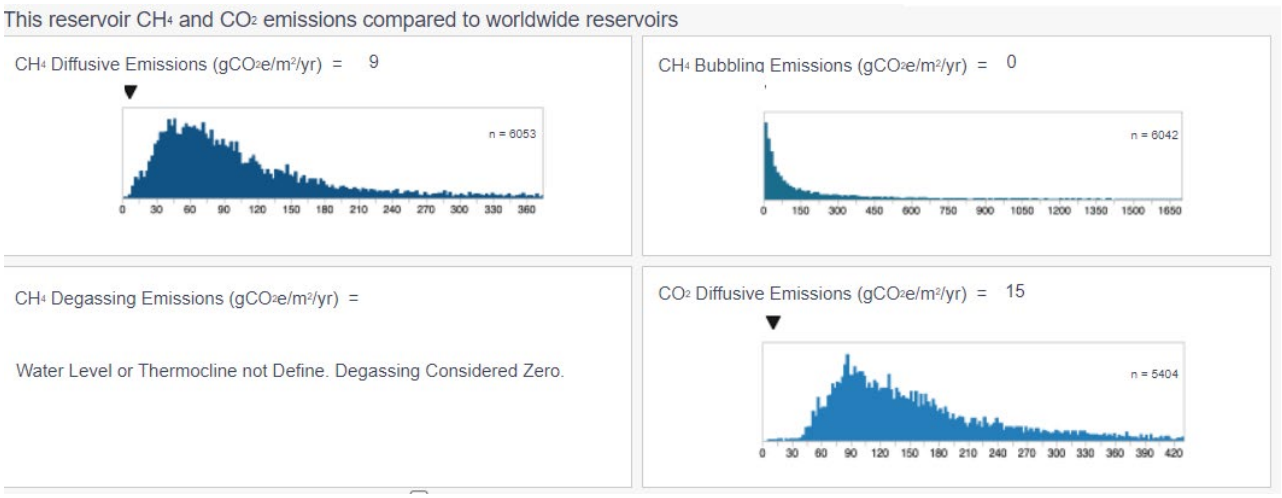

Figure B 11 Results from Falningsjøen compared to worldwide data

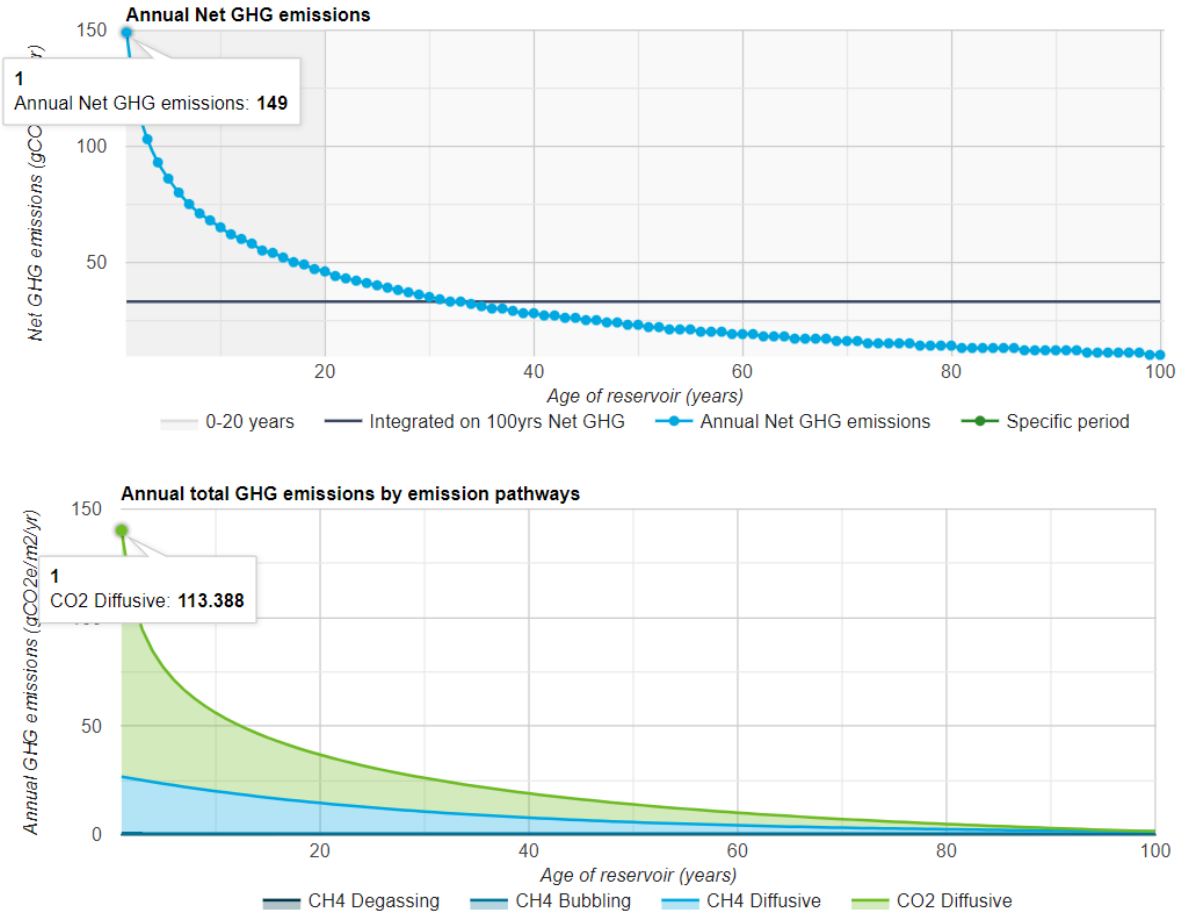

Figure B 12 Falningsjøen annual GHG emissions and total GHG emissions by pathway

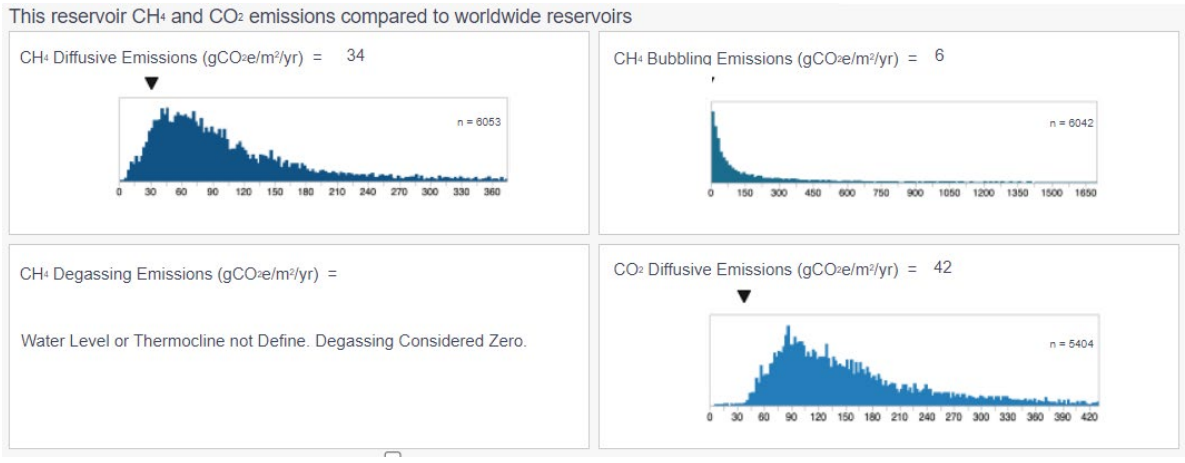

Figure B 13 Results from Sverjesjøen compared to worldwide data

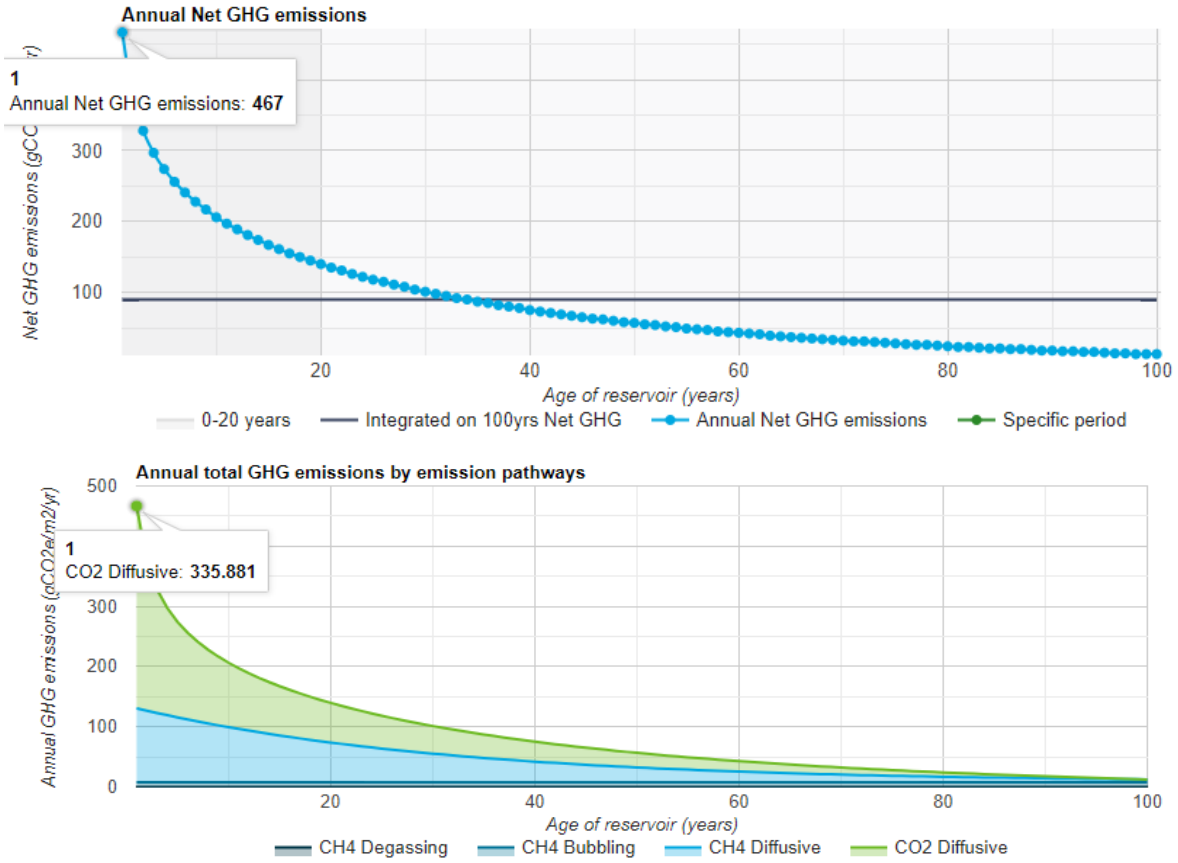

Figure B 14 Sverjesjøen annual GHG emissions and total GHG emissions by pathway

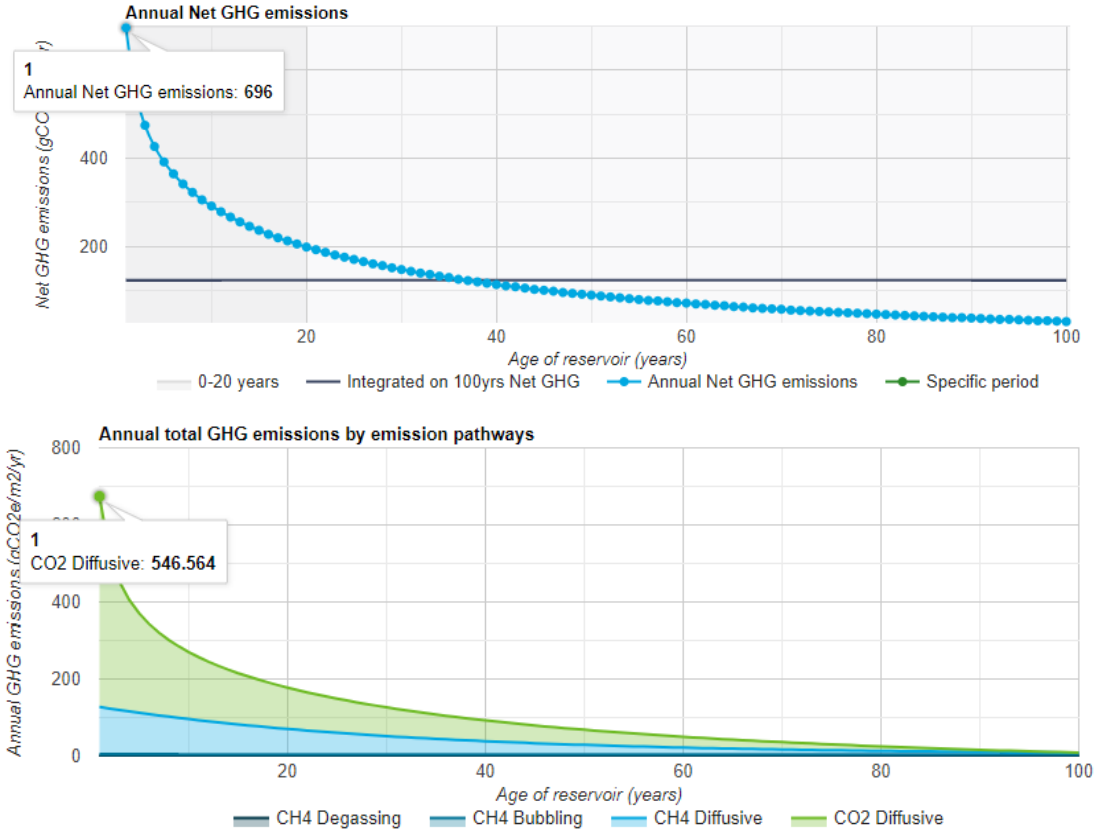

Figure B 15 Flothølen annual GHG emissions and total GHG emissions by pathway

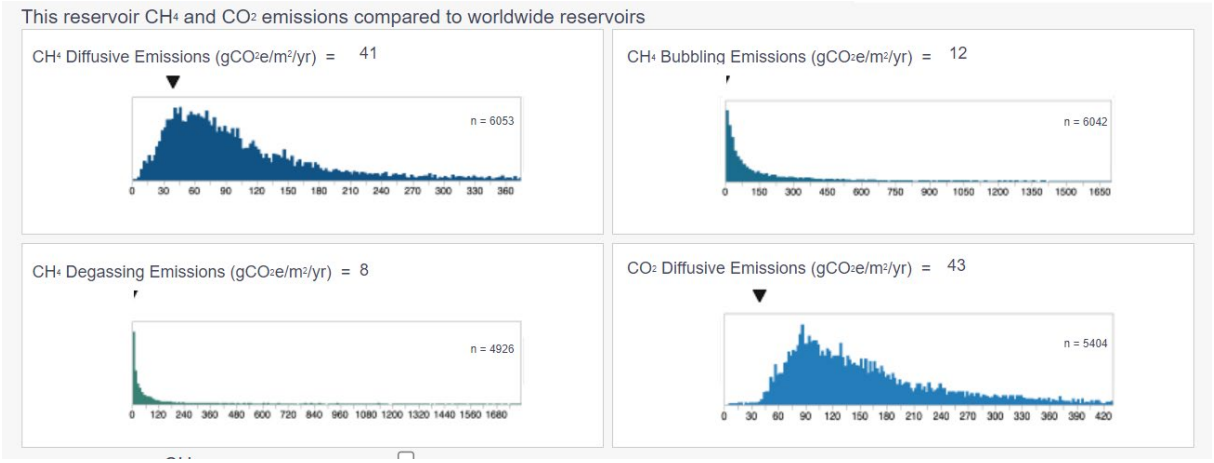

Figure B 16 Results from Valevatn compared to worldwide data

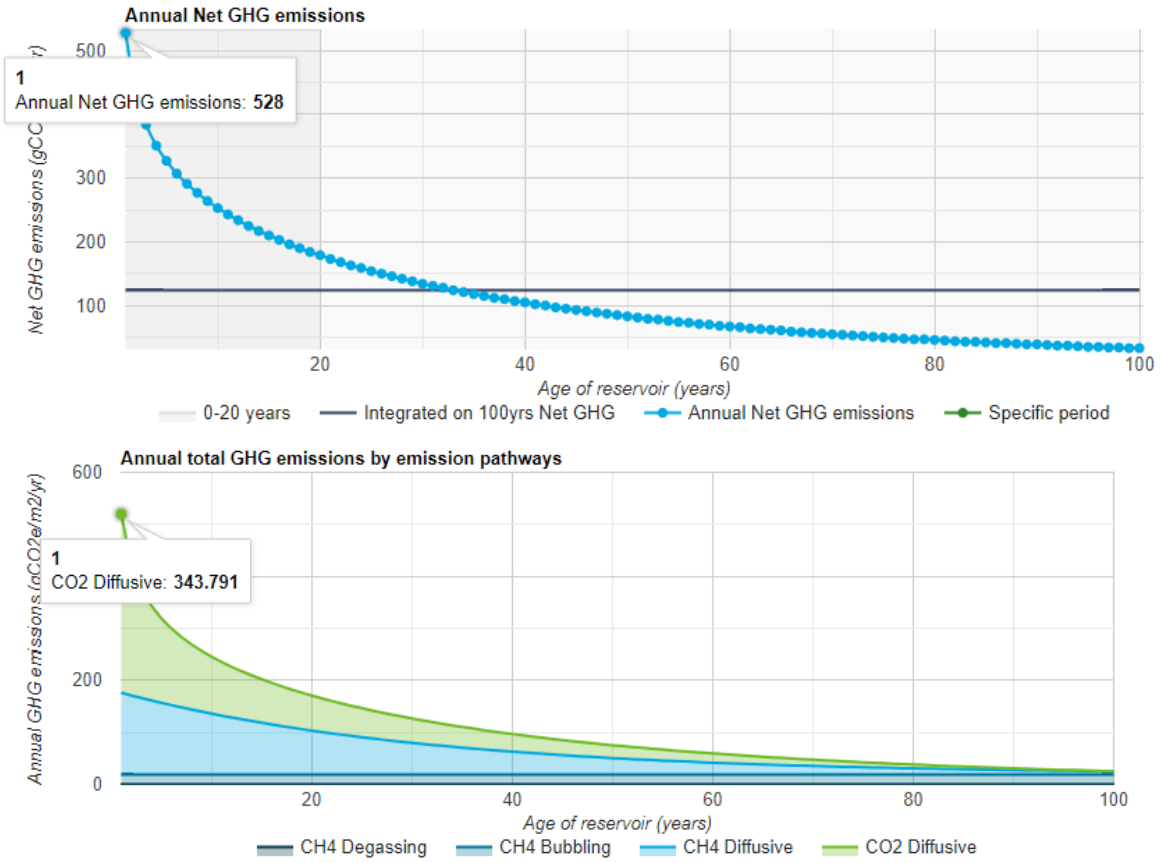

Figure B 17 Valevatn annual GHG emissions and total GHG emissions by pathway

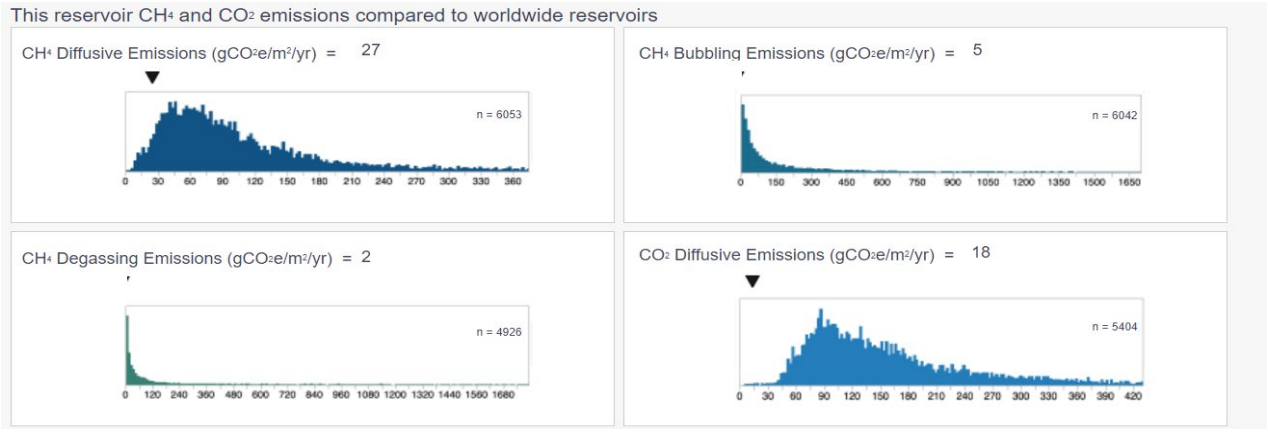

Figure B 18 Results from Gravatn compared to worldwide data

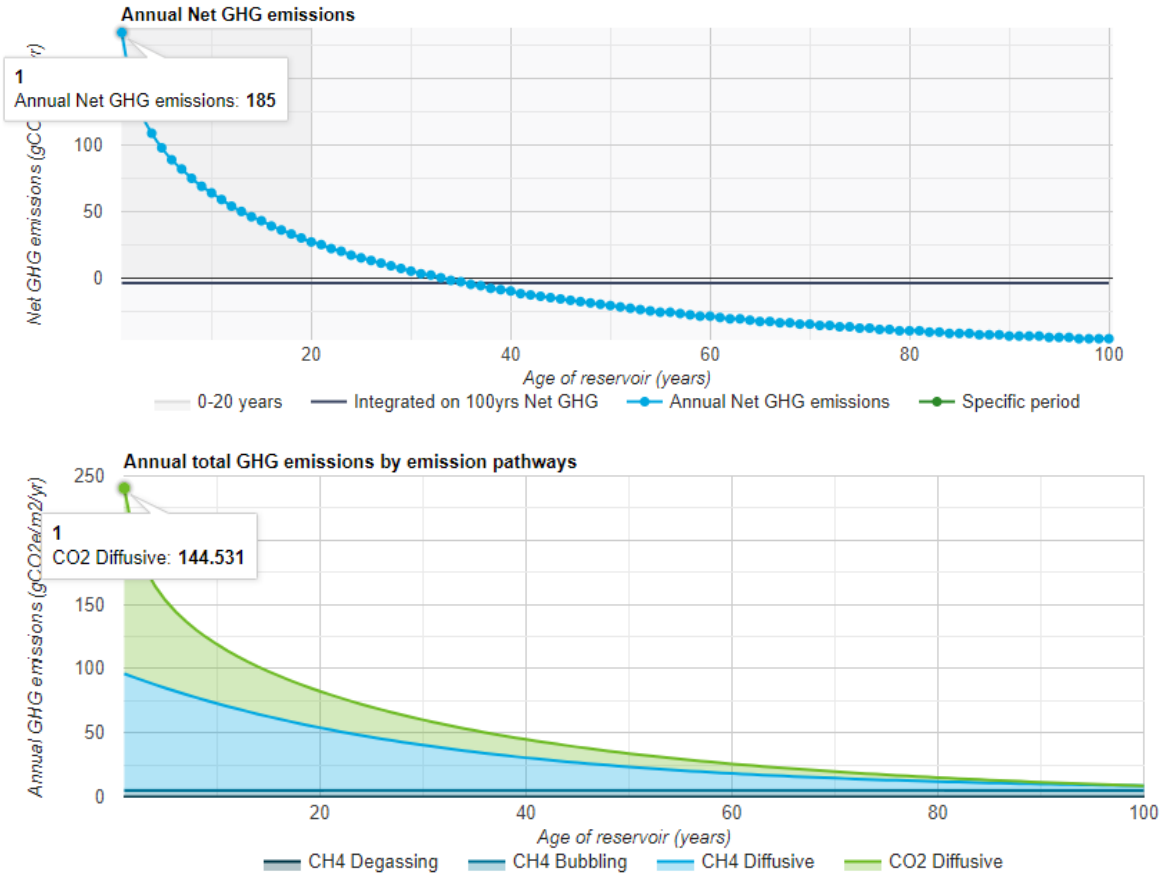

Figure B 19 Gravatn annual GHG emissions and total GHG emissions by pathway

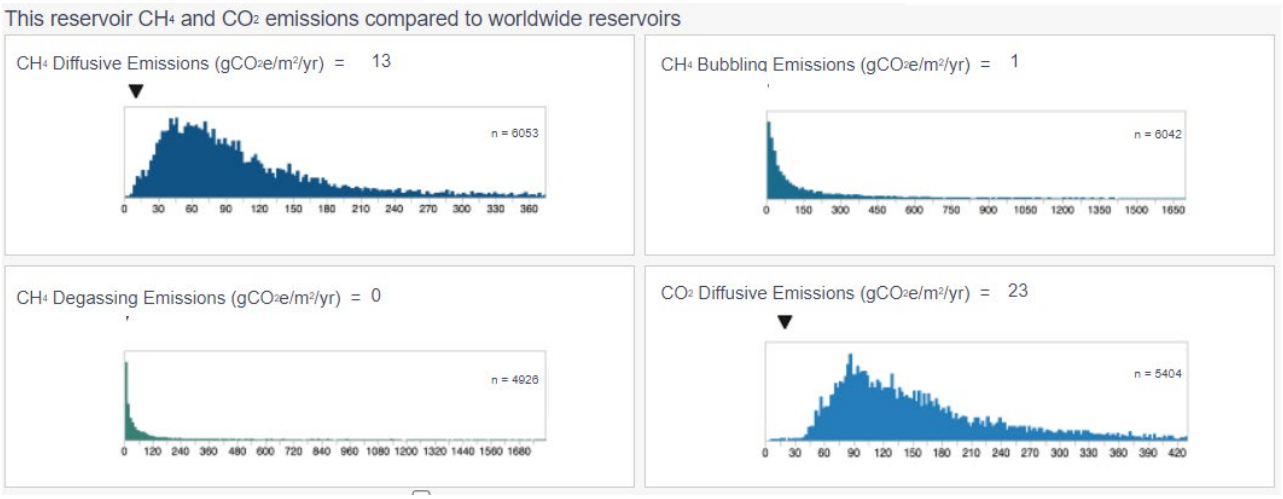

Figure B 20 Results from Roskreppfjord-Kverevatn compared to worldwide data

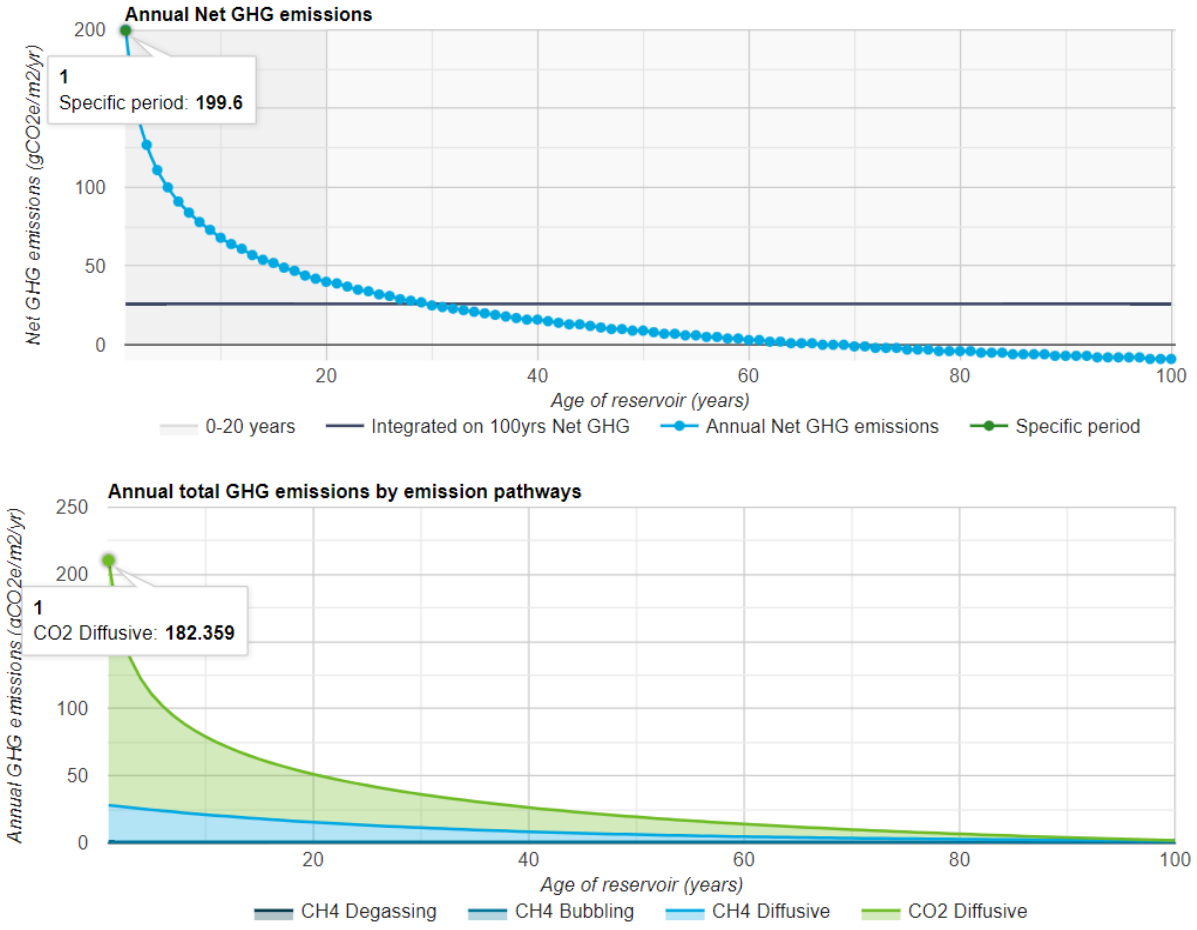

Figure B 21 Roskreppfjord-Kverevatn annual GHG emissions and total GHG emissions by pathway

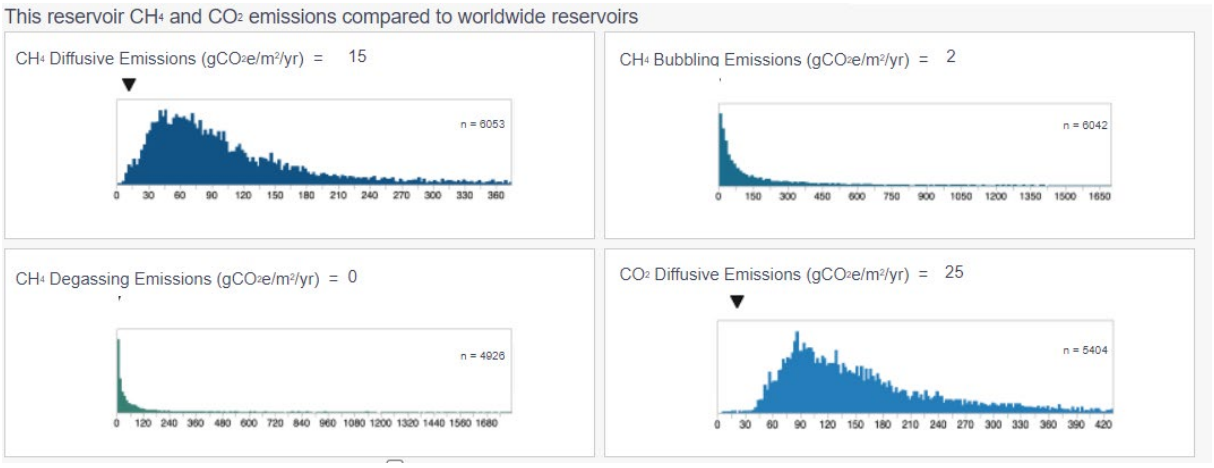

Figure B 22 Results from Øysteinsevja compared to worldwide data

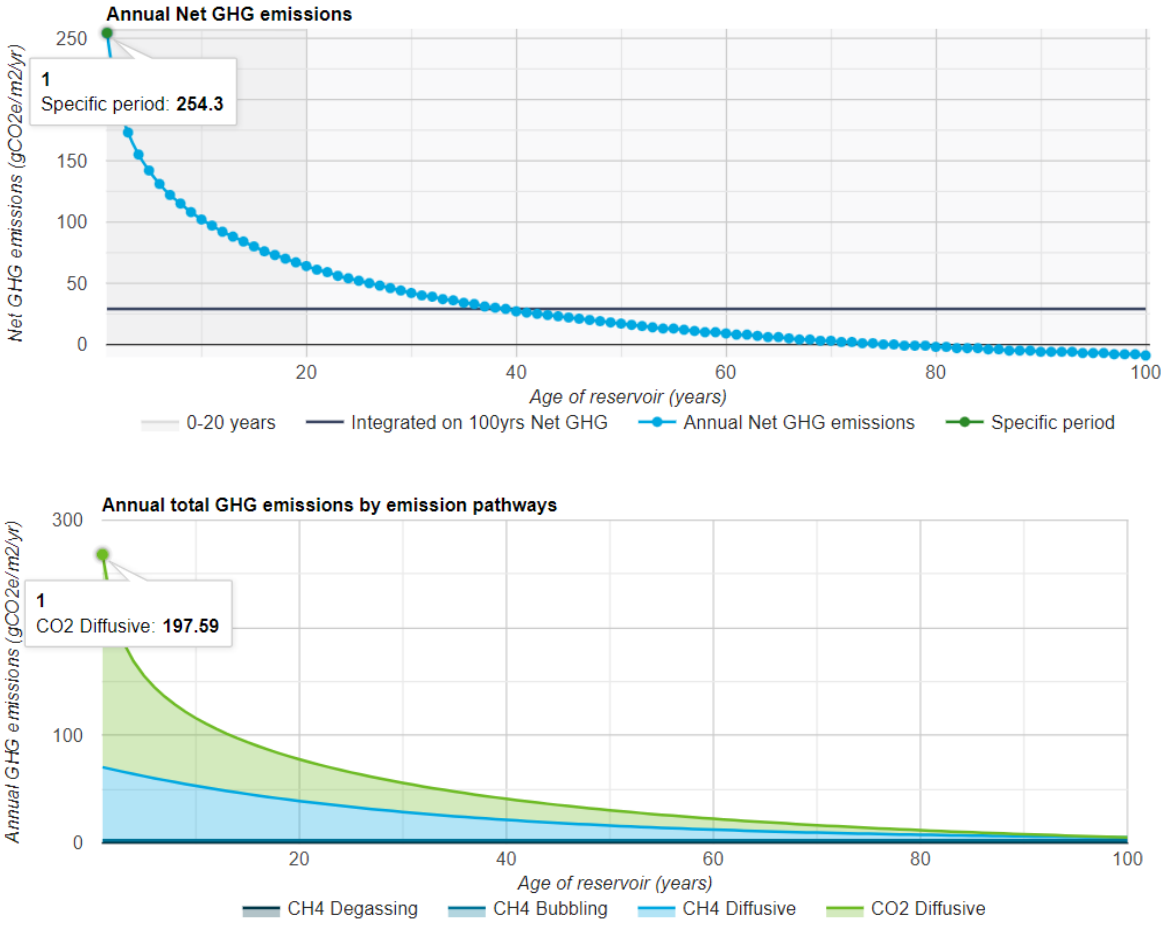

Figure B 23 Øysteinsevja annual GHG emissions and total GHG emissions by pathway

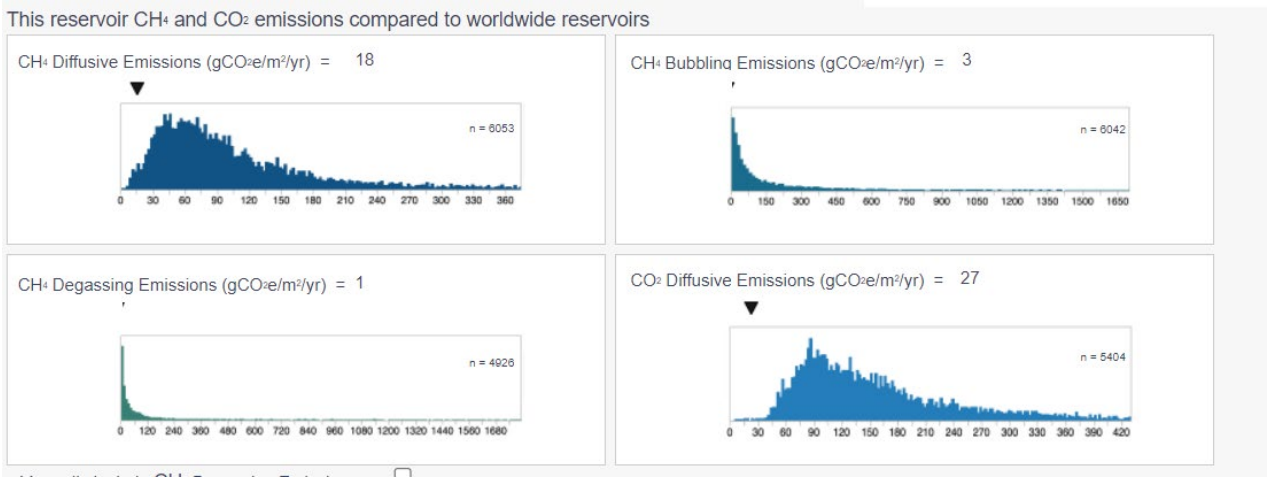

Figure B 24 Results from Kvifjorden (Nesjen) compared to worldwide data

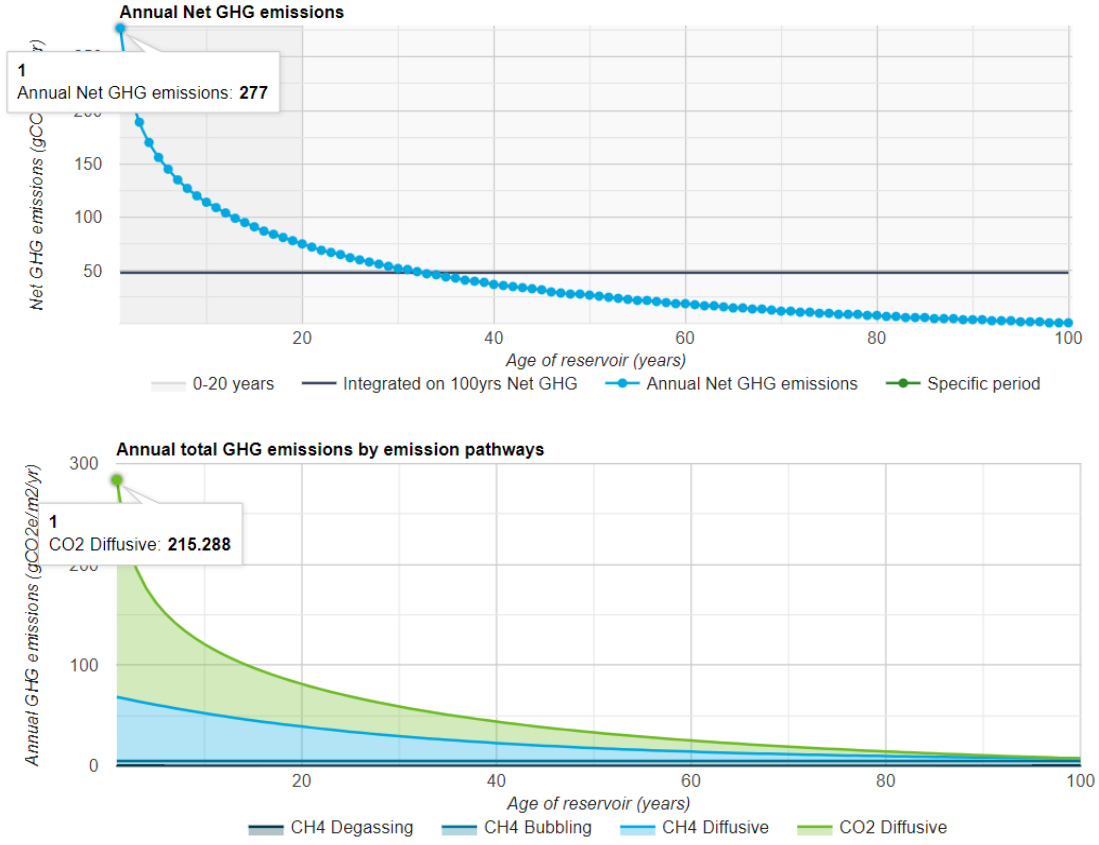

Figure B 25 Kvifjorden (Nesjen) annual GHG emissions and total GHG emissions by pathway

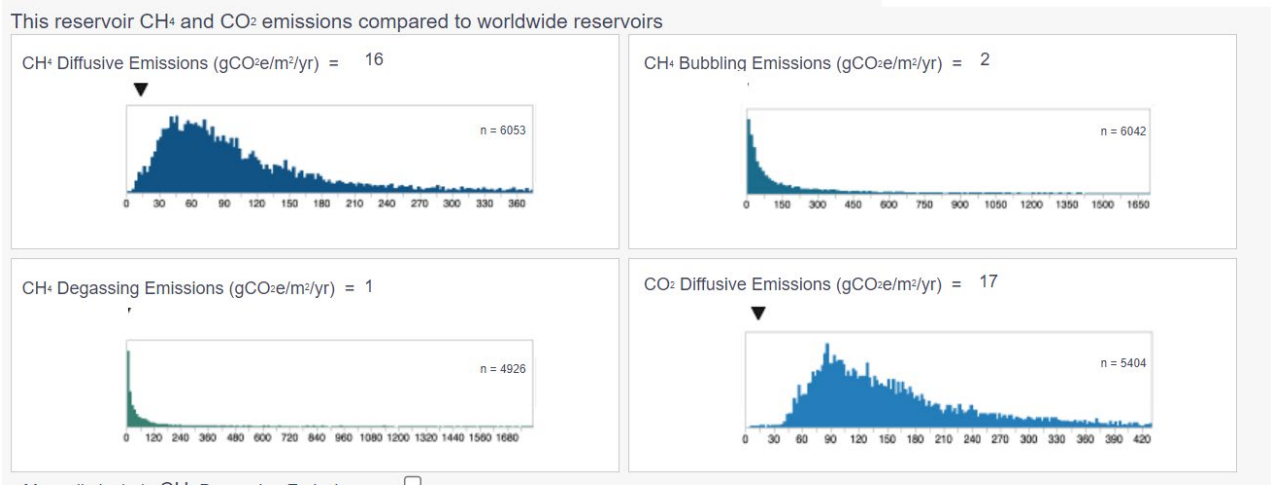

Figure B 26 Results from Homstølvatnet compared to worldwide data

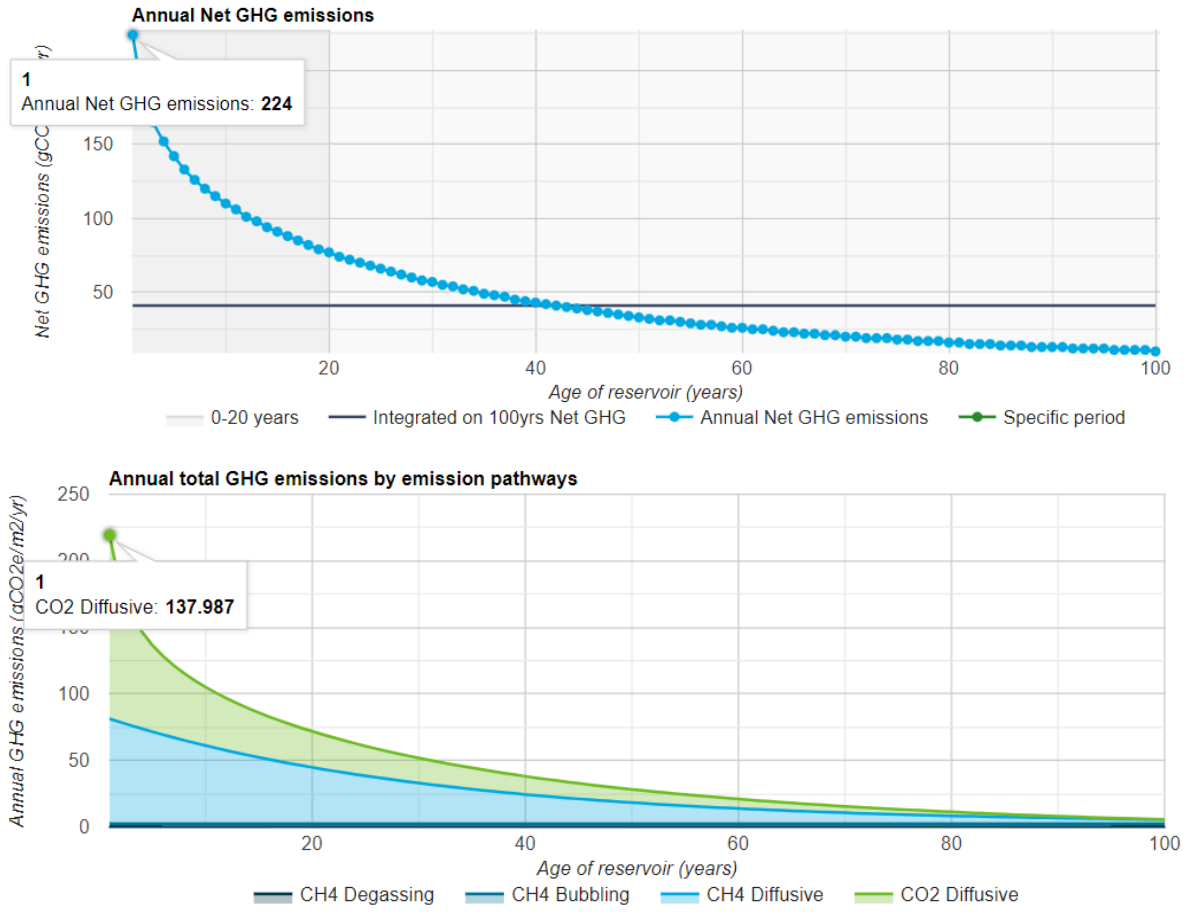

Figure B 27 Homstølvatnet annual GHG emissions and total GHG emissions by pathway

Appendix B1 – Wind and solar results overview

From	To	Change (t C)
Forest	Pasture	−5.91
Forest	Agriculture	−19.72
Forest	Bare land	−42.91
Forest	Artificial surface	−39.56
Forest	Wetlands and water surfaces	−5.97
Pasture	Forest	5.91
Pasture	Agriculture	−13.81
Pasture	Bare land	−36.99
Pasture	Artificial surface	−33.65
Pasture	Wetlands and water surfaces	−0.06
Agriculture	Forest	19.72
Agriculture	Pasture	13.81
Agriculture	Bare land	−23.18
Agriculture	Artificial surface	−19.84
Agriculture	Wetlands and water surfaces	13.75
Bare land	Forest	42.91
Bare land	Pasture	36.99
Bare land	Agriculture	23.18
Bare land	Artificial surface	3.34
Bare land	Wetlands and water surfaces	36.94
Artificial surface	Forest	39.56
Artificial surface	Pasture	33.65
Artificial surface	Agriculture	19.84
Artificial surface	Bare land	−3.34
Artificial surface	Wetlands and water surfaces	33.59
Wetlands and water surfaces	Forest	5.97
Wetlands and water surfaces	Pasture	0.06
Wetlands and water surfaces	Agriculture	−13.75
Wetlands and water surfaces	Bare land	−36.94
Wetlands and water surfaces	Artificial surface	−33.59

Figure B1 1 SOC change amounts per 1 ha of land cover change (Ozge Isik Pekkan, 2021)

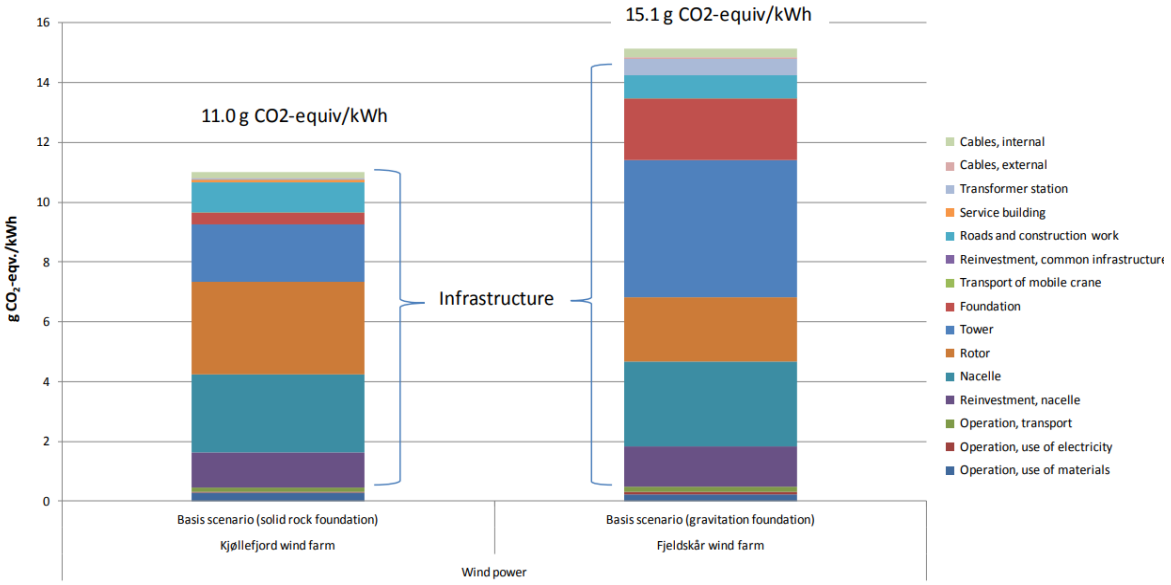

Figure B1 2 GHG emissions for the main scenarios for Kjøllefjord and Fjeldskår wind farms separated into the different life cycle stages/main components

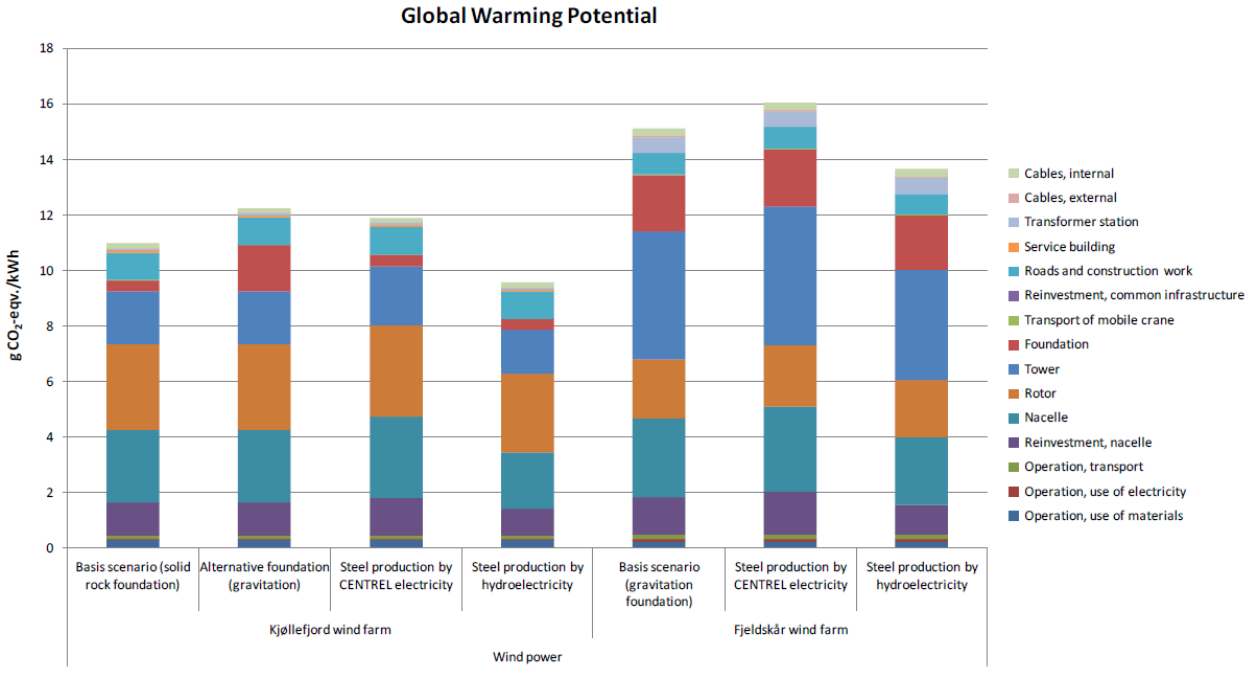

Figure B1 3 GHG emissions for additional scenarios compared to the basic scenarios for Kjøllefjord and Fjeldskår wind farms.

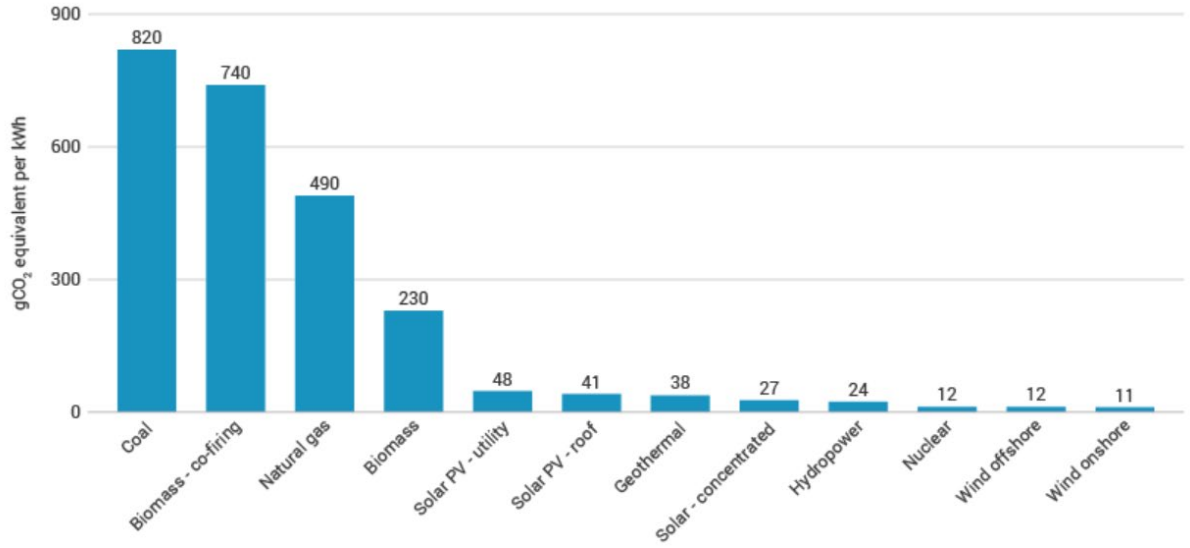

Figure B1 4 Average life-cycle CO2 equivalent emissions (IPCC, n.d.)

Focus region	Solar penetration by 2050[a]	Rooftop PV generation share of solar (2050)	Occupation of land suitable for commercial purposes ([b]) by 2050		Relative solar land occupation by 2050[c]			Occupation of land suitable for commercial purposes ([b])
	% of total electricity (PWh in 2050)	% of solar penetration by 2050	Solar energy	Bioenergy (% within region)	% of total land area	Compared to urban area in 2010 (%)	Compared to crop area in 2050 (%)	km² per TWh solar (average 2020–2050)
			1000 km²					
European Union	26 (1.19)	24.3–23.0	21–28	366 (45)	0.5–0.7	20–27	1.9–2.5	19.4–24.2
	53 (2.54)	12.3–11.6	53–69	614 (38)	1.3–1.7	50–66	4.8–6.3	22.1–28.0
	79 (3.87)	8.1–7.6	85–111	969 (32)	2.1–2.8	81–106	7.7–10	23.5–29.7
India	30 (1.8)	10.6–9.9	10–14	596 (16)	0.3–0.5	46–62	0.6–0.9	6.4–8.2
	54 (3.29)	5.9–5.5	20–26	1051 (12)	0.7–0.9	88–118	1.2–1.6	6.5–8.5
	78 (4.88)	3.6–3.3	30–41	1516 (10)	1.0–1.4	137–182	1.9–2.5	6.9–8.8
Japan and South-Korea	28 (0.5)	25.0–22.1	5–6	185 (17)	1.2–1.6	36–48	8.3–11	12.9–15.6
	46 (0.8 PWh)	15.6–13.8	9–12	279 (13)	2.3–3	68–89	16–21	13.3–16.4
	74 (1.3 PWh)	9.0–8.1	16–21	429 (10)	4–5.2	120–157	29–39	13.9–17.1

Figure B1 5 Land occupation characteristics at different solar penetration levels by 2050. (Dirk-Jan van de Ven, 2021)

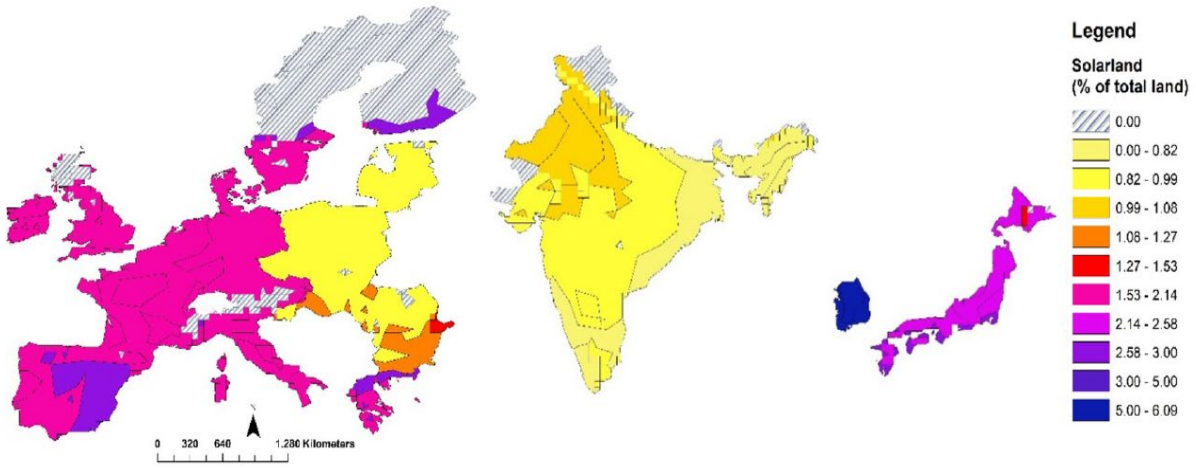

Figure B1 6 Geographical distribution of the share of total land occupied by solar energy within each region (Dirk-Jan van de Ven, 2021)

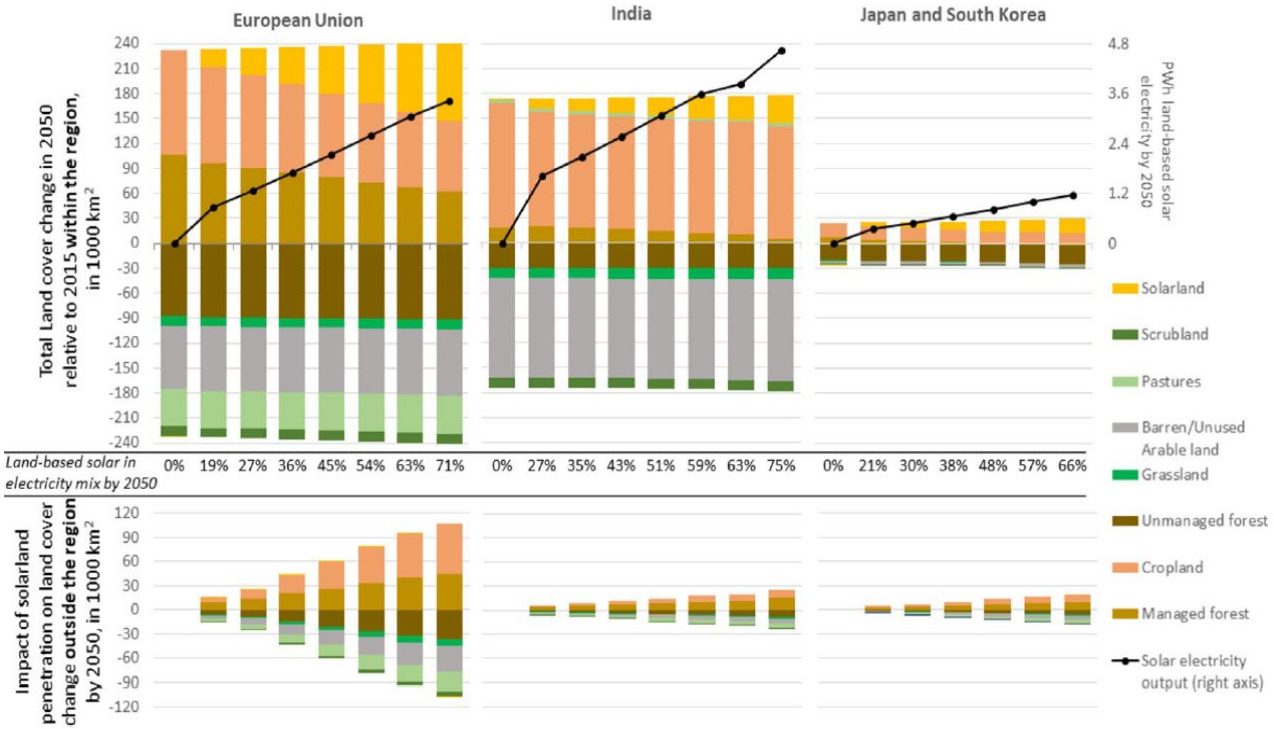

Figure B1 7 Global land-cover changes by 2050 due to solar expansion (Dirk-Jan van de Ven, 2021)

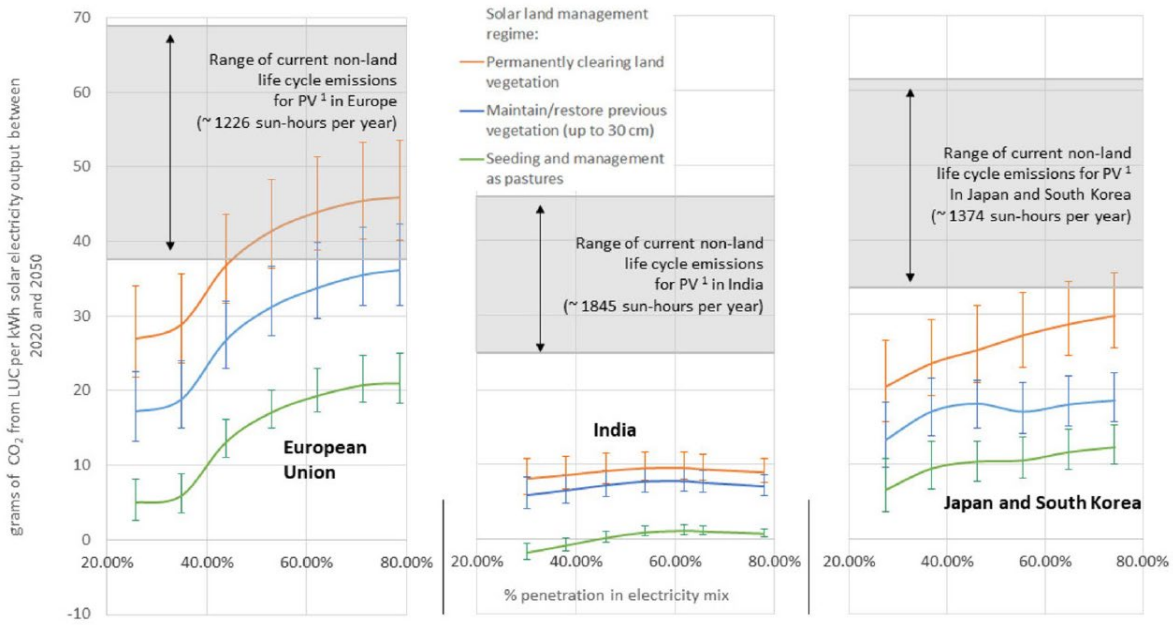

Figure B1 8 Land use change emissions related to land occupation per kWh of solar energy from 2020 to 2050 (Dirk-Jan van de Ven, 2021)

	Solar penetration level		Direct and indirect land use change (LUC) emissions due to solar energy[b]			LUC emissions per occupied m^2[c]		LUC CO_2 payback period when replacing gas-fired electricity[d]	
			Within region	Outside region	Total	Solar energy	Bio-energy	Solar energy	Bio-energy
	% and PWh in 2050 elect. mix	Land management scenario in solarland[a]	Grams of CO_2 per kWh of solar electricity output between 2020 and 2050 (average)			kg CO_2 (2020–2100) per m^2 of dedicated land in 2050		Months	
European Union	26% (1.19 PWh)	CLEAR	28.1 to 38.6	−6.4 to −4.6	21.8 to 34.0	4.4 to 5.2	3	4.7 to 7.1	46.9
		MAINT	19.7 to 27.1		13.3 to 22.5	3.1 to 3.7		3.2 to 5.2	
		SEED	9.0 to 12.7		5.0 to 8.1	1.1 to 1.7		1.2 to 2.4	
	53% (2.54 PWh)	CLEAR	33.0 to 43.5	3.3 to 4.7	36.3 to 48.3	6.7 to 6.8	3.1	6.2 to 8.2	49.2
		MAINT	24.0 to 30.9		27.3 to 36.6	5.3 to 5.4		4.8 to 6.5	
		SEED	11.7to 15.4		15.0 to 20.1	~3.1		2.9 to 3.8	
	79% (3.87 PWh)	CLEAR	34.6 to 46.7	5.6 to 6.9	40.2 to 53.6	7.2 to 7.3	3	6.4 to 8.3	49.3
		MAINT	25.8 to 35.5		31.4 to 42.4	~5.9		5.2 to 6.7	
		SEED	12.7 to 18.1		18.3 to 24.9	3.5 to 3.6		3.2 to 4.0	
India	30% (1.8 PWh)	CLEAR	10.0 to 12.5	−4.0 to −1.6	6.0 to 10.8	1.3 to 2.4	2.3	0.3 to 0.8	41.7
		MAINT	8.1 to 10.0		4.1 to 8.4	0.6 to 1.7		0.2 to 0.6	
		SEED	1.1 to 1.3		−2.7 to −0.6	−5.2 to −6.2		−1.5 to −1.7	
	54% (3.29 PWh)	CLEAR	10.8 to 13.0	−2.8 to −1.3	8.0 to 11.7	2.5 to 3.1	2.3	0.6 to 1.0	43.2
		MAINT	9.1 to 10.8		6.3 to 9.5	1.9 to 2.4		0.5 to 0.8	
		SEED	3.0 to 3.2		0.4 to 1.7	−4.5 to −5.0		−1.2 to −1.5	
	78% (4.88 PWh)	CLEAR	9.7 to 11.7	−2.1 to −0.9	7.6 to 10.8	2.9 to 3.2	2.4	0.7 to 1.1	43.9
		MAINT	8.0 to 9.5		5.9 to 8.6	2.1 to 2.5		0.5 to 0.8	
		SEED	2.3 to 2.5		0.4 to 1.4	−4.4 to −4.8		−1.2 to −1.5	
Japan and South-Korea	28% (0.5 PWh)	CLEAR	18.9 to 25.8	−3.2 to 0.8	15.7 to 26.6	4.8 to 6.8	2.7	2.9 to 5.2	47.7
		MAINT	12.8 to 17.5		9.6 to 18.2	2.2 to 4.1		1.4 to 3.1	
		SEED	6.8 to 10.0		3.6 to 10.7	−0.3 to −2.2		−0.2 to −1.3	
	46% (0.8 PWh)	CLEAR	23.0 to 30.6	−2.1 to 0.6	20.9 to 31.1	6.1 to 7.2	2.6	3.3 to 5.0	47.3
		MAINT	16.9 to 20.5		14.8 to 21.1	3.9 to 4.3		2.1 to 2.9	
		SEED	9.9 to 12.5		7.7 to 13.1	−0.2 to −1.2		−0.2 to −0.7	
	74% (1.3 PWh)	CLEAR	25.6 to 33.3	0.0 to 2.3	25.6 to 35.6	7.1 to 7.7	2.7	3.6 to 5.0	48.9
		MAINT	15.6 to 20.0		15.6 to 22.2	3.5 to 3.9		1.8 to 2.6	
		SEED	10.0 to 12.9		10.0 to 15.2	−0.5 to 0.0		−0.3 to 0.0	

Figure B1 9 Land use change emissions and payback periods for solar penetration and solar land management (Dirk-Jan van de Ven, 2021)

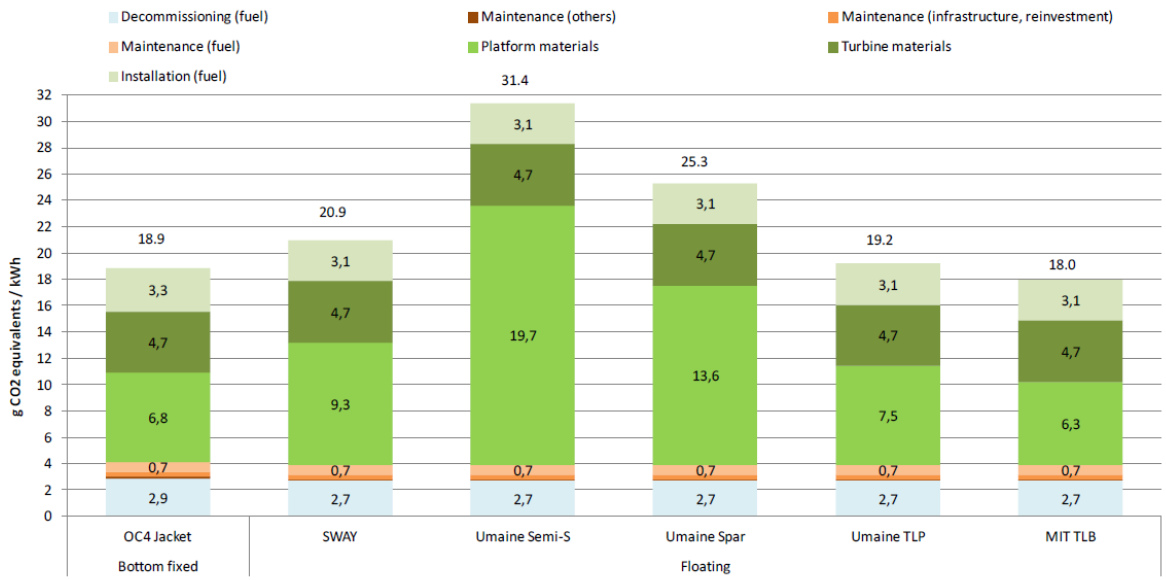

Figure B1 10 GHG emissions (g CO2 -equivalents//kWh) for the investigated offshore wind park concepts (The Norwegian Research Council, 2020)

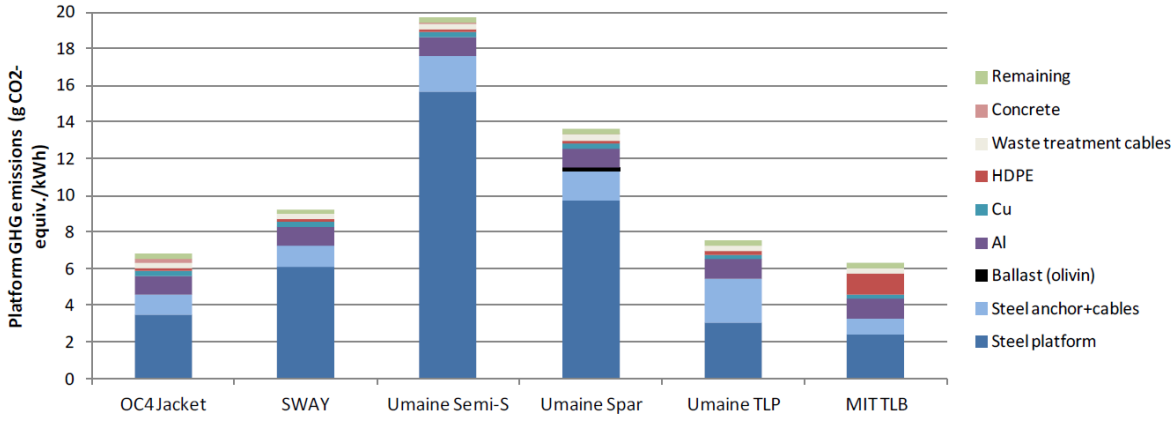

Figure B1 11 Platform GHG emissions separated into the main contributors (The Norwegian Research Council, 2020)

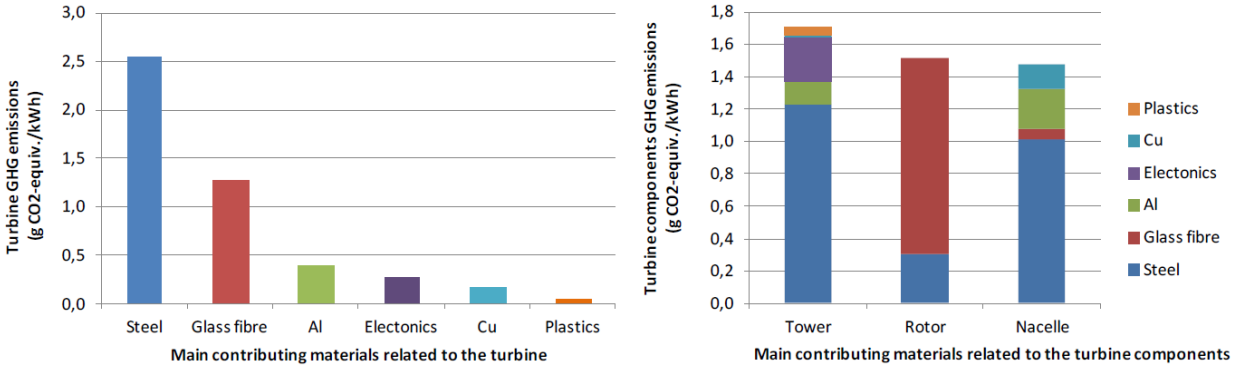

Figure B1 12 Turbine GHG emissions separated into the main contributors (The Norwegian Research Council, 2020)

Appendix C – GIS map

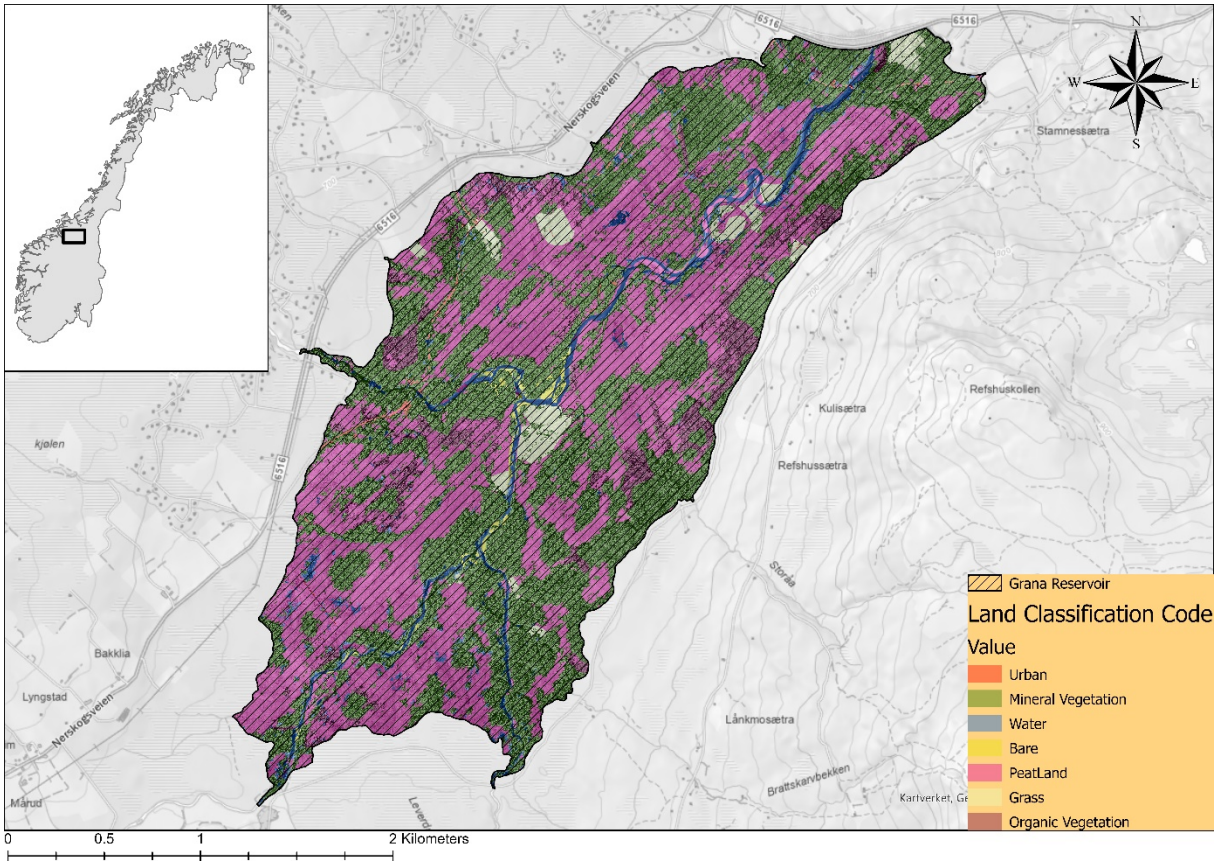

Figure C 1 Granasjøen reservoir land classification

NTNU
Norwegian University of Science and Technology

Faculty of Engineering

Department of Civil and Environmental Engineering

M.Sc. Thesis in Water Resources Modelling and Engineering

Candidate: Elene Gotsiridze

Title: Assessment of greenhouse gas emissions from hydropower projects using G-RES tool

1 BACKGROUND

Initiated by extensive plans to develop new renewable energy sources in Norway it has been an intense debate about the environmental footprint of the development of the different renewable electricity technologies. It is, however, limited scientific studies and literature that compare the environmental performance of off-shore and on-shore wind power, small and large hydropower as well as refurbishment and extension of existing hydropower plants and the development of solar power. A large set of environmental factors, such as land use occupation, greenhouse gas emissions, biodiversity impacts and more must be assessed individually before they can be summed up and the total environmental footprint assessed.

This study aims at comparing the environmental footprint of renewable energy technologies by the means of greenhouse gas emissions (GHG). The main focus will on the calculation of greenhouse gas emissions for a selection of Norwegian hydropower projects where the land use occupation has already been comprehensively assessed, providing input to the calculation of the greenhouse gas emissions. The results found for hydropower, will be further be compared against results from other renewable energy sources, i.e. mainly wind power and possibly solar power.

The study will be carried out with use of the internationally accepted (state-of-the-art) calculation tool G-RES, hosted by the International Hydropower Association (IHA), and the study and findings will be discussed with key personnel in IHA.

2 MAIN QUESTIONS FOR THE THESIS

Key questions to be addressed in the thesis are;

1. Identify and select 5-10 reservoirs for the assessment of greenhouse gas emissions in Norway, based on hydropower projects where land use changes (due to hydropower regulations) have been detailed assessed
2. Get familiar with the G-RES tool hosted by the International Hydropower Association (IHA) and configure the model for the selected reservoirs
3. Calculate the net greenhouse gas emissions from the selected case studies and discuss the results.
4. Compare the calculated results from hydropower projects in Norway, with published values on the greenhouse gas emissions from wind power projects (and possibly other renewable sources), from similar/comparable climatic conditions.

3 SUPERVISION, DATA AND INFORMATION INPUT

Professor Tor Haakon Bakken will be the main supervisor of the thesis work, with PhD-candidate Mahmoud Kenawi (NTNU), on the selection of case studies/provision of input data, and Researcher Håkon Sundt (SINTEF) on the configuration of the G-RES tool, as co-supervisors. Discussion with and input from colleagues and other researchers or engineering staff at NTNU, power companies or consultants are recommended, if considered relevant. Significant inputs from others shall, however, be referenced in a convenient manner.

The research and engineering work carried out by the candidate in connection with this thesis shall remain within an educational context. The candidate and the supervisors are therefore free to introduce assumptions and limitations, which may be considered unrealistic or inappropriate in a contract research or a professional engineering context.

4 REPORT FORMAT AND REFERENCE STATEMENT

The report shall be typed by a standard word processor and figures, tables, photos etc. shall be of good report quality. The report shall include a summary, a table of content, lists of figures and tables, a list of literature and other relevant references. All figures, maps and other included graphical elements shall have a legend, have axis clearly labelled and generally be of good quality.

The report shall have a professional structure and aimed at professional senior engineers and decision makers as the main target group, alternatively written as a scientific article. The decision regarding report or scientific article shall be agreed upon with the supervisor. The thesis shall include a signed statement where the candidate states that the presented work is his/her own and that significant outside input is identified.

This text shall be included in the report submitted. Data that is collected during the work with the thesis, as well as results and models setups, shall be documented and submitted in electronic format together with the thesis.

The thesis shall be submitted no later than 30th of June, 2023.

Tor Haakon Bakken

Tor Haakon Bakken, professor

Trondheim 15th of January 2023

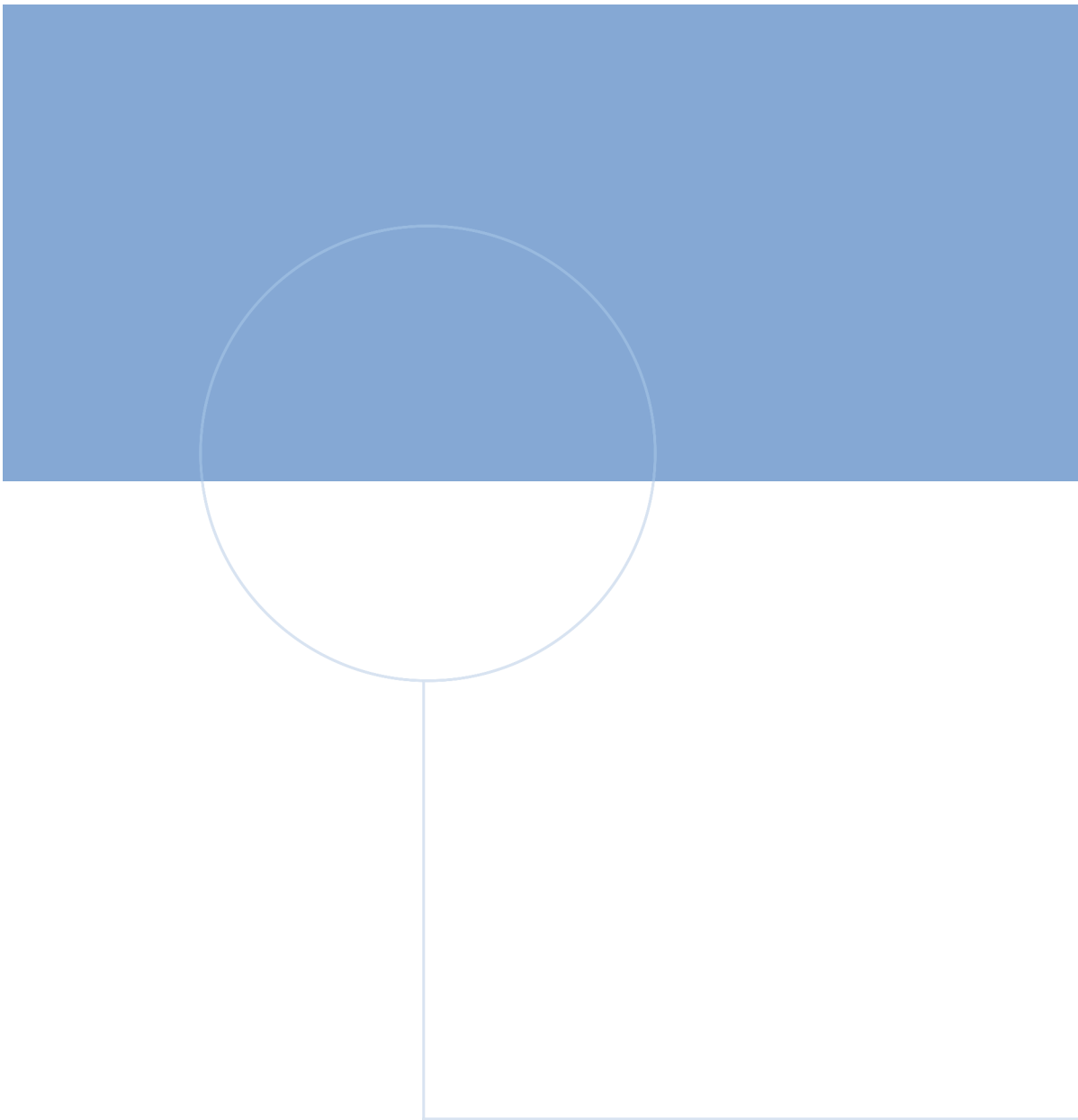

NTNU
Norwegian University of
Science and Technology

SINTEF
iha